Evaluation of Anti-E6 Single Domain Antibodies for the Treatment of Human Papillomavirus-related Cancer

A thesis presented to

The Faculty of Graduate Studies

of

Lakehead University

by

ASHLEY FAULKNER

In partial fulfillment of requirements
for the degree of
Master of Science in Biology

June 24th, 2022

ABSTRACT

The HPV16 genome encodes two oncoproteins, E6 and E7, which are essential for viral carcinogenesis. While E7 promotes cell proliferation, E6 abolishes the resulting p53-dependent apoptotic response. We hypothesized that antibodies targeting the E6 protein will allow for p53 restoration and induce apoptosis of the infected cells. Our lab has previously generated a pool of 20 *Camelidae*-derived single-domain antibodies (VHHs) against the E6 protein (Togtema et al. 2019). VHHs have several properties making them well-suited for therapeutic purposes including low immunogenicity, high stability, and capacity to bind epitopes not accessible to any other type of antibody. In the current project, we used dot blots to evaluate the VHHs binding potential to various recombinant E6 proteins, identifying several successful VHH candidates. Co-immunoprecipitation using Affigel resin was used to confirm the VHH's endogenous E6 binding capacity in CaSki cells. Therein, two clones, C26 and A37, were identified as efficient E6 binders, in triplicate. Interestingly, in denaturing Western Blot analyses, C26 was found to react with the maltose-binding protein (MBP)-containing proteins but not with E6 6C/6S lacking an MBP tag, supporting the hypothesis that C26 binds MBP or E6 through different parts of the antibody. To deliver the VHHs to target cells, cationic lipid-based protein transfection proved inadequate, however mRNA transfection resulted in improved transfection efficiency. Functional assays, including proliferation assays to assess cell proliferation, and immunodetection of p53 and PARP-1 cleavage following mRNA transfection, were used to evaluate the VHH's therapeutic potential. Our results indicate that further optimization of our molecules will be needed to yield VHHs with therapeutic potential, however, our methodology may serve as a template for other researchers, creating a pipeline of analysis for the evaluation of antibodies against the E6 protein.

LAY SUMMARY

Approximatively 20% of human cancers worldwide are due to microbes such as viruses, of which a major contributor is the common human papillomavirus (HPV). Virtually all cervical cancers and an increasing amount of throat cancers affecting all genders are caused by high-risk HPV, especially type 16. While there are various vaccines against HPV (Gardasil, Gardasil 9, Cervarix) against HPV, its uptake remains low and is financially inaccessible to those needing it most. The main culprit in HPV cancer development is a viral protein known as E6. This protein is only expressed by the virus, and it is then involved in a multitude of cancer-developing processes. Due to its function, E6 is considered the most interesting target for the development of therapeutics specifically targeting the virus. For this reason, our lab has generated several llama-derived single-domain antibodies against the E6 protein. Such molecules have the potential to only target cancerous cells in a local rather than systemic manner, where unlike current systemic treatments such as chemotherapy, healthy cells will be spared. In this study, we confirmed the ability of our antibodies to bind the E6 protein using HPV-infected cancer cells, while further investigating their capacity to slow down the multiplication of cancer cells and induce cancer cell death. We have confirmed that our antibodies can bind the E6 protein, and we have developed a methodology to analyze their capacity to induce cancer cell death. Nevertheless, our data indicates that more optimization of our antibodies will be needed for them to reach their full therapeutic potential.

ACKNOWLEDGEMENTS

Professional

First and foremost, I would like to thank my supervisor, Dr. Ingeborg Zehbe, for being not only a mentor, but a confidante and friend. Your constant support and guidance truly allowed me to blossom in your lab, and I have learned more and gained more skills than I ever could have imagined when I started three years ago in my HBSc. Thank you for always encouraging me to pursue and present my research whenever possible as these experiences have been some of the most rewarding in my life. I cannot express enough gratitude for all the opportunities you have given me to grow as a student, researcher, and person throughout these last years; your influence is something I will cherish for many years to come!

To my committee members, Dr. Marina Ulanova, and Dr. Kam Leung, thank you for your guidance and many helpful suggestions; I very much appreciate you sharing you time, expertise, and knowledge with me throughout the project. Thank you also to my external reviewer, Dr. Jinqiang Hou from the Department of Chemistry at Lakehead University, and research chair at the Thunder Bay Regional Health Research Institute, for taking the time to evaluate my thesis.

To Dr. Guillem Dayer, I would like to express my sincere appreciation for your guidance and support in completing my project; your constant support and brilliance in the lab have helped shape me into the aspiring researcher I am today. Thank you for always taking the time to help me with any and everything, I will truly miss our life chats and storytelling. But don't worry, I will always be available to "fix your English" as long as you are available to check my math.

Of course, thank you to all the scientists and my colleagues at the TBRHRI for making this such an amazing experience and academic environment to work in. To my lab mates, Tanu Talwar and Dana Gummerson, I will always cherish our memories and am truly blessed to have

had the chance to work with you both. Our time spent together was some of my fondest; I will always miss my Co-IP buddy and Thermofisher sleuth! I am so happy to have made life-long friends like you along the way! I would also like to thank Melissa Togtema for her advice, guidance, and expertise on this project, and Robert Jackson for his endless guidance with all thing's biostatistics and R.

Personal

To my loving partner Adam, for your endless support, patience, and all the late-night dinners when I said I would "be home on time". Thank you for never letting me take myself too seriously, and always making me smile with the most ill-timed jokes. To my family and friends, for always believing in me, sometimes even more than I do! Mom and Dad, I can never thank you enough for all you have done for me; you have always been my #1 fans. Thank you for attending every presentation, competition, or conference, even if you don't understand a word I am saying sometimes. To my brother, Andrew, for always capturing our best memories, and to my friends whom I can never thank enough for the constant love, support, late-night drives, hot tub nights, and endless FaceTime calls. Thank you for always being there to celebrate the wins and love me through the losses.

TABLE OF CONTENTS

LIST OF TABLES

LIST OF FIGURES

LIST OF ABBREVIATIONS

4C/4S	His6MBP-4C/4S E6
CDR	Complementary Determining Regions
Co-IP	Co-immunoprecipitation
CO_2	Carbon Dioxide
DAPI	4',6-diamindino-2-phenylindole
dH_2O	Distilled Water
DMEM	Dulbecco's Modified Eagle's Medium
DMSO	Dimethyl Sulfoxide Cryopreservative
DNA	Deoxyribonucleic Acid
DPBS	Dulbecco's Phosphate Buffered Saline
DTT	Dithiothreitol
E6	HPV16 E6 protein
E6 6C/6S	E6 Protein, Without Tags, With 6 Cysteine to Serine Substitutions
EDTA	Ethylenediaminetetraacetic Acid
F47R	His6MBP-F47R 4C/4S E6
FBS	Fetal Bovine Serum
GST	Glutathione S-Transferase
HIFU	High-intensity Focusing Ultrasound
His6	Hexahistidine
His6-E6	His6-GenScript E6
HPV	Human Papillomavirus
mAb	Monoclonal Antibody

MBP	Maltose-binding Protein
mRNA	Messenger RNA
NaCl	Sodium Chloride
NLS	Nuclear Localization Signal
p53	Tumour Suppressor Protein p53
PARP-1	Poly (ADP ribose) Polymerase
PFA	Paraformaldehyde
pRb	Retinoblastoma Protein
RNA	Ribonucleic Acid
scFv	Single-chain Fragment Antibody
SDS	Sodium Dodecyl Sulfate
SUMO	SUMOylate
VHH	*Camelidae*-derived Single-chain Antibody

1 INTRODUCTION

1.1 The Human Papillomavirus

Human papillomaviruses (HPVs) are a group of DNA viruses that infect the skin and mucosal epithelium with etiological importance to not only cervical cancer, but an increasing number of oropharyngeal, penile, and anal cancers as well (Senkomago et al. 2019, Van Dyne et al. 2018). Such viruses can be classified as high- or low-risk based on their carcinogenic potential (Kanodia et al. 2007), where infection with a low-risk type typically leads to relatively benign epithelial lesions, such as warts, whereas high-risk infections (such as HPV16 or HPV18) are responsible for almost all cervical cancers, and frequently other anogenital, head, and neck cancers (D'Souza and Dempsey, 2011). In recent years, the incidence of HPV-related oropharyngeal squamous cell carcinomas is on the rise and has become comparable to cervical cancer in Canada (Canadian Cancer Statistics 2016), while surpassing cervical cancer in the United States (United States Cancer Statistics). However, cervical cancer in particular still accounts for approximately 12% of all female cancers and is one of the most common gynecological malignancies worldwide. The virus itself is sexually transmitted and extremely common, so much so that almost all individuals will become infected at some point in their life (zur Hausen 2002). The development of cervical cancer occurs after persistent infection with high-risk types of HPV, of which HPV16 is the most common (zur Hausen 2002, Chen et al. 2005). Initial infection with these high-risk oncogenic types leads to the development of low to high-grade squamous intraepithelial lesions within the mucosal cells of the cervix, which can then progress to squamous cell carcinoma and adenocarcinoma of the cervix (zur Hausen 2002, Clifford et al. 2005).

As an exclusively intracellular pathogen, the HPV life cycle depends on the differentiation of the infected epithelium. HPV infection begins in the basal layer of the stratified epithelium, establishing a stable infection with genome integration. Once confluent, the differentiating infected daughter cells leave the basement membrane and enter the mid-epithelial layers, where it would then normally exit the cell cycle and cease DNA replication (Vats et al. 2021 and references herein). However, at this stage, E6 and E7 act in tandem to degrade host cellular proteins, leading to continued proliferation. In fact, the differences in the pathophysiology of the diseases caused by low- and high-risk HPVs are directly linked to functional differences in their E6 and E7 oncoproteins (Ghittoni et al. 2010). Once infected with HPV, the virus begins to express such oncoproteins which control keratinocyte differentiation while stimulating cell proliferation and survival (Vandepol et al. 2013). Continued expression of E6 and E7 promotes tumorigenesis through the immortilization and malignant transformation of infected cells mainly including the E6- or E7-dependent degradation of host cellular proteins leading to viral infection, persistence, and tumour promotion (Ghittoni et al. 2010, Vandepol et al. 2013, Togtema et al. 2019). While E7 triggers abberent cell proliferation by degrading pRB, the E6 protein inactivates the resulting p53-dependent apoptotic response by degrading the p53 protein in an E6AP dependent manner (Hoppe-Seyler et al. 2018). In particular, the E6 protein inactivates p53 through the formation of a stable bond with p53 and E6AP, leading to ubiquitination-mediated degradation of p53 via the proteasome (Li et al. 2019).

Although E6 does interact with a number of cellular targets also involved in apoptosis, (Bak protein, MAG-1) (Vats et al. 2021 and references herein), its interactions with p53 remain the most interesting for therapeutic development. It is anticipated that molecules inactivating E6 will restore p53 activity and therefore lead infected cells to apoptosis. In addition, Considering E6 is

expressed in both precancerous and cancerous lesions, and due to its specific functions with p53, the E6 protein is considered an interesting target for the development of diagnostic tools and therapeutics for HPV-associated cancers (Hoppe-Seyler et al. 2018, Togetma et al. 2019).

1.2 Previous Antibodies Against the E6 Protein of HPV16

Due to the enticing nature of the E6 protein, several molecules aiming at abolishing E6's functions have been generated such as chemical compounds (i.e. Zinc-ejector compounds), small interfering ribonucleic acids, RNA aptamers, antibodies (conventional antibodies, single-chain fragment antibodies (scFvs), single-domain antibodies), and inhibitory peptides (reviewed in Togtema et al. 2019). In particular, several antibodies have been generated against the HPV16 E6 protein (hereafter only referred to as E6) for therapeutic purposes including conventional antibodies, scFvs, and *Camelidae*-derived single-chain antibodies (VHHs) (Togtema et al. 2019, Zhang et al. 2021) (Figure 1).

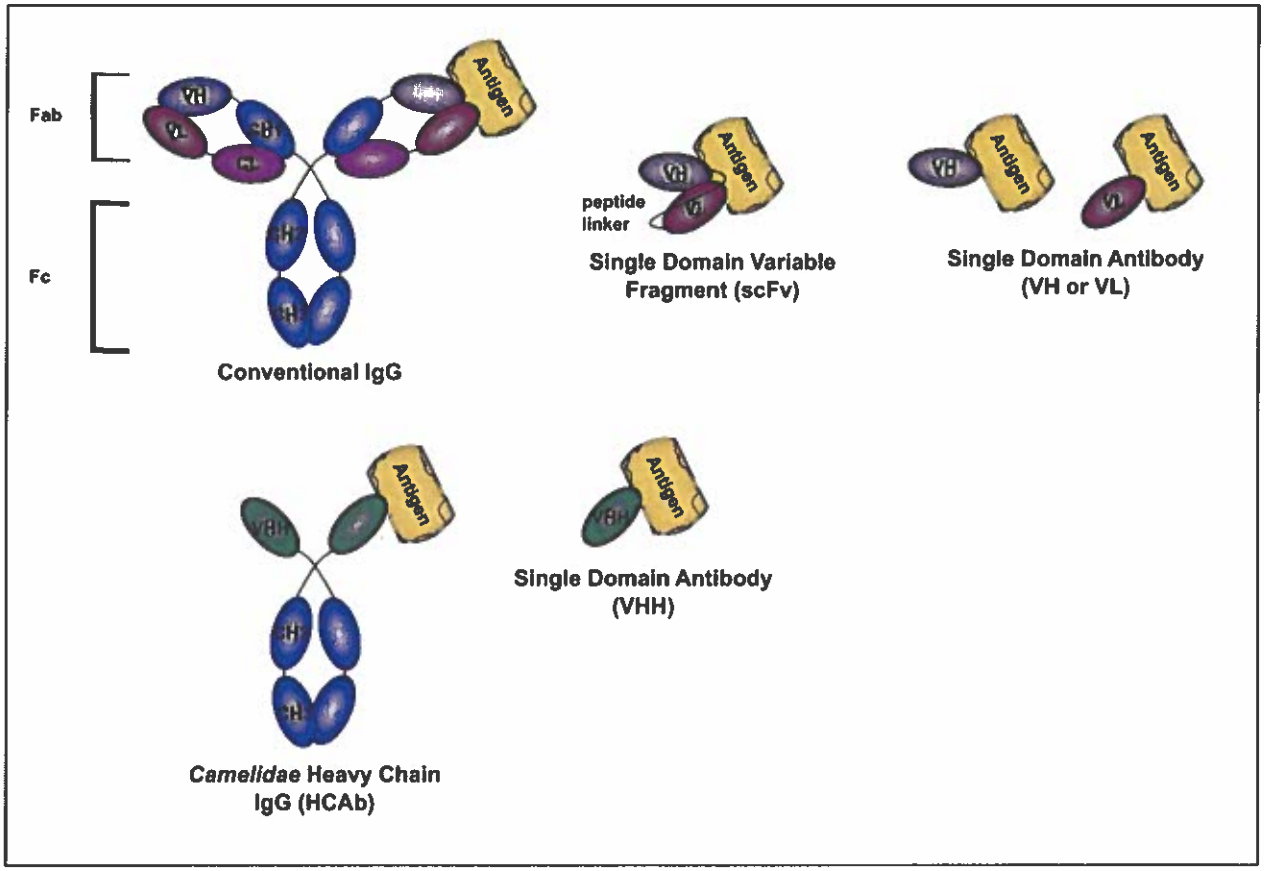

Figure 1. Schematic representation of the various types of antibodies previously developed against the HPV16 E6 protein. Images kindly provided by Dr. Melissa Togtema.

Conventional antibodies: Conventional antibodies are composed of a constant region and variable region, interacting with their antigens through the variable domain of its heavy and light chains with three complementary determining regions (CDRs) (Figure 1). Such antibodies have been very successfully used for targeting extracellular antigens, however their utilization for targeting intracellular proteins remains a challenge for researchers worldwide (Trenevska et al. 2017). In addition to the challenges associated with intracellular antibody delivery, their size (~ 150 kDa) implies that they cannot enter the nucleus by passive diffusion whereas smaller molecules such as scFv and sdAbs (~ 25 kDa) may freely enter the nucleus (Wang et al. 2007). Over the years, many conventional antibodies against the E6 protein have been reported in the literature however their translation to therapeutics and diagnostics has been notoriously challenging. As reviewed in Togtema et al. 2019, several N-terminal specific mAbs (clones 1F1, 6F4, 4C6) or zinc-binding domain-specific clones (1F5, 3B8, 3F8) of the HPV16 E6 protein have been isolated from immunized mice (Giovane et al. 1999, Masson et al. 2003, Lagrange et al. 2005, Togtema et al. 2019). During preliminary studies by both the Zehbe lab group and others, it has been demonstrated that when transiently transfected into HPV16-positive cell cultures, such mAbs showed no notable restoration of p53 protein levels leading to apoptosis (Togtema et al. 2012, Courtête et al. 2007, Togtema 2019).

The Zehbe lab evaluated the therapeutic potential of the 4C6 antibody alongside the F127-6G6 antibody (Togtema et al. 2012), both kind gifts from the Arbor Vita Corporation (Fremont, CA, USA). The F127-6G6 antibody was produced using Balb/c mice immunized with peptides corresponding in part to the E6 C-terminal region. After chemical transfection of CaSki and SiHa cells with 4C6 or F127-6G6, the amount of p53 positive cells was not significantly increased compared to cells transfected with the transfection reagent alone. However, cells

transfected with higher concentrations of F127-6G6 did show significant increases in the percentage of p53 positive cells compared to all controls (Togtema et al. 2012). Additionally, the p53 intensity per cell was also significantly increased under these conditions but no cytopathic effect of apoptosis was noted. On the other hand, sonoporation delivery of F127-6G6 did lead to a significant increase in the percentage of p53 positive CaSki but not SiHa cells compared to sonoporation alone. Unfortunately, the p53 intensity per cell was not significantly increased and only limited apoptotic cells were observed, indicating that the anticipated induction of apoptosis was not achieved (Togtema et al. 2012). Overall, these mAbs did elicit a notable restoration of p53 protein levels (Togetema at al. 2012, Courtête et al. 2007), and it is interesting to note that conjugating the mAbs to a nuclear localization signal (NLS) was able to improve their ability to access E6's mainly nuclear location, further enhancing this response (Freund et al. 2013, Postupalenko et al. 2014).

Single-chain fragment antibodies: Single-chain fragment antibodies, or scFvs are composed of the variable domain of the heavy and light chains of conventional antibodies with two variable regions held together via a peptide linker of variable length. Such scFvs are delivered to cells as cDNA for intracellular antibody expression and can therefore also be referred to as intrabodies (Figure 1). However, the reducing environment of the cytoplasm can interfere with the formation of the disulphide bonds linking their CDRs, leading to the formation of non-functional, aggregated intrabodies (Kang and Seong 2020). Bacterial expression of soluble scFvs for therapeutic purposes has also proved to be challenging due to the tendency of scFvs to form insoluble fractions in the inclusions bodies (Sarker et al. 2019). Several scFvs have been developed using the variable domains of previously mentioned monoclonal antibodies (scFv1F1, scFv6F4), through mixing the heavy and light chain variable domains of such

monoclonal antibodies (6F4 and 1F1 to scFv1F4 and scFv6F1, Giovane et al. 1999, Sibler et al. 2003), and with solubility enhancement random mutations (1F4-P41L, Lagrange et al. 2007). Additional scFvs against HPV16 E6 in the literature include GTE6-1 scFv which binds the N-terminal ZBD of E6 (Griffin et al. 2006), and I7 later modified with a nuclear localization signal to become I7nuc (Amici et al. 2016). Although scFvs are better suited for expression inside mammalian cells as intrabodies as well as by passive nuclear diffusion, their non-specific effect in HPV-negative cells as well as unexpected downstream cellular responses often observed (Lagrange et al. 2007, Amici et al. 2016) indicate that much research is still needed for their translation to a clinical setting.

Camelidae-derived single-domain antibodies: Members of the *Camelidae* family naturally express heavy chain only antibodies lacking the light chain found in conventional antibodies. The variable domain of these antibodies can be expressed as VHHs retaining the full antigen-binding capacity of the parent molecules (Figure 1). As VHHs are smaller (~15 kDa) and more soluble than scFvs, and the disulphide bridges linking the scFv's CDRs are less commonly found in VHHs, this facilitates their soluble expression in bacteria or mammalian cells (Harmsen et al. 2000, Soetens et al. 2020). Similar to scFvs, companies such as Hybrigenics, have created libraries of synthetic VHHs using a randomized mutation within the CDR regions of VHHs. In a previous study, the Zehbe lab group has generated several VHHs by immunizing two llamas with different recombinant E6 proteins (Togtema et al. 2019), the production of which will be discussed in section 1.3. Even more recently, a new anti-E6 VHH was developed by Zhang et al. (2021) through Bactrian camel immunization with a sumoylated (SUMO)-tagged E6 protein and the selection of E6 binders performed using a bacterially expressed His-tag E6 protein. Candidate VHHs were sequenced and the VHH corresponding to the most frequently identified

sequence (named Nb9) was further investigated. Nb9 was found to bind the denatured E6 protein indicating that the VHH recognizes a linear epitope, shown using a bacterially expressed E6 protein in Western blot probed using the Nb9 antibody. Immunolocalisation of E6 using Nb9 showed mainly nucelar detection of E6 as expected, however intracellular expression of Nb9 in CaSki and SiHa cells lead to the sequestration of the E6 protein into the cytoplasm, losing its common nuclear localization (Zhang et al. 2021). Intracellular expression of Nb9 also led to increased p53 and p21 levels as observed by Western blot although no quantification was performed. Finally, CaSki and SiHa cells transfected with Nb9 for intracellular expression had reduced proliferation while AnnexinV-PE/7-AAD staining of the cells showed increased apoptosis rates compared to untransfected controls cell lines (Zhang et al. 2021).

Interestingly, a humanized VHH, Caplacizumab (Cablivi™) has been approved in Europe and in the USA for the treatment of acquired thrombotic thrombocytopenic purpura (Sanofi Press Release 2019). As new therapeutic applications for VHHs continue to be identified, and with the antibody-based therapy market undergoing explosive growth, expected to reach $300 billion US in 2025 (Lu et al. 2020), it can be anticipated that more investment in the development of new anti-E6 antibodies or the optimization of existing molecules will occur in the upcoming decade.

1.3 Previous Production of *Camelidae*-derived Single-domain Antibodies in the Zehbe Lab

In a previous study, the Zehbe lab group generated several VHHs by immunizing two llamas with different recombinant E6 proteins (Togtema et al. 2019). The first llama was immunized with the His6-GenScript E6 (His6-E6) that corresponds to the cervical carcinoma-derived HPV16-positive cell line CaSki with the following amino acid substitutions: R10G and L83V compared to the reference sequence (GenBank Accession #: K02718.1, Meissner 1999,

Pattillo et al. 1977, Zehbe et al. 2009) (Figure 2). The second llama was immunized with two recombinant E6 proteins expressed from plasmids kindly provided to us by Dr. Gilles Travé. These proteins have a maltose-binding protein (MBP) tag to enhance solubility proprieties and are denoted as His6MBP-4C/4S E6 (4C/4S) and His6MBP-F47R 4C/4S E6 (F47R). Both MBP-E6 proteins have a hexahistidine (His6) and MBP tag. The 4C/4S E6 protein contains the following mutations: C80S, C97S, C111S, C140S and the F47R E6 protein contains F47R, C80S, C97S, C111S, C140S mutations (Figure 2).

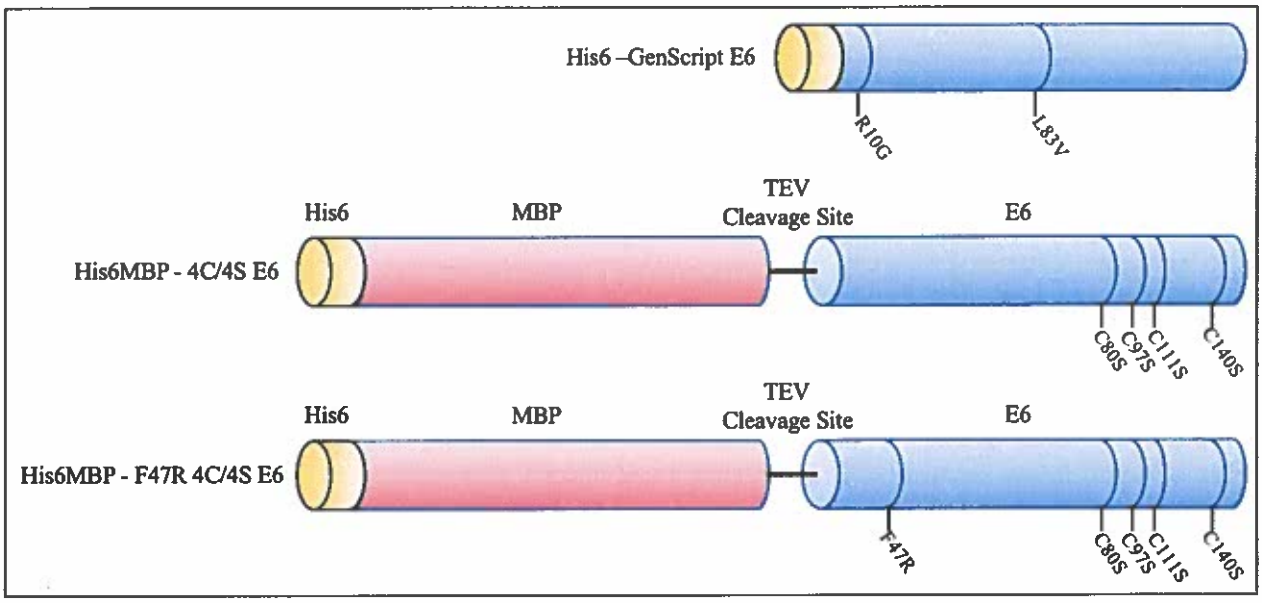

Figure 2. Recombinant E6 proteins used to produce anti-E6 single-domain antibodies. His6-GenScript E6 (His6-E6) corresponds to the cervical carcinoma-derived HPV16-positive cell line CaSki with the amino acid substitutions R10G and L83V compared to the reference sequence. Both His6MBP-4C/4S E6 (4C/4S) and His6MBP-F47R 4C/4S E6 (F47R) have a hexahistidine (His6) and MBP tag. 4C/4S contains the following mutations: C80S, C97S, C111S, C140S and F47R contains F47R, C80S, C97S, C111S, C140S mutations. Image adapted from Togtema et al. 2019, Figure 1.

Blood samples from both llamas were collected post-immunization and tested in ELISA to screen for anti-E6 VHHs. Blood samples were added to wells coated with His6-E6 or MBP-E6 proteins, followed by a secondary antibody recognizing the llama VHHs to detect antibodies binding to the recombinant E6 proteins. From these wells, lymphocytes were collected to form two VHH phage libraries, one for each llama immunization. In both libraries, DNA coding for the VHHs was inserted into phages which then expressed the given VHH on their surface. Two rounds of subtractive panning were used to remove the MBP binders, enriching the E6-binding VHH pool. Briefly, phages were incubated with the MBP protein to separate the MBP-binding VHHs from the rest of the pool. Next, the rest of the phage library was exposed to MBP-E6 proteins, to again separate the non-MBP-E6 binders from the VHHs of interest. In the second round, the same process was used but with increased amounts of MBP and decreased MBP-E6 proteins to increase the specificity of the selected VHHs. The VHH DNA from the selected phages was then subcloned into *E. coli* bacteria due to their ability to be produced quickly, easily, and abundantly in bacteria (Togtema et al. 2019).

Altogether, 18 VHHs were obtained: 15 from the llama immunized with the His6-E6, and 3 from the llama immunized with the additional recombinant E6 proteins (Togtema et al. 2019). To further evaluate their activity, they were analyzed using soluble ELISA against recombinant E6 proteins followed by characterization using western blotting under denaturing and native conditions. Under denaturing conditions, none of the VHHs were detectable, however, using Western blot under native conditions, it was observed that C26 reacts with 4C/4S, F47R, and MBP while 2A17 reacted only with 4C/4S and F47R. From this point, a subset of VHHs was further analyzed using surface plasmon resonance to determine their binding affinity to 4C/4S and F47R, the results of which showed that 2A17 had the highest binding affinity to the target

protein. Altogether, the data obtained indicated that 17 VHHs bind preferentially to the folded 4C/4S and F47R proteins while C26 binds a linear epitope in the MBP protein. As of 2019, 2A17 was the most attractive anti-E6 VHH as it was successful in all experiments performed, and C26 was a successful MBP binding control (Togtema et al. 2019).

1.4 Previous dot blot results

As previously mentioned, Togtema et al. 2019 performed several experiments using MBP, 4C/4S, and F47R to further characterize the VHHs. In particular, using dot blot experiments, it was determined that 17 VHHs bind preferentially to 4C/4S and F47R while C26 binds the recombinant E6 proteins and MBP, suggesting that C26 was an MBP binder. The dot blot results also indicated that the 2A17 was the strongest 4C/4S and F47R binder, which was further confirmed using surface plasmon resonance. The next step was to then confirm the binding of the VHHs to the endogenous E6 protein. Several preliminary co-immunoprecipitation (co-IP) experiments were performed using CaSki cell lysate and 2A17 under different conditions, however, 2A17 failed to capture the native E6. Due to this surprising result, we decided to re-evaluate the VHHs in new dot blot experiments (Figure 3), however with two key changes. Compared to previous experiments (Togtema et al. 2019), our improved dot blots used a secondary antibody specific to the VHH rather than a secondary antibody detecting the VHH's HA tag. More importantly, in addition to the MBP, 4C/4S, and F47R proteins, we spotted a recombinant E6 protein without any tags but with 6 cysteine to serine substitutions (E6 6C/6S). Although we had previously shown which VHHs can bind recombinant E6 proteins with an MBP tag (Togtema et al. 2019), it was crucial to verify that each VHH can bind an E6 protein lacking the MBP tag, as the endogenous E6 protein expressed in HPV16 infected cells does not

exist naturally with a tag of any kind. Although dot blots are qualitative rather than quantitative, the relative intensity of each dot is indicative of E6 binding by our VHHs.

As expected, some VHHs reacted similarly to 4C/4S, F47R, and E6 6C/6S while not binding to MBP alone (Figure 3), including A05, A37, A45, A46, A47, C38, 2A03, 2A04 and 2A78. The VHHs C11, 2A12, and 2A15 also reacted to the 3 recombinant E6 proteins, however, the signal detected was extremely low and only observed at higher exposures. Other VHHs showed more disparity in their binding capacity to the different E6 proteins, such as C36 which bound strongly to both 4C/4S and F47R but had a very low affinity to E6 6C/6S (Figure 3). Although A34 and 2A51 bound 4C/4S and F47R in previous dot blot experiments (Togtema et al. 2019), they did not react with any of the proteins in the current dot blot (Figure 3), indicating that a higher concentration of A34 and 2A51 could be needed to detect the recombinant E6 protein. It is also possible that the secondary anti-VHH antibody used to detect our VHHs in the current dot blot was not efficient at detecting A34 or 2A51, however due to the amout of positive E6-binders observed, we did not explore either hypothesis for these particular VHHs.

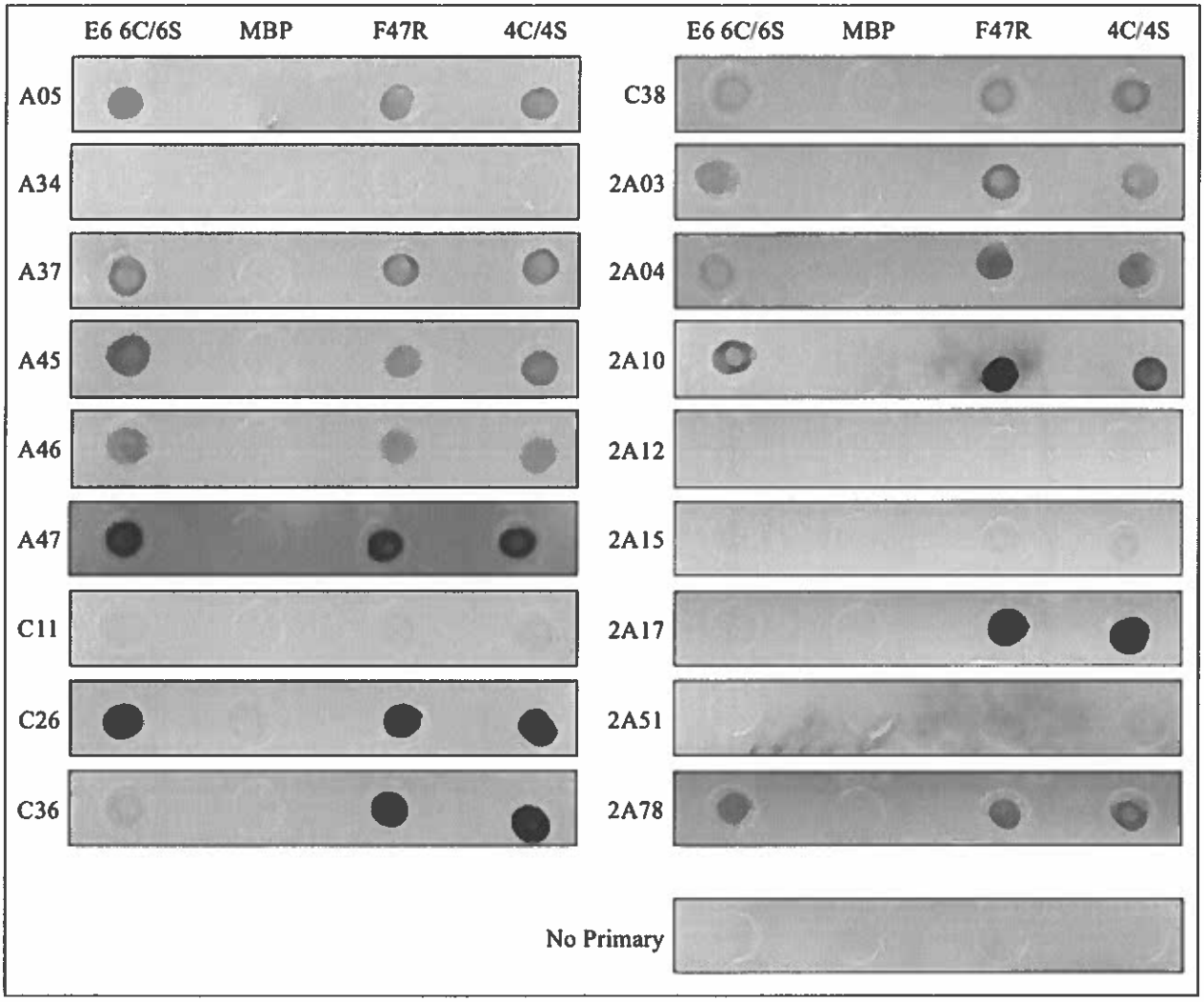

Figure 3. Dot blot results for previously developed anti-E6 VHHs. Each spot contains 4 µL of the respective recombinant E6, E6-MBP, or MBP protein at a concentration of 0.5 µg/µl. Membranes were incubated overnight in a 5 mL blocking solution containing 5.4 µg/µL of the respective VHH, followed by a secondary antibody incubation with MonoRabTM: Rabbit Anti-Camelid VHH Antibody [HRP] in blocking solution overnight. Membranes were visualized through chemiluminescence, UVP™ Gel Imaging System, and VisionWorks software.

Some of the most interesting results were revealed for 2A17 and C26. Based on previous dot blots experiments (Togtema et al. 2019), 2A17 was considered an interesting candidate, however failed at immunoprecipitating the endogenous E6 protein in pre-liminary co-IP experiments. In the current dot-blot, 2A17 reacts strongly with 4C/4S and F47R, but reacts extremely weakly with E6 6C/6S and the MBP protein alone (Figure 3). Additionally, 2A17's detection of E6 6C/6S and MBP was visible only at a higher exposure. Although 2A17 originates from a llama immunized with CaSki E6 without an MBP tag, the antibody selection was performed using ELISA and the recombinant MBP tagged E6 proteins (Togtema et al. 2019). These new results indicate that the 2A17 epitope is likely composed of a fragment of both MBP and E6, but fails to interact with each protein independently.

The results obtained with C26 were also interesting, as C26 was raised against the 4C/4S E6 and F47R proteins, with previous experiments (dot blot, Western blot under denaturing and native condition, SPR) leading to the conclusion that C26 is an MBP binder (Togtema et al. 2019). However, in the current dot blot with the addition of E6 6C/6S, it appears that C26 preferentially binds the recombinant E6 proteins and has almost no interaction with MBP alone (Figure 3). Interestingly, previous ELISA performed using 4C/4S, F47R, and MBP alone also suggested an increased binding affinity to the recombinant E6 protein compared to MBP (about 10 fold). Taken together, these results lead to an interesting hypothesis. As mentioned previously, VHHs contain 3 CDRs involved in antigen interaction, however, 30% of the VHH paratope is composed of only one or two CDRs while this is the case for only 10% of conventional antibodies (Mitchell and Colwell 2018). Additionally, the CDR3 is the main region in VHH affinity and specificity to their target. Considering the loop containing CDR3 is also longer, CDR3 is the antibody region involved in the binding of a folded epitope (Mitchell and

Colwell 2018). As C26 does not react with CaSki E6 in Western blot under denaturing conditions but does react with recombinant MBP-E6 and the MBP protein (Togetema et al. 2019), we speculate that C26 interacts with each protein using different CDRs. In addition, we believe that C26 binds a folded epitope with higher affinity via CDR3 (and potentially another between CDR 1 or 2) and binds a linear MBP epitope via CDR1, 2, or both.

1.5 Delivery Strategies

As the primary barrier between the cytoplasm of the cell and the extracellular environment, the plasma membrane prevents both diffusions of intracellular molecules out of the cell and spontaneous uptake of large external molecules making it a fundamental obstruction to macromolecule delivery in vivo. Over the years, many methods have been explored to overcome this blockade and deliver both proteins (i.e., antibodies, VHHs), and genetic material (i.e., DNA, RNA) into targeted cells. To deliver conventional antibodies, many researchers have explored transfection, cell-penetrating peptides, fragments of bacterial toxins, lipid-based molecules, along with physical methods such as electroporation and microinjection (Slastnikova et al. 2018). In relation to VHHs, methods range from those requiring transient physical disruption of the cell membrane including micro-injection, electroporation, and nanoparticle-based photoporation, those manipulating electrostatic interaction with the cell surface including cell-penetrating peptides and polycationic resurfacing, and expression-based methods including mRNA delivery, DNA transfection, and viral transduction (Soetens et al. 2020).

Common laboratory techniques allowing large therapeutic antibodies to cross the cell membrane such as chemical transfection are an easy solution in vitro, however, their cytotoxic nature and potential to cause unwanted side effects limits their use for in vivo and clinical

environments (Zhao et al. 2003, Rui et al. 2002, Togtema et al. 2012). Chemical transfection is commonly used for in vitro cell studies, causing pores in the membrane of living cells allowing small molecules like our own to enter. The HiPerFect transfection reagent is one of many cationic lipid-based transfection reagents originally designed for RNA/DNA delivery, although it has been further adapted for the delivery of mouse monoclonal antibodies against the E6 protein (Courtête 2007, Togtema et al. 2012). However, for efficient protein delivery using HiPerFect, the protein must contain a sequence of anionic residues to interact with the cationic lipids, allowing the transfection to occur. Previous research in the Zehbe lab has used HiPerFect to deliver two mouse monoclonal antibodies to CaSki and SiHa cells (Togtema et al. 2012), evaluating their ability to reactivate p53 expression in the infected cells. However, as previously discussed, although the p53 intensity per cell was significantly increased under some conditions, no cytopathic effect of apoptosis was noted (Togtema et al. 2012). It was concluded that chemical transfection was not the optimal method for antibody delivery to cells in our case, however, it was a functional baseline for comparison between different methods of delivery. Alternatively, it was shown using a tubulin antibody, that sonoporation may be a more efficient antibody delivery approach (Togtema et al. 2012).

In recent years, high-intensity focusing ultrasound (HIFU) has emerged as an accurate and non-invasive method for the treatment of some cancers. During this process, an ultrasound beam focusing on a specific location results in irradiation with high-intensity energy, leading to transiently increased permeability of cellular membranes. Such a technique can be used alone or in combination with numerous therapeutic agents including anti-cancer drugs, liposomes, siRNA, and microbubbles (Han et al. 2017). When used in combination with microbubbles, the process is known as sonoporation which has been reportedly used for ultrasound delivery of

dextrans, calcein, plasmid DNA, siRNA, and antibodies, summarized in Togtema et al. 2012, Table 1. Due to both the temperature and mechanistic effects of the HIFU treatment, a significant amount of the delivered nanoparticle will be extravasated from the blood vessels in the surrounding areas, accumulating in the tumour site (Han et al. 2017). To this end, sonoporation delivery is more well suited for clinical application and therapeutic delivery. In the same Togtema et al. 2012 paper mentioned previously, the F127-6G6 antibody was evaluated using sonoporation delivery to CaSki or SiHa cells as well. It was found that sonoporation of F127-6G6 did lead to a significant increase in the percentage of p53 positive CaSki cells compared to sonoporation alone, although the p53 intensity per cell was not significantly increased and only limited apoptotic cells were observed (Togtema et al. 2012).

1.6 Research Rationale

To date, there is no commercially available antibody which can specfically target the E6 protein of HPV16 in either a laboratory or clinical setting. To further explore this crucial oncoprotein in the development of HPV16-related cancers, a molecule targeting E6 would be invalubable to both research and clincial staff alike. Due to E6's mainly nuclear location and the challenges associated with intracellular antibody delivery of traditional monoclonal antibodies (~150 kDa) (Wang et al. 2007), it is clear that novel molecules derived from unconventional sources are needed. Members of the *Camelidae* family naturally express heavy chain only antibodies, of which the variable domain can be expressed as a VHH. Such VHHs retain the full antigen-binding capacity of the parent molecules, while being smaller (~15 kDa) and more soluble compared to other alternative forms (monoclonal anitbodies, scFvs) (Harmsen et al. 2000, Soetens et al. 2020). Our lab has previously generated several anti- E6 VHHs and

identified various candidates with recombinant E6-MBP and E6 binding ability (Togtema et al. 2019) (Figure 3). However, in vivo, the E6 protein does not exist with any tags or solubility-enhancing amino acid substituitions. It is therefore key to identify VHHs with the ability to bind the endogenous E6 protein, allowing for its use in detection, identification, and potential therapeutic intervention when dealing with HPV16-related cancers. In addition, in order to explore our VHHs ability to interact with the E6 protein in vitro, they must be able to be succesfully delivered intracelluarly. Once delivered, if they are to be used as therapeutics, they must exert an effect on target cell lines expressing the E6 protein, including interactions with known interactors of E6 (p53) leading to apoptosis of infected cells, identified by early markers of apoptosis such as cleavage of poly (ADP ribose) polymerase (PARP-1).

1.7 Hypotheses

Based on previous dot blot results (Togtema et al. 2019) (Figure 3) we hypothesize that some of our VHHs will have the ability to bind and immunoprecipitate E6 from CaSki cells. In addition, we hypothesize that of the VHHs able to successfully bind endogenous E6, some will be successfully delivered to CaSki, SiHa, and C33A cell lines efficiently. Finally, we hypothesize that these delivered VHHs will increase p53 expression in targeted cells, and show signs of apoptosis through PARP-1 cleavage.

1.8 Research Aims

1. Use co-immunoprecipitation experiments to identify VHHs capable of binding the endogenous E6 protein in an HPV16 positive cell line (CaSki).

2. Optimize our co-immunoprecipitation protocol for both acidic (isoelectric point below 7.0) and basic (isoelectric point below 7.0) VHHs.
3. Use in vitro transfection methods to deliver our VHHs into CaSki, SiHa, and C33A cell lines.
4. Quantify the effects of our VHHs on CaSki, SiHa, and C33A cell lines using CCK8 proliferation assays.
5. At a cellular level, observe the effects of our VHHs on known interactors of E6, such as p53, and known markers of apoptosis, such as PARP-1 cleavage using immunoflourensence microscopy and immunodetection.

2 MATERIALS AND METHODS

2.1 Cell Culture

2.1.1 Cell Lines and Routine Maintenance

All mammalian cell cultures were cultured in T-75 flasks (75 cm2, Fisher, Cat. # 1368065) and maintained in a 5% CO_2, 37°C humidified incubator. CaSki (ATCC CRL-1550), SiHa (ATCC HTB-35), and C33A (ATCC HTB-31) were used for *in vitro* experiments. The HPV16-positive cell line, CaSki and SiHa were used as an HPV16 E6 positive control while C33A, an HPV negative cervical carcinoma cell line, was used as an HPV16 E6 negative control. The culture medium was changed every second day and routine verification of mycoplasma contamination was done once a month. The working area was decontaminated with 70% ethanol before and after use and cell culture work was performed under sterile conditions. CaSki and C33A were maintained in Dulbecco's modified eagle's medium (DMEM, Fisher Scientific, Cat. # SH3024301) supplemented with 10% FBS (Fisher Scientific, Cat. #SH3039603) and 1% antibiotic/antimycotic (Fisher Scientific, Cat. #SV3007901). Cells were passaged when they reached 70%-80% confluency. Cells were sub-cultured 2 times per week and 3-5 x 10^5 cells were reseeded. For subculture, cells were harvested using 3 mL of trypsin (Trypsin, Fisher Sci., Cat# SH3023602). Cells were incubated for 10 min in a 37°C humidified incubator. Detached cells were collected, and the trypsin solution was neutralized using DMEM (3 mL per mL of trypsin). Cells were centrifuged at 350 x g for 5 minutes to collect cell pellets. The supernatant was aspirated, and cells were then resuspended in a fresh medium. For cell culture, cells (3-5 x 10^5) were reseeded in a new T-75 flask, while the rest of the cells were centrifuged as before. Media was removed, and the cells were washed using 5 mL DPBS (HyClone, Cat # SH300028.02). After centrifugation, the

cells were resuspended in 1 mL DPBS and transferred into a microcentrifuge tube. Cells were pelleted as before, DBPS was removed, and the pelleted cells were stored in a -80°C freezer.

2.1.2 Cryogenic Cell Storage

To preserve stocks of cells, freeze back stocks were made and preserved in liquid nitrogen. Cells were trypsinized, followed by centrifugation at 350 x g for 5 minutes to remove the neutralizing solution. Cell pellets were then resuspended in a freezing medium. The freezing medium consisted of 90% culture medium and 10% dimethyl sulfoxide cryopreservative (DMSO; Sigma-Aldrich-Aldrich, Cat. # 34869). Aliquots of 1 mL were placed in 1.5 mL cryogenic vials (Nalgene, Fisher, Cat. # 03-337-7Y). The cryogenic vials were kept in a controlled rate freezing container (Nalgene, Fisher, Cat. # 5100-0001) filled with isopropanol at -80°C overnight and were then transferred into liquid nitrogen for long-term storage.

2.1.3 Thawing Cells

To bring up cells from cryogenic storage, the cryogenic vial was removed from the liquid nitrogen and immediately thawed in a 37°C bath. The contents of the cryogenic vial were added directly to the T75 cell culture flask containing 10 mL of culture medium to dilute the concentration of DMSO to non-toxic levels for the cells. The culture medium was changed the following morning after the cells had adhered to remove any traces of DMSO.

2.2 Dot Blot for VHH Selection

2.2.1 Recombinant Proteins

Due to intrinsic proprieties, the E6 protein is poorly soluble when expressed in bacteria. Therefore, different recombinant E6 proteins with increased solubility proprieties were used in these experiments. The E6 6C/6S protein (R&D Systems Inc., Cat# AP-120-025) contains six cysteine to serine substitutions (positions 23, 58, 87, 104, 118, 147) compared to the reference protein sequence (UniprotDB Q547J2). The 4C/4S protein contains an N-terminal hexahistidine (His6)-maltose-binding protein (MBP) tag and lacks 7 N-terminal residues found in Q547J2. The protein also has four cysteine to serine substitutions (position 80, 97, 111 and 140 equivalent to E6 6C6S substitutions at position 87, 104, 118, 147). The F47R protein has the same modifications as 4C/4S with an additional phenylalanine to arginine substitution at position 47. Note that 4C/4S and F47R were previously produced (Togtema et al. 2019) using expression plasmids kindly provided to us by Dr. Gilles Travé. Finally, the MBP protein (Abnova, Cat. # P4989) was used to identify VHHs interacting with the MBP tag.

2.2.2 Dot blot

For the dot blot, 2 µg of E6 6C/6S (0.5 µg/µL), MBP (1 µg/µL), F47R (stock concentration 1.23 µg/µL), and 4C4S (stock concentration 1.05 µg/µL) diluted in 4 µL PBS were spotted on a 0.45 µm nitrocellulose membrane (BioRad, Cat. # 162-0116) and allowed to dry at room temperature for 1 hour. Once dry, each membrane was incubated in blocking solution for 1 hour at room temperature on a tube twirler (Labnet Mini Labroller™). The blocking solution consisted of 10 mL TBST 0.01% and 0.5 g instant skim milk powder (Safeway Brand). The TBST 0.01% consisted of 100 mL 10X TBS and 0.1 mL Tween® 20 (Fisher, Cat. # BP337-500) made up to 1L

in distilled H_2O. The 10X TBS consisted of 30.3 g Tris Base (Fisher, Cat. # BP152-1) and 87.6 g of NaCl sodium chloride (NaCl, Fisher, Cat. # S271-3) made up to 1L in distilled H_2O and pH adjusted to 7.5. Following blocking, membranes were cut and divided into respective 50 mL Falcon tubes containing primary antibody solution. The primary antibody solutions consisted of 5 mL TBST 0.01% and 5.4 μg/μL of the respective VHH. Membranes in primary antibody solution were incubated overnight at 4°C on a tube twirler. After incubation, membranes were washed three times 5 minutes with 5 mL of TBST 0.01%. Following washes, membranes were incubated in secondary antibody solution overnight at 4°C on a tube twirler. The secondary antibody solution consisted of 1 μL MonoRabTM: Rabbit Anti-Camelid VHH Antibody [HRP], mAb (GenScript Cat No. A01861-200) in 5 mL of blocking solution. Following incubation, membranes were washed three times for 5 minutes with 5 mL of TBST 0.01%. Once washed, a chemiluminescent solution (Clarity™ Western ECL Substrate, BioRad, Cat. # 170-5061) was applied, and membranes were visualized using a UVP™ Gel Imaging System and VisionWorks software.

2.3 Western Blot for Recombinant E6 Proteins

The Precision Plus Protein™ Dual Color Standards (BioRad, Cat #1610374) was used as the protein ladder. All samples were thawed, pulse centrifuged, and combined with 6X sodium dodecyl sulfate (SDS) loading dye with 6.66M Dithiothreitol (DTT, Fisher, Cat. # BP172-25) for a final concentration of 1X SDS. The 6X SDS consisted of 2.5 mL 1.5 M Tris Base, 1 g SDS (Sigma, Cat. # L4390), 5 mL glycerol and 0.03 g bromophenol blue (Fisher Sci., Cat# FLB3925). The samples were heated to 95°C for 10 minutes to denature the protein, pulse centrifuged and stored at -80°C until Western Blot analyses. For Western Blot analyses, samples were removed from -80°C storage and boiled at 95°C for 10 minutes before being loaded into precast gels (Mini-

PROTEAN® TGX™ Precast Protein Gels, BioRad, Cat #4561094, 4561096). Gels were run in 4°C 1X running buffer (100 mL 10X running buffer and 900 mL dH_2O) at 120V for 75 minutes. The 10X running buffer consisted of 144 g glycine (Fisher, Cat# BP381-5), 30.3 g Tris Base, and 5 g SDS (Sigma, Cat# L4390) made up to 1L in dH_2O. After the run, the proteins were transferred to a PVDF membrane (Fisher, Cat. # PI88518) which had been activated by soaking in methanol (Fisher, Cat. # A454-1) for 15 minutes. The transfer was done at 100V, 0.35A for 60 minutes in chilled 1X transfer buffer (100 mL 10X transfer buffer, 200 mL methanol, and 700 mL dH_2O) with an ice pack and a stir bar in the container to keep the temperature cool. The 10X transfer buffer consisted of 144 g glycine, and 30.3 g Tris Base made up to 1L in dH_2O. Following the transfer, membranes were incubated with 5% skim milk powder in TBST 0.05% for 1 hour at room temperature on a tube twirler. The TBST 0.05% consisted of 100 mL 10X TBS and 0.5 mL Tween® 20 made up to 1L in distilled H_2O. Following blocking, membranes were incubated in primary antibody solution overnight at 4°C on a tube twirler. The primary antibody solutions consisted of 5% skim milk powder in TBST 0.05% with respective primary antibodies (Anti-E6 6F4, Stock Concentration: 2.69 µg/mL, kind gift from Arbor Vita Corporation; C26, Stock Concentration: 2.69 µg/mL). Following overnight incubation, membranes were washed for 5 minutes on a tube twirler with 5 mL of TBST 0.05% for a total of 3 washes. Once washed, membranes were incubated in secondary antibody solution (HRP-Anti Mouse, 1:1000, Jackson Immunoresearch Laboratories Inc., Cat# 115-035-062; Anti-HA-HRP, 1:5000, Rat mAb [3F10], Roche, Cat# 12013819001) for 1 hour at room temperature on a tube twirler. Membranes were washed for 5 minutes on a tube twirler with 5 mL of TBST 0.05% for a total of 3 washes. Once washed, the chemiluminescent solution was applied, and membranes were visualized using a UVP™ Gel Imaging System and VisionWorks software.

2.4 Co-immunoprecipitation of E6 by Single-domain Antibodies

2.4.1 Binding Single-domain Antibodies to Affi-Gel Resin

Affi-Gel resin (BioRad, Cat. #1536099 (Affi-Gel 10), Cat. # 1536051 (Affi-Gel-15) was aliquoted (12.5 uL resin per column) and resuspended using HPLC-grade distilled water (Fisher Chemical, Cat. # W5-4). Affi-Gel resin was divided equally into Pierce™ Spin Columns (Fisher, Cat. # PI69725). Unless otherwise specified, centrifugation was performed at 1000 x g, 4°C, for 30 seconds. Columns were centrifuged (Eppendorf, Centrifuge 5417R) to discard flow-through. The resin was resuspended using 500 µL of HPLC-grade distilled water, incubated for five minutes at 4°C on a tube twirler, and centrifuged to discard flow-through for a total of three washes. Following washes, 250 µL of VHH dilutions or 100 mM MOPS pH 7.0 buffer was added to respective columns and incubated overnight at 4°C on a tube twirler. The 100 mM MOPS buffer consisted of 2.0926 g MOPS (Fisher, Cat. # BP308-100) diluted in 100 mL of HPLC-grade distilled water, pH adjusted to 7.0. Additionally, 10 – 20 µL of the VHH dilutions were stored at -80°C and used as the input sample for dot blot/Western blot analysis. This method of resin division will be known as Method A (Figure 4).

Alternatively, Affi-Gel resin was aliquoted (12.5 µL resin per column), resuspended using HPLC-grade distilled water, and divided into master mix columns containing enough resin for two samples (25 µL resin per tube). Master mix columns were centrifuged to discard flow-through. The resin was resuspended using 500 µL of HPLC-grade distilled water, incubated for five minutes at 4°C on a tube twirler, and centrifuged to discard flow-through for a total of three washes. Following washes, 500 µL of VHH dilutions or 250 µL of 100 mM MOPS pH 7.0 buffer was added to respective columns and incubated overnight at 4°C on a tube twirler. VHH dilutions samples were stored at -80°C as before. The following day, master mix columns were split equally

into two sample columns (one for CaSki, one for C33A) following ProteOn Ethanolamine hydrochloride pH 8 (BioRad, Cat. # 1762450) incubation (see section 2.4.5). This method of resin division will be known as Method B (Figure 4).

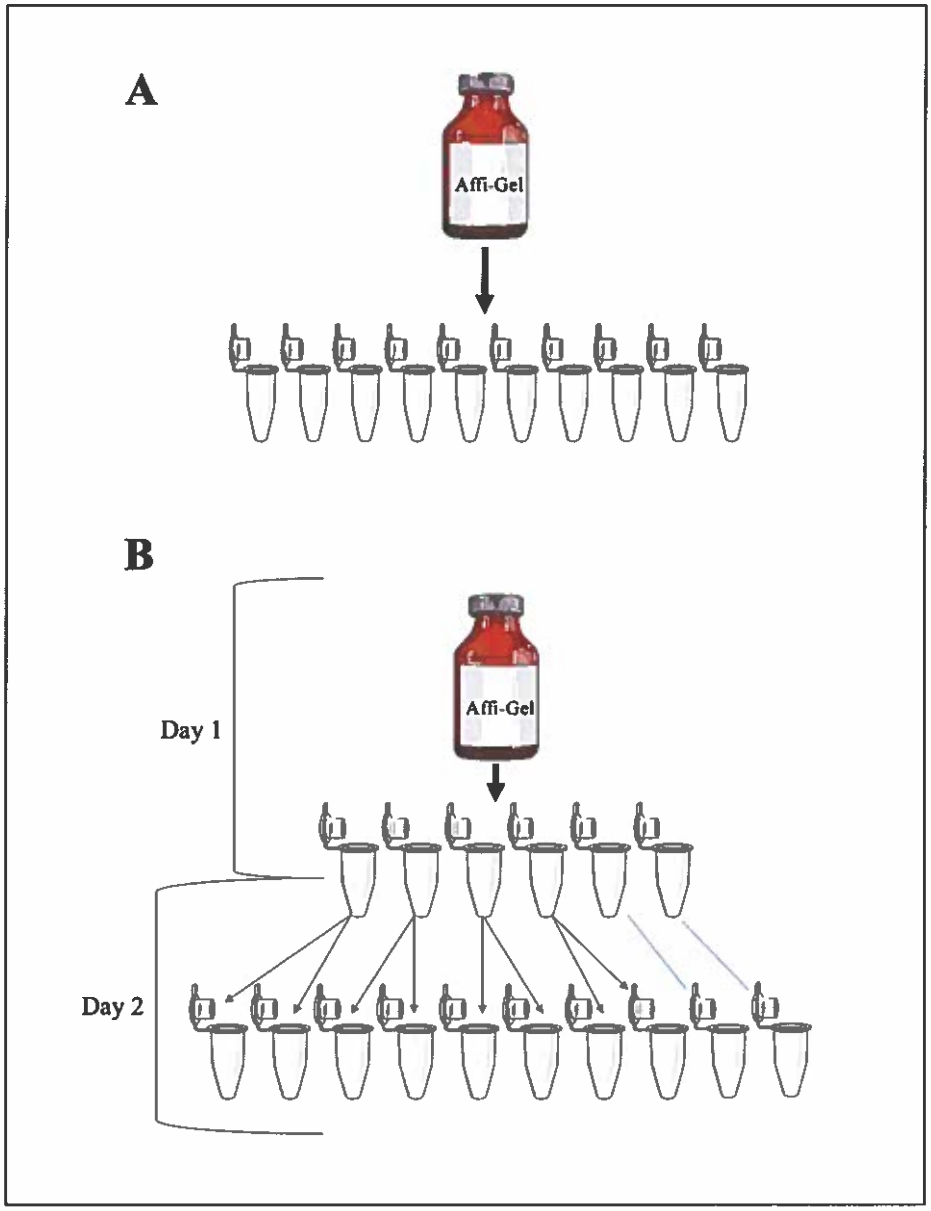

Figure 4. Resin division methods used for co-immunoprecipitation of E6 by various VHHs. Panel A: Method A Day 1 division. Affi-Gel resin is divided into all columns on the first day of the experiment. No further divisions occur during the experiment. Panel B: Method B 2-Day division. Affi-Gel resin is divided into master mix VHH columns on Day 1, and further divided into CaSki or C33A columns on Day 2 immediately before protein lysate edition. Control columns are only divided on Day 1 and carry over for the rest of the experiment.

2.4.2 Dot Blot to Confirm the Binding of the VHHs to the Resin

2 µLs of each sample were spotted on a 0.45 µm nitrocellulose membrane and allowed to dry at room temperature for 30 minutes. Once dry, the membrane was incubated in blocking solution for 30 minutes at room temperature on a tube twirler. The membrane was then incubated with a detection antibody solution consisting of 1:20 000 Anti-HA-HRP for 1 hour at room temperature on a tube twirler. The membrane was then washed with 5 mL TBST 0.05% for 5 minutes at room temperature on a tube twirler for a total of three washes. Once washed, the chemiluminescent solution was applied, and membranes were visualized using a UVP™ Gel Imaging System and VisionWorks software.

2.4.3 Cell Lysis

CaSki and C33A cell pellets were frozen at -80°C for at least 1 hour prior to lysis. Lysis buffer composed of Mammalian Protein Extraction Reagent (Fisher, Cat. # PI78501), 150 mM sodium chloride, 1X HALT™ phosphatase inhibitor cocktail (Fisher, Cat. # PI78428), 1X cOmplete EDTA free protease inhibitor (Roche, Cat. # 04 693 159 001), and 1 mM phenylmethylsulphonyl fluoride was mixed and chilled at 4°C. Each fresh pellet was resuspended with 10 µL per mg of pellet weight in chilled lysis buffer and incubated on a tube twirler for 30 minutes at 4°C. The solutions were centrifuged at 14 000 x g for 15 minutes at 4°C to remove cell debris and obtain the protein-containing supernatant.

2.4.4 Bradford Assay

The Bradford Assay was done to determine protein concentration. A 5 µL volume of bovine serum albumin (BSA, VWR Life Science, Amresco, LLC, Cat# 0332-100G) standards (1-10 µg), CaSki

or C33A cell protein lysate, or lysis buffer was mixed with 25 µL of Reagent A' and 200 µL of Reagent B (DC™ Protein Assay Reagent B, BioRad, Cat. # 500-0114). Reagent A' consisted of 500 µL Reagent A (Alkaline copper tartrate, DC™ Protein Assay Reagent A, BioRad, Cat. #500-0113) and 10 µL Reagent S (Surfactant solution, DC™ Protein Assay Reagent S BioRad, Cat. # 500-0115). The reactions were incubated at room temperature for 15 minutes and 230 µL of each mixture was transferred to a 96-well plate (Falcon, Cat. # 353072) where protein concentration was analyzed at 750 nm using a plate reader (PowerWave XS; BioTek).

2.4.5 Co-immunoprecipitation of E6

Columns were centrifuged and flow-through was collected. Columns were washed using 500 µL of 100 mM MOPS pH 7.0 buffer, incubated for five minutes at 4°C on a tube twirler, and centrifuged to discard flow-through for a total of three washes. Each column then received 200 µL of ProteOn Ethanolamine hydrochloride pH 8 and was incubated at 4°C on a tube twirler. A dot blot was used to assess VHH binding to the resin (see section 2.4.2). Freshly harvested frozen CaSki and C33A cell pellets were lysed, and protein concentration was determined using the Bradford Assay (see sections 2.4.3 and 2.4.4). Columns were centrifuged to discard flow-through and washed with 500 µL of 100 mM MOPS buffer pH 7.0 on a tube twirler for 5 minutes at 4°C for a total of three washes. Each column received 500 µg of protein lysate and was filled up to 200 µL using chilled lysis buffer and was incubated overnight at 4°C on a tube twirler.

2.4.6 SDS Elution and Western Blot

Columns were centrifuged and flow-through was collected. Columns were washed with 500 µL of lysis buffer without inhibitors containing Mammalian Protein Extraction Reagent and

150mM NaCl and incubated for five minutes at 4°C on a tube twirler. Columns were then centrifuged to discard flow-through for a total of three washes. Columns were then eluted using 30 µL of fresh 1X SDS loading dye with 6.66M DTT and were incubated on a rocker (Stoval Lifer Science Incorporated, The Belly Dancer®, US Patent #:4,702,610) for 30 minutes at room temperature. The 1X loading dye with 6.66M DTT consisted of 50 µL of 6X SDS loading dye in 300 µL of distilled water. Columns were centrifuged for 1 minute at 1000 x g at 4°C to remove resin and obtain the eluate containing supernatant. The samples were heated to 95°C for 10 minutes to denature the protein, pulse centrifuged, and stored at -80°C until Western Blot analyses. All other western blot samples were prepared as described in section 2.3. Samples were analyzed by Western Blot as described in section 2.3 with the following primary and secondary antibodies respectively; Primary (For E6: Anti-E6 6F4, 2.69 µg/mL), Secondary (For E6: HRP-Anti Mouse, 1:1000, For VHHs: Anti-HA-HRP, 1:20 000, For C26B: Anti-VHH, 1:20 000)

2.5 HiPerFect Transfection

2.5.1 24-well Plate HiPerFect Transfection

For each well, 25 000 cells (CaSki, SiHa, C33A) were seeded in a 24-well plate (Fisher Sci. Cat. # 08-772-1) and allowed to grow overnight in a 37°C incubator. Transfection complexes were prepared according to Table 1. Once prepared, tubes were vortexed and allowed to incubate for 10 minutes at room temperature. During incubation, old media was aspirated and 150 µL of incomplete DMEM (DMEM without 10% FBS or antibiotic/antimycotic) was added to each well. Once the incubation was complete, the transfection reactions were added dropwise to their respective wells, with the plate gently tilted to distribute. The plate was incubated at 37°C for 3 hours. After initial incubation, 250 µL of complete DMEM media with 20% FBS was added to

each well and the plate was returned to the incubator for the remaining 48-hours. After 48-hours, the plate was prepared for staining and analysis as described in section 2.5.2.

Table 1. HiPerFect transfection complex components. Components for experiment wells (VHH + HiP), transfection controls (Tubulin +HiP), and control wells (VHH + PBS, PBS + HiP). Note that VHH dilutions varied based on the concentration of VHH tested.

VHH + HiP	**Tubulin + HiP (Transfection Control)**	**VHH + PBS (VHH Control)**	**PBS + HiP (HiP Control)**
10µL VHH dilution 10µL HiP 80µL DMEM Free Media	10µL Tubulin dilution 10µL HiP 80µL DMEM Free Media	10µL VHH dilution 10µL PBS 80µL DMEM Free Media	10µL 1X PBS 10µL HiP 80µL DMEM Free Media

2.5.2 Immunofluorescence Assay Staining and Analysis Preparation: 24-well Plate

After 48-hours, wells were gently rinsed twice with 500 µL cold 1X PBS. The 1X PBS consisted of 100 mL of 10X PBS diluted in 900 mL dH_2O. The 10X PBS consisted of 17.8 g of sodium phosphate dibasic anhydrous ($Na_2HPO4 \bullet H_2O$, Fisher Scientific, Cat# BP332-500), 2.4 g of potassium phosphate monobasic (KH_2PO_4, Fisher Biotech, Cat# BP362-1), 80g of NaCl, and 2 g of potassium chloride (KCl, Sigma Chemical Co., Cat# P-9541), diluted in 900 mL of dH_2O and pH adjusted to 7.4. Following rinses, 500 µL of 4% paraformaldehyde in PBS (PFA-PBS) was added to each well and incubated at room temperature for 10 minutes. PFA-PBS was then removed, and the wells were washed three times with 500 µL of cold 1X PBS for 5 minutes. Once washed, 500 µL of cold 0.1% Triton X-100 solution was added to each well and incubated at room temperature for 10 minutes. The 0.1% Triton X-100 solution consisted of 50 mL of 1X PBS and 50 µL of Triton-X 100 (US Biological, T8655). Following incubation, wells were washed three times with 500 µL of cold 1X PBS for 5 minutes. After washing, 500 µL of cold 1% BSA-PBS solution was added to each well and incubated at room temperature for 30 minutes. The 1% BSA-PBS consisted of 50 mL of 1X PBS and 0.5 g of bovine serum albumin. After incubation, to detect the VHHs or tubulin respectively, 300 µL of a 1/400 dilution of Alexa Fluor 594 + (1/400, Jackson Immunoresearch Inc., Cat #: 128-585-230) or Alexa Fluor 488 Donkey anti-mouse IgG, Invitrogen by Thermo Fisher Scientific, Cat# A21202) in 1% BSA-PBS was added to their respective wells and incubated in the dark at room temperature for 1 hour. Following incubation, wells were washed three times with 500 µL of cold 1X PBS for 5 minutes, followed by one wash with 1mL of cold distilled water for 5 minutes. Finally, water was removed from the wells, and the plate was allowed to dry for ~10 minutes. Once dry, DAPI (Cedarlane Cat. # H-1200) and coverslips (Fisher Scientific, Cat# 1254581) were applied before imaging using Zeiss Axiovert 200 fluorescence

microscope (Carl Zeiss Canada Ltd., North York, Ontario, Canada) equipped with an LD A-Plan 40x/0.50 Ph2 objective (Carl Zeiss Canada Ltd.) and a CCD camera with 12-bit capability (Q Imaging, Surrey, British Columbia, Canada)

2.6 mRNA Transfection

2.6.1 mRNA Transfection in Chamber Slides

Each well of the chamber slides (Lab-Tek, Cat# 177402) was treated with 300 µL of 0.15% Poly L Lysine diluted in dH_2O to improve the cell's ability to attach and grow efficiently. Once treated, the slides were incubated in a 37°C incubator for 2 hours. After incubation, the wells were washed 3 times for 5 minutes with 300 µL of dH_2O before 24 000 (CaSki, C33A) or 12 000 (SiHa) cells were seeded in each well and allowed to grow for 48-hours in a 37°C incubator. Transfection reactions were prepared according to Mirus *Trans*-IT-mRNA Transfection Kit (Mirus, Product No. MIR 2225), following guidelines for a 48-well plate (Table 2), and incubated for 3 minutes. During incubation, the existing media was aspirated, and 300 µL of fresh complete DMEM was added to each well. After incubation, the transfection reactions were added dropwise to their respective wells, with the plate gently tilted to distribute, and incubated at 37°C for 4-hours. After 4 hours, the existing media was removed and replaced with 300 µL of fresh complete DMEM. The chambers were then incubated at 37°C for the remaining 48-hours. After 48 hours, the chamber slides were prepared as described in section 2.6.2.

Table 2. Supplier recommendation for mRNA transfections with the Mirus *Trans*IT-mRNA Transfection Kit.

Culture vessel	96-well plate	48-well plate	24-well plate	12-well plate	6-well plate	10-cm dish	T75 flask
Surface area	0.35 cm^2	1 cm^2	1.9 cm^2	3.8 cm^2	9.6 cm^2	59 cm^2	75 cm^2
Complete growth medium	92 µl	263 µl	0.5 ml	1 ml	2.5 ml	15.5 ml	19.7 ml
Serum-free medium	9 µl	26 µl	50 µl	100 µl	250 µl	1.5 ml	1.9 ml
RNA (1µg/µl stock)	0.09 µl	0.25 µl	0.5 µl	1 µl	2.5 µl	15.5 µl	19.7 µl
*Trans*IT-mRNA Reagent	0.18 µl	0.5 µl	1 µl	2 µl	5 µl	31 µl	39.4 µl
mRNA Boost Reagent	0.18 µl	0.5 µl	1 µl	2 µl	5 µl	31 µl	39.4 µl

2.6.2 Immunofluorescence Assay Staining and Analysis Preparation: Chamber Slide

After 48-hours, wells were gently rinsed once with 300 µL of cold 1X PBS before adding 300 µL of 4% PFA-PBS to each well, incubating at room temperature for 10 minutes. After incubation, the PFA-PBS was removed along with the detachable plastic chamber piece of the chamber slide, leaving behind the slide. Using a Coplin jar, slides were washed three times with cold 1X PBS for 5 minutes. Once washed, slides were incubated with cold 0.1% Triton X-100 solution for 10 minutes. Following incubation, slides were washed three times with cold 1X PBS for 5 minutes. After washing, slides were incubated with cold 1% BSA-PBS solution at room temperature for 30 minutes. After incubation, to detect the VHHs, 50 µL of 1/400 diluted Alexa Flour 594 + antibody in 1% BSA-PBS was added to each spot and incubated in the dark at room temperature for 1 hour. Following incubation, slides were washed three times with cold 1X PBS for 5 minutes, followed by one wash with cold distilled water for 5 minutes. Finally, slides were allowed to dry for 10-minutes and once dry, DAPI and coverslips (BIPEE, Product Code: X000Y42UNX) were applied before imaging using Zeiss Axiovert 200 fluorescence microscope and a CCD camera.

2.6.3 Co-Staining with p53 and PARP-1

Cells were transfected in chamber slides as outlined in section 2.6.1 and prepared for staining and analysis as outlined in section 2.6.2 with the following changes. After the 30 minute incubation with 1% BSA-PBS, p53 and PARP-1 cleavage were probed using 50 µL of the following primary antibodies diluted in 1% BSA-PBS: p53 Monoclonal Antibody [DO1] (1/400, Invitrogen by Thermo Fisher Scientific, Stock Concentration: 0.2 mg/mL, Cat # AH00152), Mouse mAb to cleaved PARP [4B5BD2] (1/760, Abcam, Stock Concentration: 0.76 mg/mL, Cat #

ab110315); slides were incubated overnight in the dark at 4°C. Following incubation, slides were rinsed once and washed three times with cold 1X PBS for 5 minutes. After washing, 50 µL of secondary antibody diluted in 1% BSA-PBS was added to their respective spots and used to detect the following: VHHs (1/400, Alexa Flour 594 +), p53 and PARP-1 cleavage (1/400, Alexa Fluor 488 Donkey anti-mouse IgG). Slides were incubated in the dark at room temperature for 1 hour and finished according to section 2.6.2.

2.6.4 Actinomycin D Treatment

After seeding as outlined in section 2.6.1, cells (CaSki, SiHa, C33A) were allowed to grow for 24-hours. After 24-hours, existing media was aspirated and replaced with Actinomycin D treatment solution. Actinomycin D is a known apoptosis inducer as it damages cell's DNA, leading to cancer cell death. CaSki cells were treated with a solution containing 2.5 µL of Actinomycin D (Actinomycin D from Streptomyces species diluted in DMSO, Sigma, Cat# A9415-2MG, 1 mM) in 5 mL of DMEM complete, while SiHa and C33A cells were treated with a solution containing 0.25 µL of Actinomycin D in 5 mL of DMEM complete. In all cases, 300 µL of treatment solution was added to respective wells and incubated at 37°C for 24-hours. After incubation, the treatment solution was removed, and chamber slides were prepared for p53, and PARP-1 cleavage analysis as outlined in section 2.6.3 without addition of the VHH secondary antibody, as no VHH was present.

2.7 Proliferation Assays

In a 96-well plate, 8000 cells (CaSki and C33A) or 4000 (SiHa) per well were seeded and allowed to grow in a 37°C incubator overnight. After incubation, mRNA transfection was

performed as outlined in section 2.6.1, using a total volume of 100 µL per well and following supplier recommendations for a 96-well plate (Table 2). Following the 48-hour incubation, the Cell Counting Kit (Sigma-Aldrich, Cat# 96992) was removed from the fridge and warmed to room temperature for 10 minutes. Once warmed, 540 µL of the cell counting solution was added to 5.4 mL of complete DMEM media and vortexed gently to combine. Existing media was aspirated from each well and replaced with 105 µL of the cell counting dilution and allowed to incubate at 37°C for 4 hours. After 4 hours, absorbance was measured at 450 nm/650 nm using a plate reader.

2.8 Statistical Analyses

Raw data from triplicate proliferation assays was averaged for each trial was averaged and normalized against the No Transfection control for their respective cell type. Calculations and data collection were performed using Excel Version 16.59. Following normalization, statistical analyses were done using the open-source programing language R, version 4.0.3 (GUI 1.73 Catalina build). Assumptions of normality were assessed using boxplots, diagnostic plots, and an Anderson-Darling normality test. Homogeneity of variance was assessed using diagnostic plots and a Levene's test for homogeneity of variance. A two-way ANOVA was used to determine global mean differences. If significant differences were found, post-hoc Tukey HSD analyses were performed. Significance was set, *a priori*, at 0.05.

3 RESULTS

3.1 Initial VHH Selection Using Co-immunoprecipitation

Based on the initial dot blot (Figure 3), 5 VHHs were selected for preliminary co-IP analysis (C26, A37, A45, A46, 2A78). Co-IP was performed using the Affi-Gel 10 resin and several samples were analyzed by Western blot. To confirm the binding of the VHHs to the resin, the diluted antibody was analyzed alongside the unbound VHH collected after incubation with the resin. C26, A37, and 2A78 were bound to the resin using 100 mM MOPS pH 7.0 which works well for antibodies with an isoelectric point above 7.0 (C26: 7.21, A37: 8.91, 2A78: 8.63). However, for proteins with an isoelectric point below 7.0 (A45: 5.55, A46: 6.03), the supplier suggested the buffer 100 mM MOPS + 80 mM $CaCl_2$ pH 7.5 for the coupling of acidic proteins to the resin.

For the co-IP itself, the CaSki and C33A input were loaded to confirm the presence of E6 in CaSki and its absence in C33A. The elution sample from the resin coated with VHH incubated with CaSki lysate or with C33A lysate were also analyzed. The presence of a band at E6's molecular weight (~18 kDa) from CaSki indicates immunoprecipitation of E6. The presence of bands at the same molecular weight in C33A is unlikely of E6 immunoprecipitation as C33A does not express E6. However, the VHH themselves have a molecular weight of roughly 15 kDa and could be released from the resin during the elution. In some instances, we noticed that the antibodies used to probe for E6 could have unspecific reactions with the released VHHs. The last sample loaded is CaSki incubated with the resin in the absence of any VHH. A band observed at the E6 molecular weight indicates unspecific binding of the E6 protein to the resin itself.

The preliminary co-IP experiments were performed in duplicate. In the first experiment, the 5 VHHs tested immunoprecipitated E6, however a very faint band was observed in CaSki

incubated with the resin alone (CaSki + Affi-Gel 10) (Figure 5). In the second experiment, only 3 VHHs (C26, A37, and A46) immunoprecipitated E6, however the bands observed were less intense compared to the previous experiment. Interestingly, no band was observed in CaSki + Affi-Gel 10. Although some VHHs were capable of immunoprecipitating E6, either the results were not reproducible (A45, 2A78) and/or the amount of E6 immunoprecipitated was very low (C26, A37, A45, A46, A47, 2A78). Furthermore, the input CaSki sample only contains 10% of the samples subjected to immunoprecipitation, yet the bands corresponding to E6 precipitation for each VHH is faint suggesting that a limited amount of E6 was captured. Additionally, in Figure 5 it can be observed in CaSki + Affi-Gel 10 that a limited amount of E6 was also immunoprecipitated in the absence of any VHHs indicative of unspecific binding of E6 to the resin. Although these initial data were encouraging, more optimization was need in our experimental procedure to yield more efficient E6 immunoprecipitation and eliminate any unspecific results in the control.

Unfortunately, due to the low amounts of A45 and 2A78, further experiments could not be carried out using these antibodies. To expand our pool of candidates, we analyzed different VHHs selected based on the previous dot blot analyses (Figure 3). In the first group of experiments, A47, 2A03, 2A04, and 2A10 were selected as they worked well in dot blot. 2A15 was also selected based on ELISA experiments using recombinant E6 proteins performed by our NRC collaborators, however, 2A15 did not work in our dot blot experiments. Of the 5 candidates, only A47 was able to immunoprecipitate E6 in duplicate with no bands observed in the control (Figure 6). For 2A03, no bands were observed in the immunoprecipitated sample or in the control, however the VHH was properly bound to the resin (Figure 6). For 2A04, 2A10, and 2A15 the results were similar to 2A03, showing no bands in the immunoprecipitated sample or in the control (Appendix A). Based on these preliminary experiments, C26, A37, A46, and A47 were selected to optimize our methods.

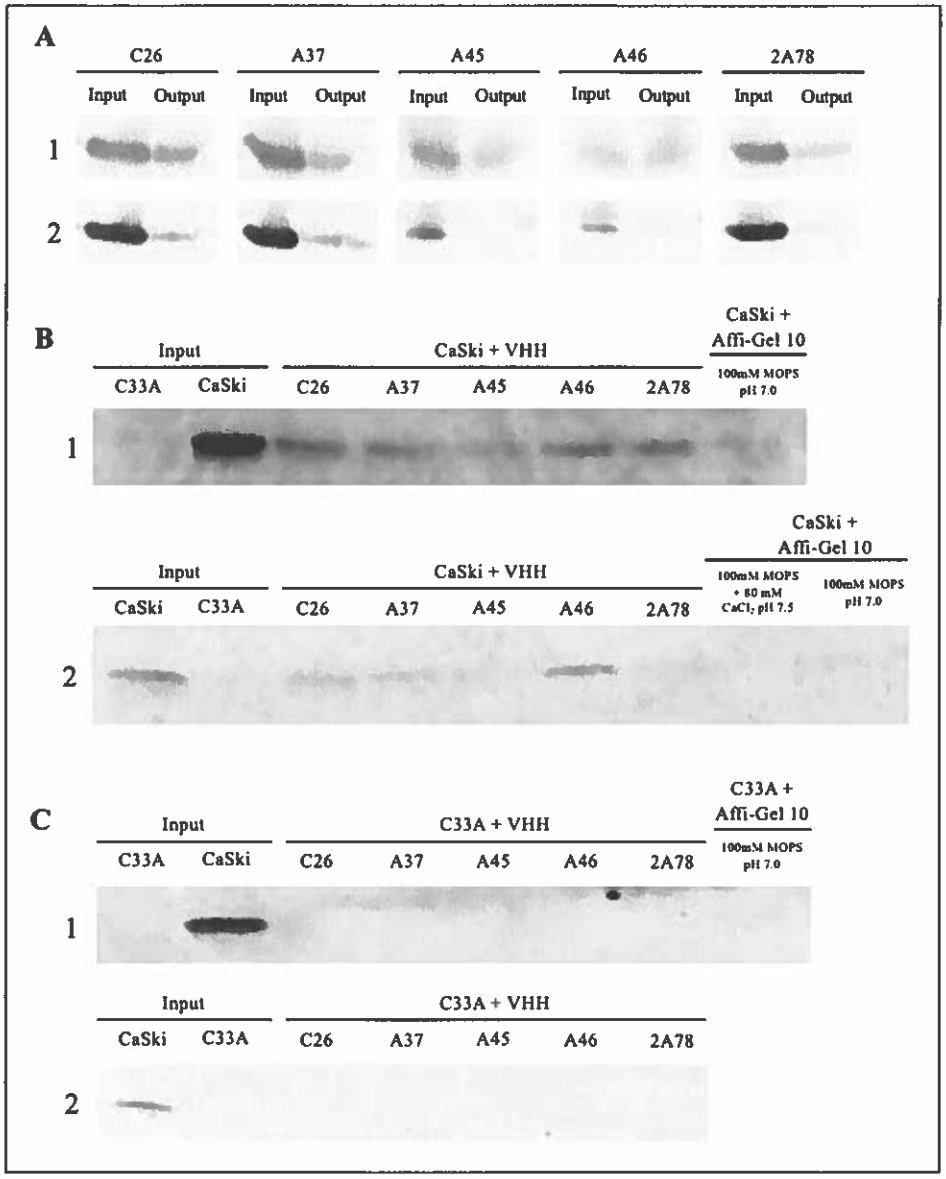

Figure 5. Preliminary co-immunoprecipitation results for C26, A37, A45, A46, and 2A78 using the Affi-Gel 10 resin and 100 mM MOPS pH 7.0- or 100 mM MOPS + 80 mM $CaCl_2$ pH 7.5 respectively. (A) VHH inputs and outputs for trial 1 and 2. Each input contains 10ug of the respective VHH. Method B resin division was used in both trials. Membranes were visualized using 0.25uL/5mL HA-HRP antibody. (B) CaSki and C33A immunoprecipitation results, and resin alone control results for Trial 1 and 2. Membranes visualized using 12.33uL 6F4 anti-E6 antibody. 500 μg of protein lysate for both CaSki and C33A were used in both trials.

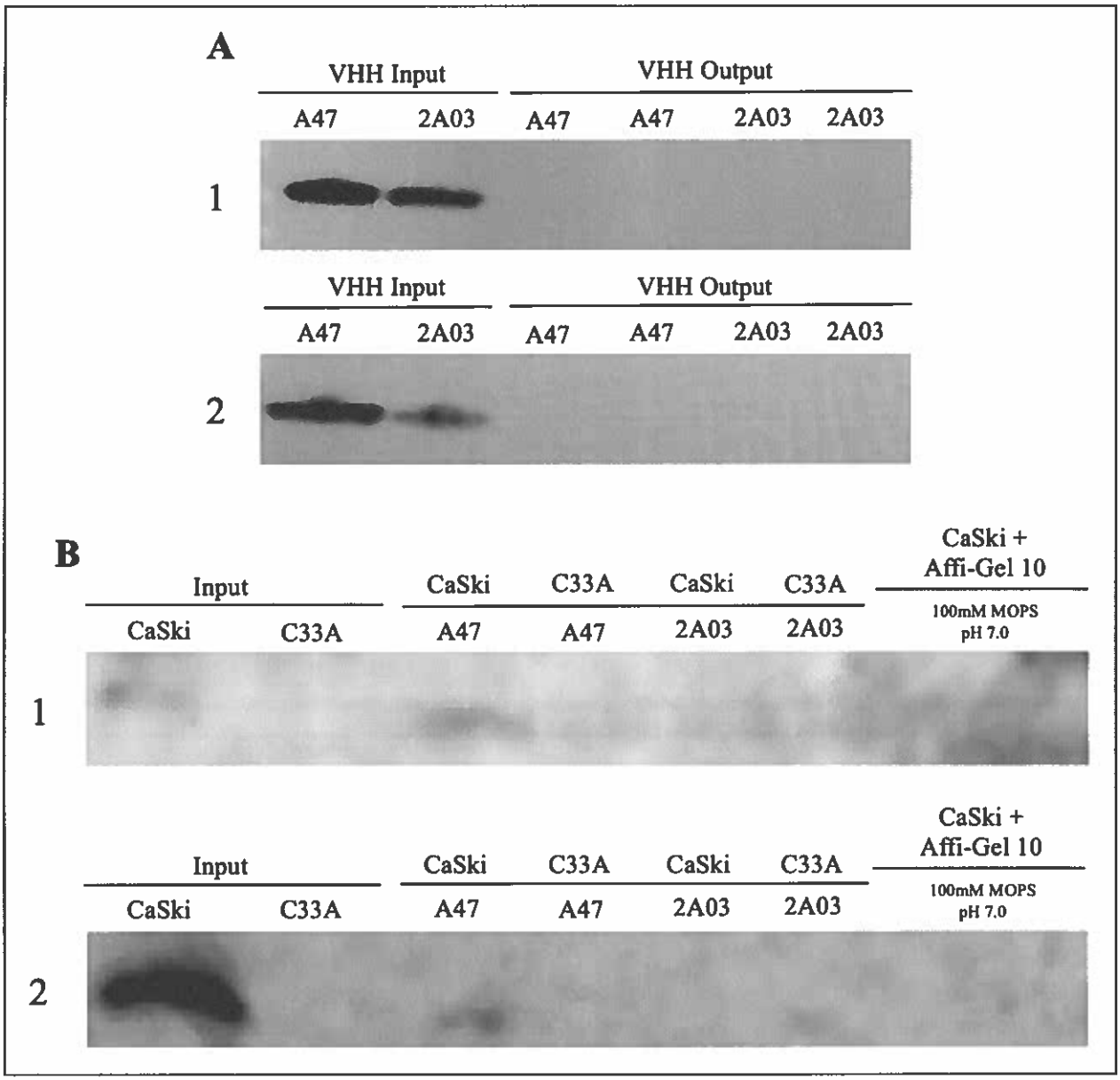

Figure 6. Co-Immunoprecipitation results for A47 and 2A03. (A) VHH inputs and outputs for Trial 1-3. Each input contains 10ug of the respective VHH. Method A resin division was used for all three trials. Membranes visualized using 0.25uL/5mL HA-HRP antibody. (B) CaSki and C33A immunoprecipitation results, and resin alone control results for Trial 1-3. Membranes visualized using 12.33uL 6F4 anti-E6 antibody. 500 μg of protein lysate for both CaSki and C33A were used in both trials.

3.2 Optimization of General Co-immunoprecipitation Protocol

3.2.1 VHHs at 40μg

Based on the previous co-IP results where a limited amount of E6 was immunoprecipitated by our VHHs, we decided to increase the amount of VHH added to the resin to capture more E6. These conditions were tested in duplicate, increasing the amount from 10 μg to 40 μg (due to low amount, only 20 μg was used for A47) per immunoprecipitation reaction.

In each trial, the VHHs were successfully bound the resin, observed by comparing the VHH input to the VHH output (Figure 7A). VHH input and output for C26 and A37 differed between trial 1 and 2, with increased output in trial 2 for both VHHs (Figure 7A.1 and 7A.2 respectively). This was however not a concern as the VHH input remained more intense than the output in both trials, still indicating strong coupling of the VHH to the resin. A46 showed consistent VHH input and output in both trials while a limited amount of A47 was detected in trial 1, likely due to poor transfer of the protein during Western blot (Figure 7A).

E6 was successfully immunoprecipitated by all four VHHs in both trials (CaSki + VHH), however in trial 2 a band corresponding to E6's molecular weight was also detected in CaSki + Affi-Gel 10 (Figure 7B). Comparing CaSki + C26, A37, and A47 to CaSki + Affi-Gel 10 + 100 mM MOPS pH 7.0 (the buffer used to dilute these antibodies) more E6 was detected in the C26 and A47 lanes compared to the control, however this was not the case for A47. As for A46, more E6 was detected in the CaSki + A46 lane compared to the CaSki + Affi-Gel 10 + 100 mM MOPS + 80 mM $CaCl_2$ pH 7.5 (the buffer used to dilute this antibody, Figure 3B). Finally, no bands were detected in the C33A + VHH lanes for any of the VHHs (Figure 7C). Nevertheless, an improved amount of E6 was immunoprecipitated especially for C26 and A46. Therefore, we decided to

continue with the increased amount of VHH (40 μg per immunoprecipitation reaction) in future experiments.

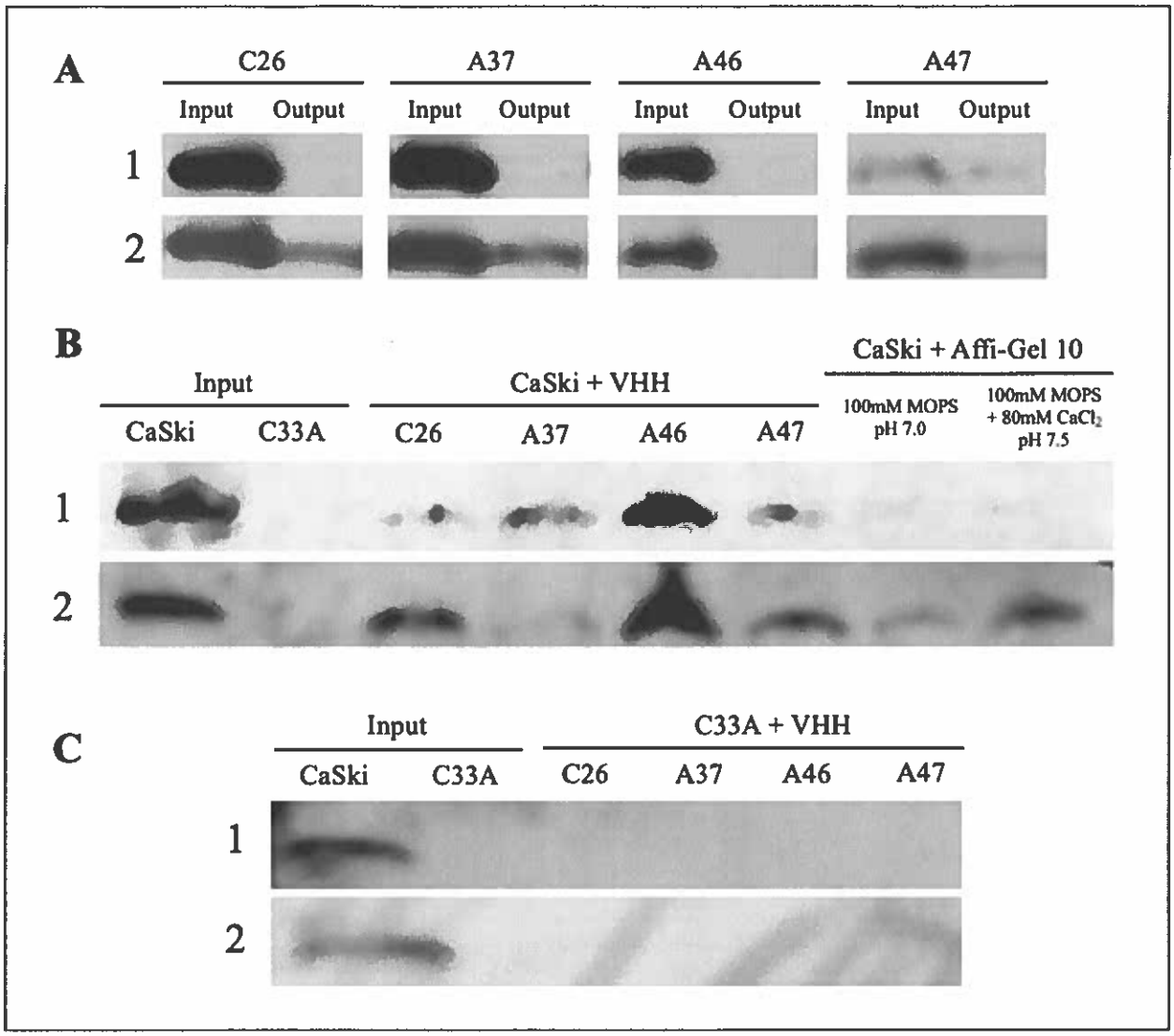

Figure 7. Co-immunoprecipitation results for C26, A37, A46, and A47. (A) VHH inputs and outputs for trial 1 and 2. C26, A37, and A46 contain 40ug of the respective VHH while A47 contains 20ug. Method B resin division was used for both trials. Membranes were visualized using 0.25uL/5mL HA-HRP antibody. (B) CaSki immunoprecipitation and resin alone control results for trial 1 and 2. Membranes visualized using 12.33uL 6F4 anti-E6 antibody. (C) C33A control immunoprecipitation results for trial 1 and 2. Membranes visualized using 12.33uL 6F4 anti-E6 antibody. 500 μg of protein lysate for both CaSki and C33A were used in both trials.

3.2.2 Increased PBS Washes

To help remedy non-specific bands present in the resin alone controls for both buffers (Figure 7B.2), three 1X PBS washes were added to the protocol following lysis buffer washes prior to elution. Unfortunately, due to low stock and its very low concentration, we were unable to continue using A47 for subsequent experiments. Despite this, C26, A37, and A46 were able to be continually tested throughout the following experiments.

As shown in Figure 8A, the VHHs were efficiently bound to the resin in both experiment 1 (C26 and A46), and experiment 2 (C26 and A37). Hereafter, all experiments have been performed using Method A for resin division, hence two coupling reactions were performed, resulting in two VHH output samples; the first to be used for CaSki IP and the second for C33A IP. Additionally, note that VHH output 1 corresponds to sample then used for CaSki, and VHH output 2 corresponds to the sample then used for C33A.

In experiment 1, both C26 and A46 showed strong immunoprecipitation of E6 (Figure 8B.1). Although this trial showed positive improvement in the resin alone control for C26 (CaSki + Affi-Gel 10 + 100 mM MOPS pH 7.0), A46 still presented non-specific binding in both controls (CaSki + Affi-Gel 10 + 100 mM MOPS + 80 mM $CaCl_2$ pH 7.5 and C33A + A46), especially with the resin alone. The faint band observed in the C33A + A46 lane is more likely due to unspecific detection of A46 itself. In experiment 2, C26 and A37 immunoprecipitated E6 efficiently, and a very faint band was observed in the CaSki + Affi-Gel 10 and the C33A + A37 controls (Figure 8B.2). Based on these results, it was concluded that the extra 1X PBS washes did not help alleviate non-specific interactions in the resin alone control and did not help with any non-specific interactions in the C33A control for A46. However, they did have a positive impact on CaSki + Affi-Gel 10 + 100 mM MOPS pH 7.0.

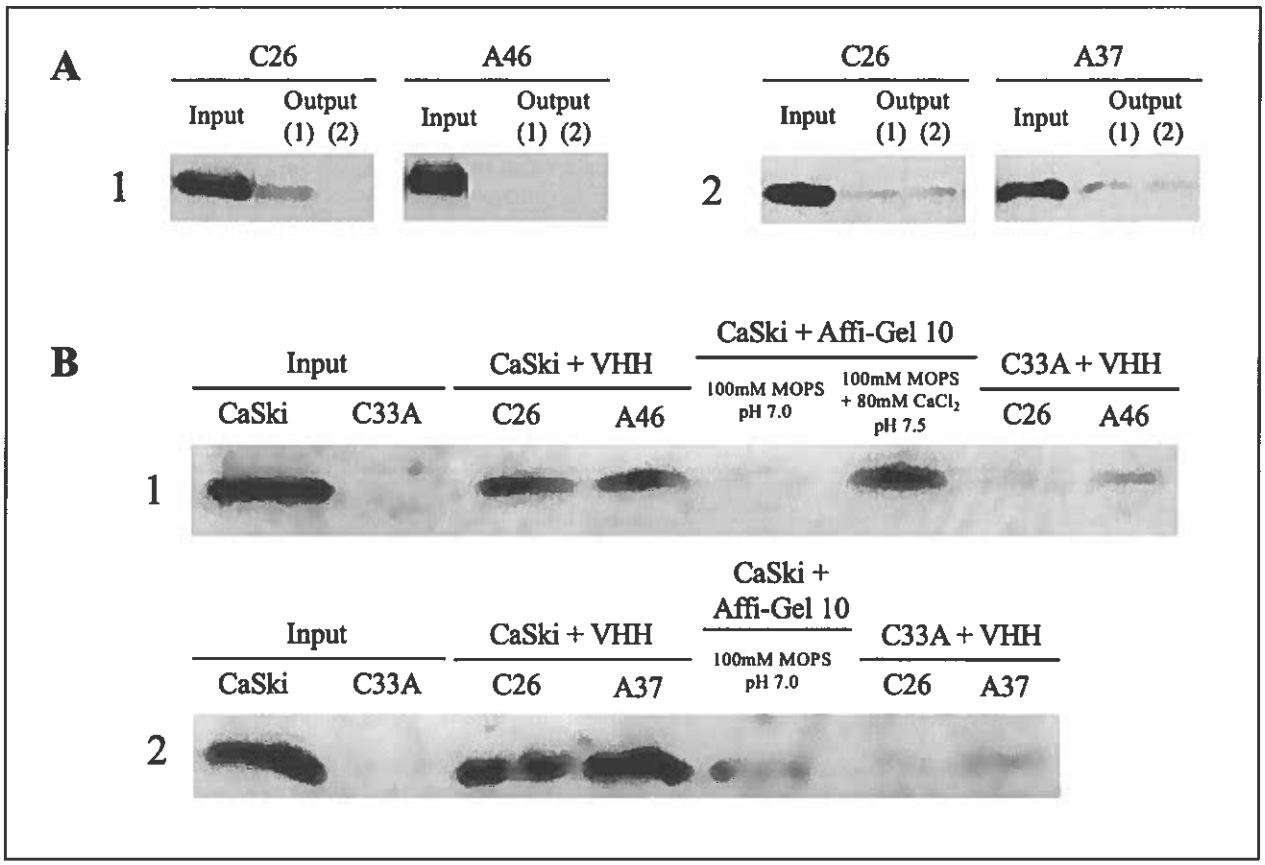

Figure 8. Co-immunoprecipitation results for C26, A46, and A37 with increased PBS washes. (A) VHH inputs and outputs for experiment 1 and 2. Each input contains 40ug of the respective VHH. Method A resin division was used for both trials. Membranes visualized using 0.25uL/5mL HA-HRP antibody. (B) CaSki and C33A immunoprecipitation and resin alone control results. Membranes visualized using 12.33uL 6F4 anti-E6 antibody. 500 μg of protein lysate for both CaSki and C33A were used in both experiments.

3.2.3 Shortened Protocol

In previous experiments, the coupling of the VHHs to the resin was performed overnight. Similarly, the resin was incubated with the respective MOPS buffers for the same time. Since more unspecific interactions with E6 and the resin were observed in the resin treated with $CaCl_2$, we hypothesize that the treatment applied to the resin increases unspecific binding of E6. Therefore, we tried reducing the amount of time the 100mM MOPS + 80mM $CaCl_2$ pH 7.5 buffer was in contact with the Affi-Gel-10 resin. For this experiment, C26 was also evaluated alongside A46 to determine if C26 would retain its E6 binding capacity under these conditions. In this protocol, initial VHH coupling was done for the 4 hours followed by ethanolamine HCl incubation for 1 hour. Protein lysate was then added to each column and incubated overnight, with the rest of the protocol remaining the same.

Despite the shorter VHH-resin coupling time, our VHHs still bound efficiently to the resin allowing further co-IP (Figure 9A). Unfortunately for A46, this approach did not fix the non-specific interactions observed in the 100mM MOPS + 80mM $CaCl_2$ pH 7.5 control and resulted in increased non-specific interactions in the C33A control as well (Figure 9B). This approach also appeared to decrease the immunoprecipitation efficiency of E6 for both C26 and A46. Therefore, we concluded that this method was not best for the optimization of immunoprecipitation results for either C26 or A46.

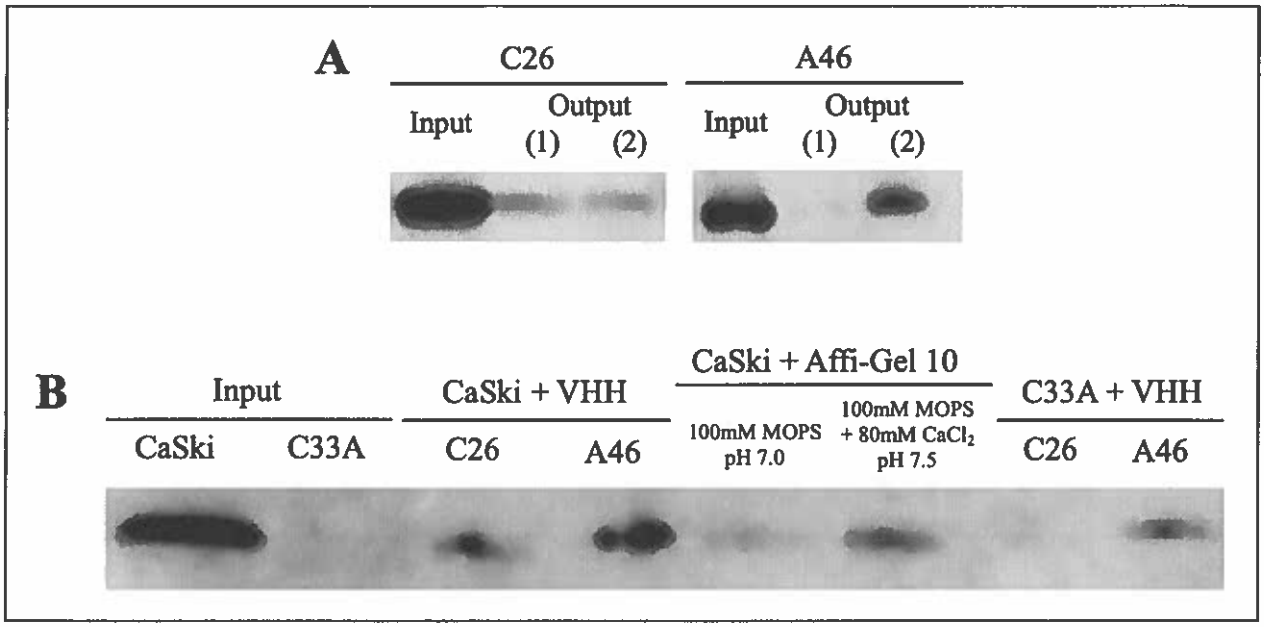

Figure 9. Co-immunoprecipitation results for C26 and A46 with a shortened protocol. (A) VHH inputs and outputs. Each input contains 40ug of the respective VHH. Method A resin division was used. Membranes visualized using 0.25uL/5mL HA-HRP antibody. (B) CaSki and C33A immunoprecipitation and resin alone control results. Membranes visualized using 12.33uL 6F4 anti-E6 antibody. 500 μg of protein lysate for both CaSki and C33A were used.

3.3 Optimization of Co-Immunoprecipitation Protocol for Acidic VHHs (A46)

3.3.1 Affi-Gel 15

An additional consideration we encountered was the isoelectric point of our VHHs and the recommendations of the Affi-Gel 10 resin itself. To couple VHHs with a lower isoelectric point, the addition of $CaCl_2$ was proposed. As previously mentioned, this was potentially causing the non-specific interactions seen in the resin alone controls for A46, the only VHH using this supplemented buffer at the time. However, Affi-Gel 10 couples' proteins best at a pH near or below their isoelectric point therefore making it recommended for proteins with isoelectric points of 6.5 to 11. Considering A46 has an isoelectric point of 6.03, this is outside the recommended range for Affi-Gel 10, and we decided to explore other resin options. Affi-Gel 15 couples' proteins best at a pH near or above their isoelectric point and is therefore recommended for proteins with isoelectric points below 6.5, such as A46.

For initial experimentation with Affi-Gel 15, we used the previous protocol optimizations (40 μg of VHH) however we did not implement the extra PBS washes as they did not help alleviate unspecific bands in the case of A46. Additionally, due to the optimization of Affi-Gel 15 for acidic proteins like A46, the addition of $CaCl_2$ was no longer necessary, allowing the 100 mM MOPS pH 7.0 buffer to be used in its place. Using this methodology, A46 was efficiently bound to the resin (Figure 10A) and E6 was successfully immunoprecipitated by A46 (Figure 10B). There were very little non-specific interactions seen in the resin alone control, which was a great improvement compared to previous results for A46 (Figure 7B.2, 8B.1, 9B). However, the results show a very strong band in the C33A + VHH control (Figure 9B), which appears equally as strong as the immunoprecipitation band (CaSki + VHH). It is likely that the band seen in C33A is the VHH being released from the resin and detected due to unspecific binding with the 6F4 primary

antibody, or the HRP secondary antibody in the western blot. As previously mentioned, A46 coupled very well to the Affi-Gel-15 resin, as the input is very strong with little to no output (Figure 10A). This very strong input band also supports the hypothesis that the band in C33A is the VHH, as this shows that a large amount of A46 was efficiently coupled to the resin. It is likely that A46 was released from the resin during SDS elution. At this time, considering this was the first trial with the new Affi-Gel-15 resin, needing some optimization was expected.

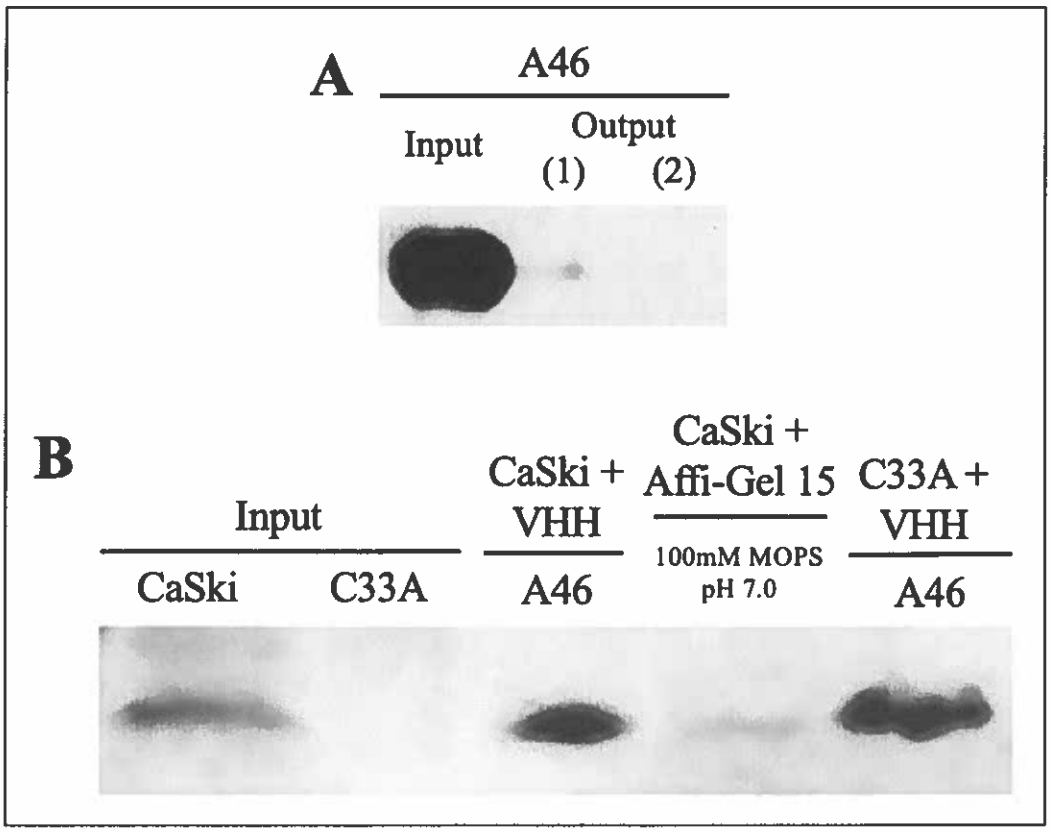

Figure 10. Co-immunoprecipitation results for A46 with Affi-Gel-15 resin and 100mM MOPS pH 7.0 buffer. (A) VHH inputs and outputs. Each input contains 40ug of the respective VHH. Method A resin division was used. Membranes visualized using 0.25uL/5mL HA-HRP antibody. (B) CaSki and C33A immunoprecipitation and resin alone control results. Membranes visualized using 12.33uL 6F4 anti-E6 antibody. 500 μg of protein lysate for both CaSki and C33A were used.

3.3.2 Altering A46 Concentrations for Affi-Gel-15

To optimize the protocol when working with Affi-Gel-15 resin and eliminate the non-specific bands seen in C33A in previous experiments (Figure 10B), three different concentrations of A46 were tried when coupling to the resin. The concentrations tried were 1X (10μg VHH), 2X (20μg VHH), and 4X (40μg VHH). The rationale being that this could reduce the released VHH observed in the C33A + VHH control while maintaining E6 binding capacity.

Observing the VHH input and output (Figure 11A), the input intensities varied logically with the concentration of VHH with 4X being the most intense, followed by 2X, and 1X. Both the 1X and 4X outputs were consistent with good coupling of A46 to the resin, however the 2X concentration appeared to have increased output. Nevertheless, this output was still weaker than the input, indicating A46 did bind to the resin overall. E6 was successfully immunoprecipitated by A46 when using all three concentrations (Figure 11B.1, 2) with varying intensities. The 4X concentration showed the strongest immunoprecipitation band, however it also elicited the strongest band in the C33A control (Figure 11B.1). Logically, the 2X concentration showed the second most intense immunoprecipitation band, however it also elicited a strong band in the C33A control (Figure 11B.2). Finally, the 1X concentration had the weakest E6 immunoprecipitation band, but also had very little in the C33A control (Figure 11B.1). Of note was that all three concentrations did not show non-specific interactions in the resin alone control, indicating that the Affi-Gel-15 resin was a marked improvement compared to the Affi-Gel-10 resin used previously. With all things considered, we concluded that the best option moving forward with the Affi-Gel-15 resin and A46 was the 1X concentration in which both controls were clean.

Due to the conclusion, 2 more experiments using these conditions were performed (Figure 12). Proper binding of A46 was obtained as before (Figure 12A). In trial 1, we observed that E6

was not immunoprecipitated, and in fact the entire membrane was blank other than the CaSki protein input lane (Figure 12B.1). In trial 2 however, E6 was immunoprecipitated, however there were non-specific interactions observed in both the resin alone and C33A controls (Figure 12B.2). Now having triplicate results for A46 at a 1X concentration, based on these results combined with those obtained in the original 1X Affi-Gel-15 trial (Figure 11B.1), it was concluded that E6 was immunoprecipitated unreliably by A46 when using Affi-Gel-15 resin with a 1X concentration of VHH (10μg). Therefore, we focused our attention on C26 and A37 for further analyses.

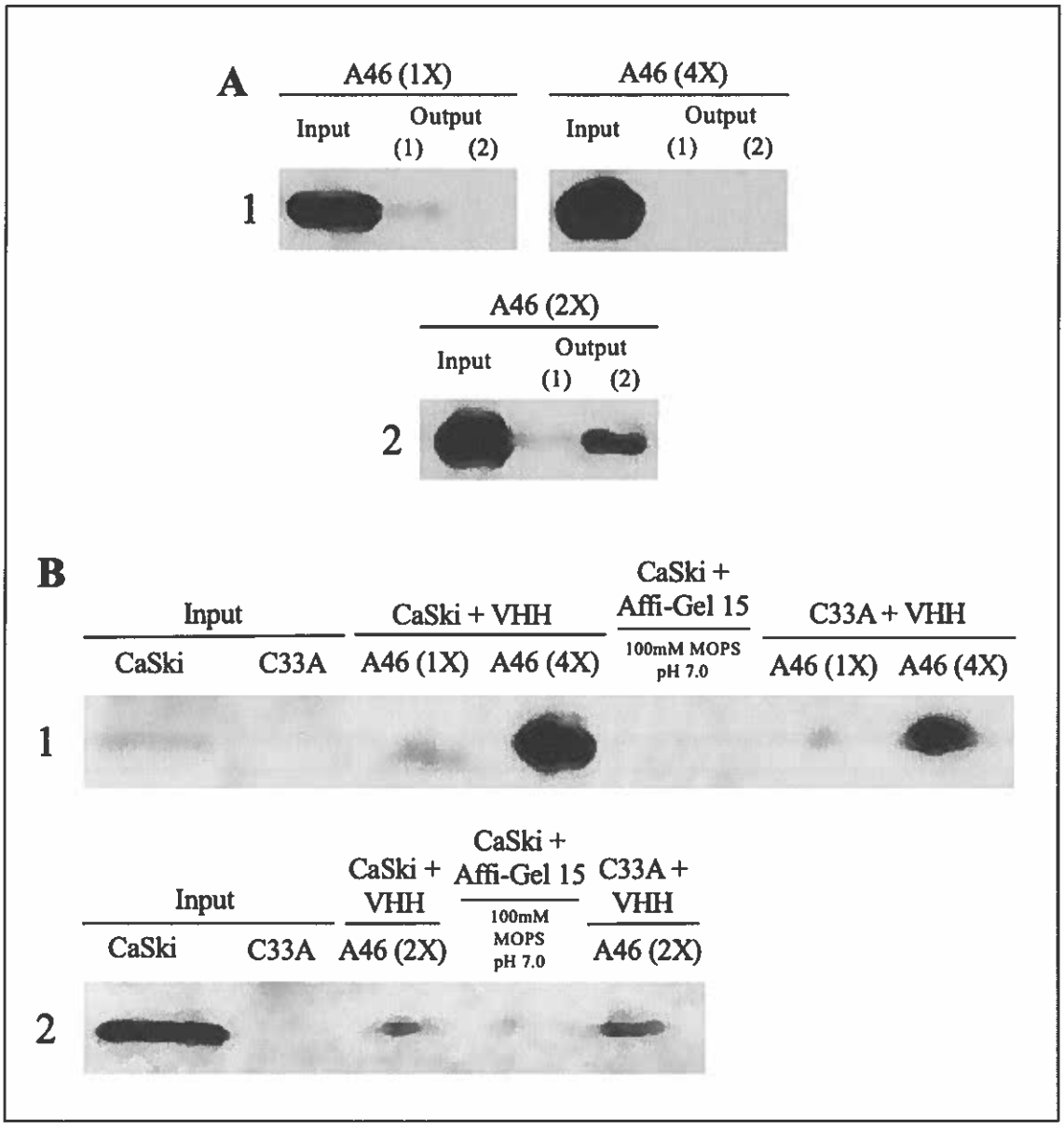

Figure 11. Co-immunoprecipitation results for A46 with Affi-Gel-15 resin and 100mM MOPS pH 7.0 buffer at 1X, 2X, and 4X concentrations of VHH. (A) VHH inputs and outputs. A46 1X input contains 10ug of VHH, A46 2X contains 20ug of VHH, and A46 4X contains 40ug of VHH. Method A resin division was used for both experiments. Membranes visualized using 0.25uL/5mL HA-HRP antibody. (B) CaSki and C33A immunoprecipitation and resin alone control results. Membranes visualized using 12.33uL 6F4 anti-E6 antibody. 500 μg of protein lysate for both CaSki and C33A were used in both experiments.

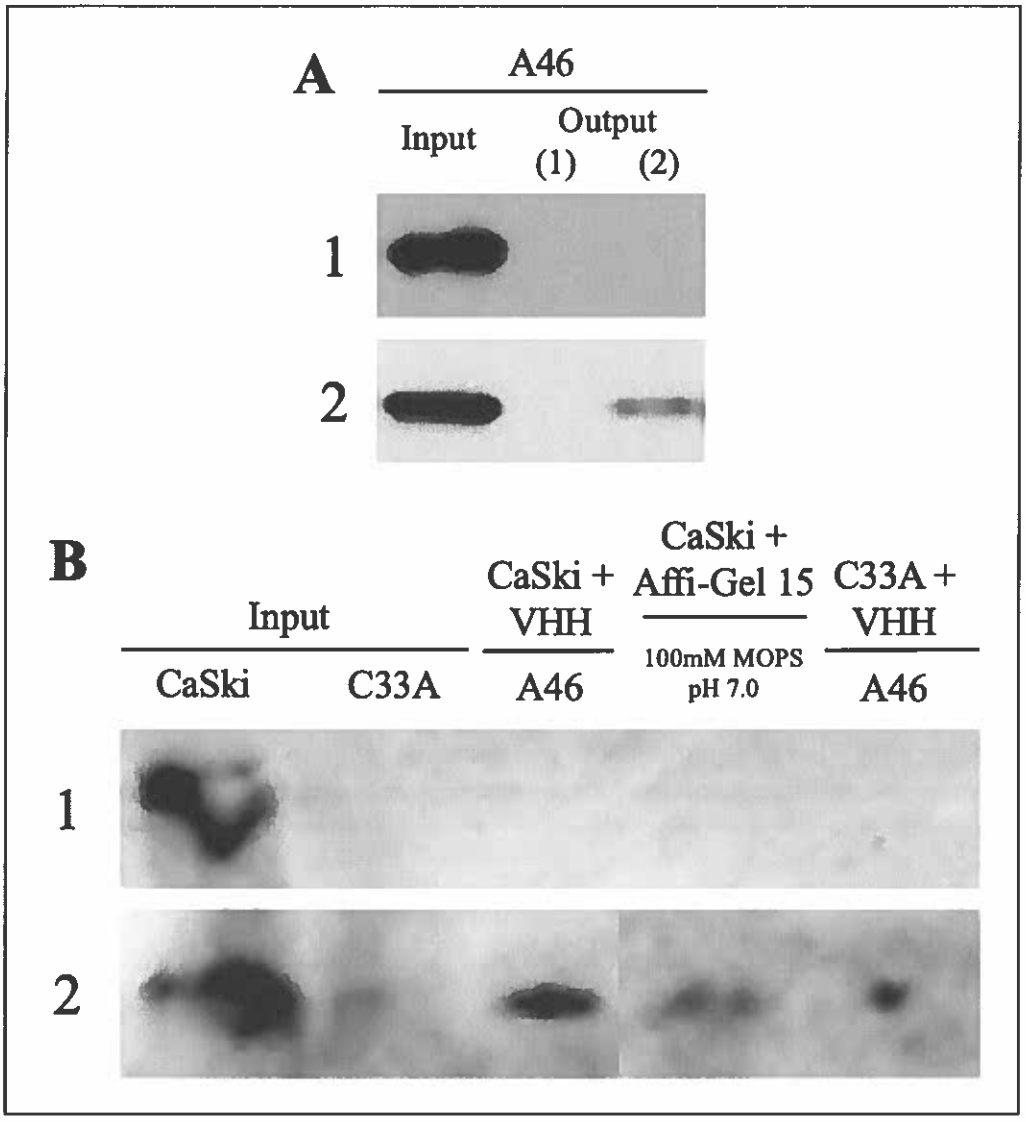

Figure 12. Co-immunoprecipitation results for 1X A46 with Affi-Gel-15 resin. (A) VHH inputs and outputs for trial 1 and 2. All VHH inputs contain 10ug of A46. Method A resin division was used. Membranes visualized using 0.25uL/5mL HA-HRP antibody. (B) CaSki and C33A immunoprecipitation and resin alone control results. Membranes visualized using 12.33uL 6F4 anti-E6 antibody. 500 μg of protein lysate for both CaSki and C33A were used in both trials.

3.4 Optimization of Co-Immunoprecipitation Protocol for Basic VHHs (C26, A37)

3.4.1 Glycine Elution

In hopes of remedying the non-specific interactions seen in the 100mM MOPS pH 7.0 buffer with Affi-Gel-10 alone (Figure 7B.2 and 8B.2), we decided to attempt using glycine to replace the SDS elution used in the standard protocol. Glycine elution has been successfully used previously in our lab; however, this method has only been used with a magnetic bead to immobilize the VHHs, not with Affi-Gel-10 resin. Glycine elution is gentler compared to SDS, and potentially gentle enough to elute only the immunoprecipitated E6 protein, avoiding non-specific interactions.

Observing the VHH input and output (Figure 13A), it appears that both C26 and A37 had good coupling to the resin, although C26 did show slightly more output compared to A37; overall, the results indicate that the VHHs were successfully coupled to the resin. Although there was a very strong band in the CaSki input (Figure 13) confirming E6' presence in the samples, we did not see bands in any other lanes, including the immunoprecipitation samples. Therefore, this lack of immunoprecipitation from previously successful VHHs was likely due to lack of elution by glycine when using the Affi-Gel-10 resin. We concluded that the glycine elution did not optimize the protocol, and therefore did not continue with its use.

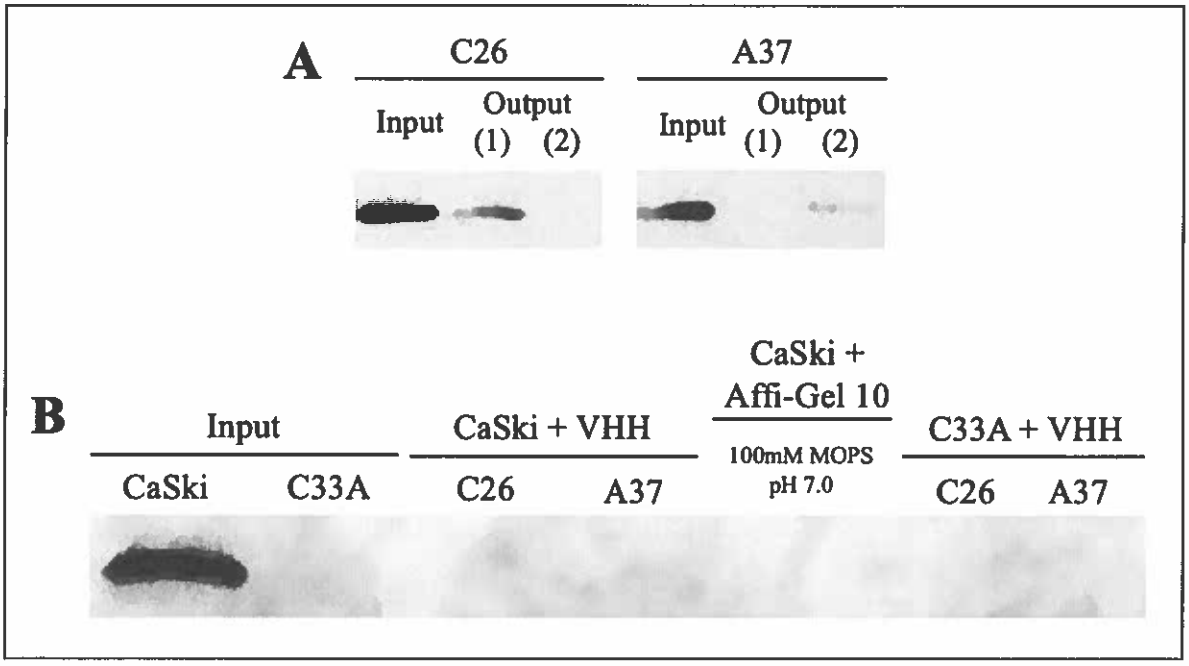

Figure 13. Co-immunoprecipitation results for C26 and A37 with glycine elution and Affi-Gel 10 resin. (A) VHH inputs and outputs. All VHH inputs contain 40ug of C26 or A37. Method A resin division was used. Membranes visualized using 0.25uL/5mL HA-HRP antibody. (B) CaSki and C33A immunoprecipitation and resin alone control results. Membranes visualized using 12.33uL 6F4 anti-E6 antibody. 500 μg of protein lysate for both CaSki and C33A were used.

3.4.2 C26, C26-Biotin, and A37 Successfully Bind Endogenous E6 in Triplicate

Although we occasionally observed non-specific signal in the controls for C26 and A37, this signal was always of lower intensity compared to the immunoprecipitated E6, indicating that overall, these VHHs do immunoprecipitate E6. Additionally, it has been observed with different monoclonal antibodies against the E6 protein such as 6F4, 3B8, and IF5 that faint bands with similar molecular weights to E6 could be observed in E6-negative cells (Lagrange et al. 2005) (Figure 2) suggesting that these antibodies could have some non-specific interactions with other proteins. Therefore, we decided to analyze C26 and A37 in triplicate using the exact same conditions (40μg, additional PBS washes) to confirm that E6 signal was consistently stronger than any bands in the control.

Around this time, we also obtained a new C26 antibody with a biotin tag (C26B). Unlike C26 which was generated with an HA tag, C26B was developed with a Biotin tag instead of the HA tag. Since antibodies have a shelf-life that could also interfere with their activity, we decided to add C26B alongside C26, to analyze if it's E6 immunoprecipitation efficiency was similar to C26.

The inputs and outputs for all three VHHs were found to be excellent, with consistently strong VHH input bands and little to no output (Figure 14A). This was consistent for C26, C26B, and A37 alike. As we anticipated, E6 was successfully immunoprecipitated by C26, C26B, and A37 while both the Affi-Gel-10 resin alone and C33A controls were found to be clean in all three trials (Figure 14B). Both C26 and C26B displayed consistently strong bands in all three trials, compared to A37 which showed a very strong band in Trial 1, however was weaker in Trial 2 and 3. Nevertheless, all three VHHs were successful in the immunoprecipitation of E6 in triplicate, which was a very encouraging result.

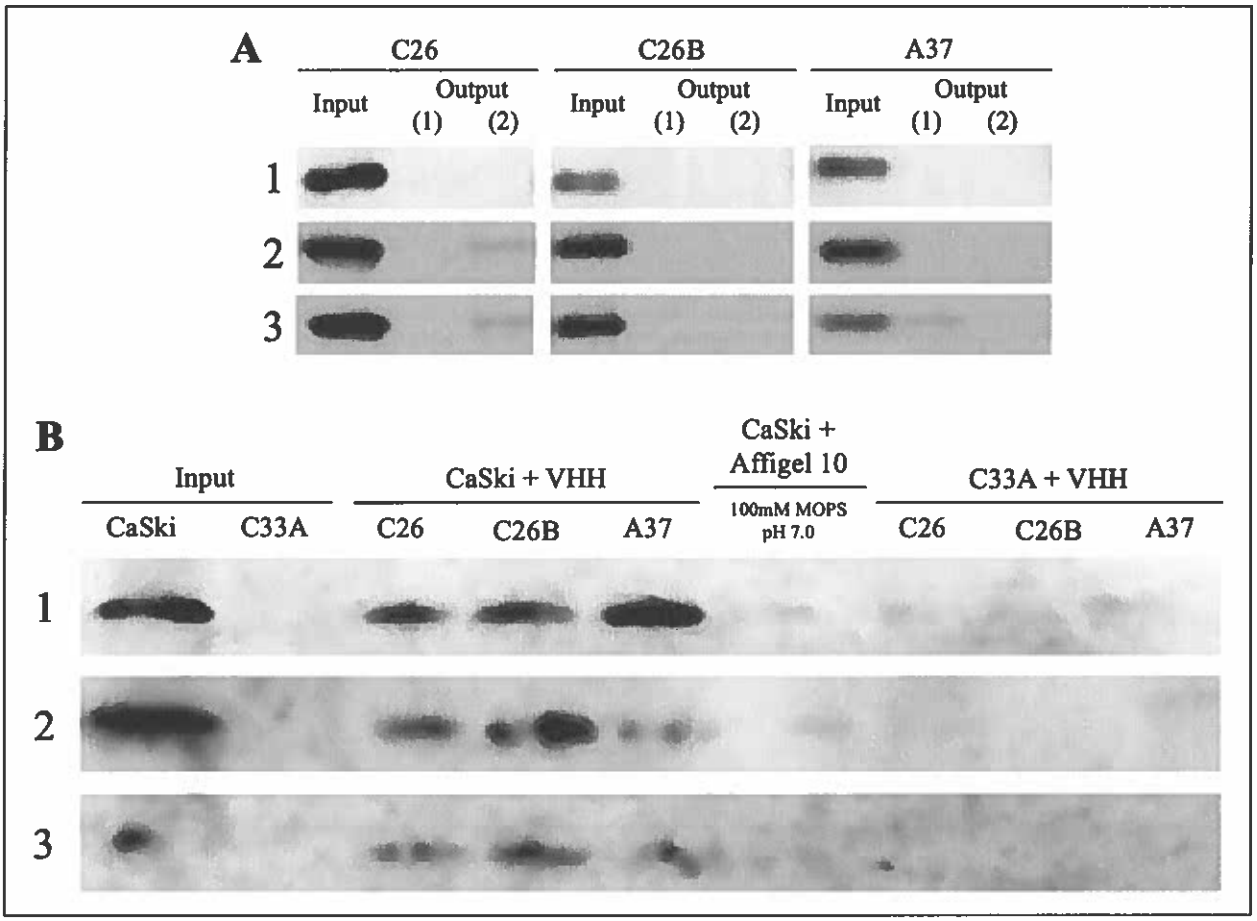

Figure 14. Co-immunoprecipitation results for C26, C26B, and A37 with Affi-Gel 10. (A) VHH inputs and outputs for trial 1-3. All VHH inputs contain 40ug of C26, C26B, or A37. Method A resin division was used. Membranes visualized using 0.25uL/5mL HA-HRP antibody. (B) CaSki and C33A immunoprecipitation and resin alone control results. Membranes visualized using 12.33uL 6F4 anti-E6 antibody. 500 μg of protein lysate for both CaSki and C33A were used in all trials.

3.5 Exploration of Additional VHHs Through Optimized Co-immunoprecipitation Protocols

Based on our dot blot experiments (Figure 3), we selected other VHHs to be evaluated using our optimized co-IP protocols. The VHHs A34, C11, C36, C38, 2A12, 2A15, 2A17, and 2A51 were not analyzed as they had limited to no binding capacity to the recombinant E6 6C/6S protein. The A47 and 2A78 VHH were not analyzed as we didn't have a sufficient amount of these proteins remaining. The 2A10 VHH was not thoroughly analyzed as its binding to the E6 6C/6S was very low compared to the binding of 4C/4S and F47R, indicating that 2A10 will need the presence of MBP to have a strong binding capacity. The remaining VHHs were analyzed using the Affi-Gel resins more suited to their isoelectric points.

3.5.1 Acidic VHHs

A05

Much like A46, A05 is another acidic VHH having an isoelectric point of 5.3. For this reason, we chose Affi-Gel-15 for our experiments to maximize our results. When observing the antibody input and output (Figure 15A), it was observed that A05 did not show efficient coupling to the Affi-Gel-15 resin, as the output bands are very intense and comparable to the input. However, in all three trials the input bands do appear to be slightly larger in comparison, indicating that some VHH was coupled to the resin. Considering Affi-Gel 15 couples' proteins through their primary amino group found on the N-termini and lysine side chains, although A05 contains 8 lysine residues, it remains possible that these residues are hidden within pockets or folded sections of the protein, rendering them inaccessible to the resin itself. Nevertheless, since some limited amounts of A05 were bound to the resin, the co-IPs were performed. A05 was found to immunoprecipitate E6 unreliably in co-IP, showing a weak band in Trial 1, however lacking

success in Trials 2 and 3 (Figure 15B). This result suggests that A05 could have some E6 immunoprecipitation capacity, however another support should be used to immobilize the antibody itself.

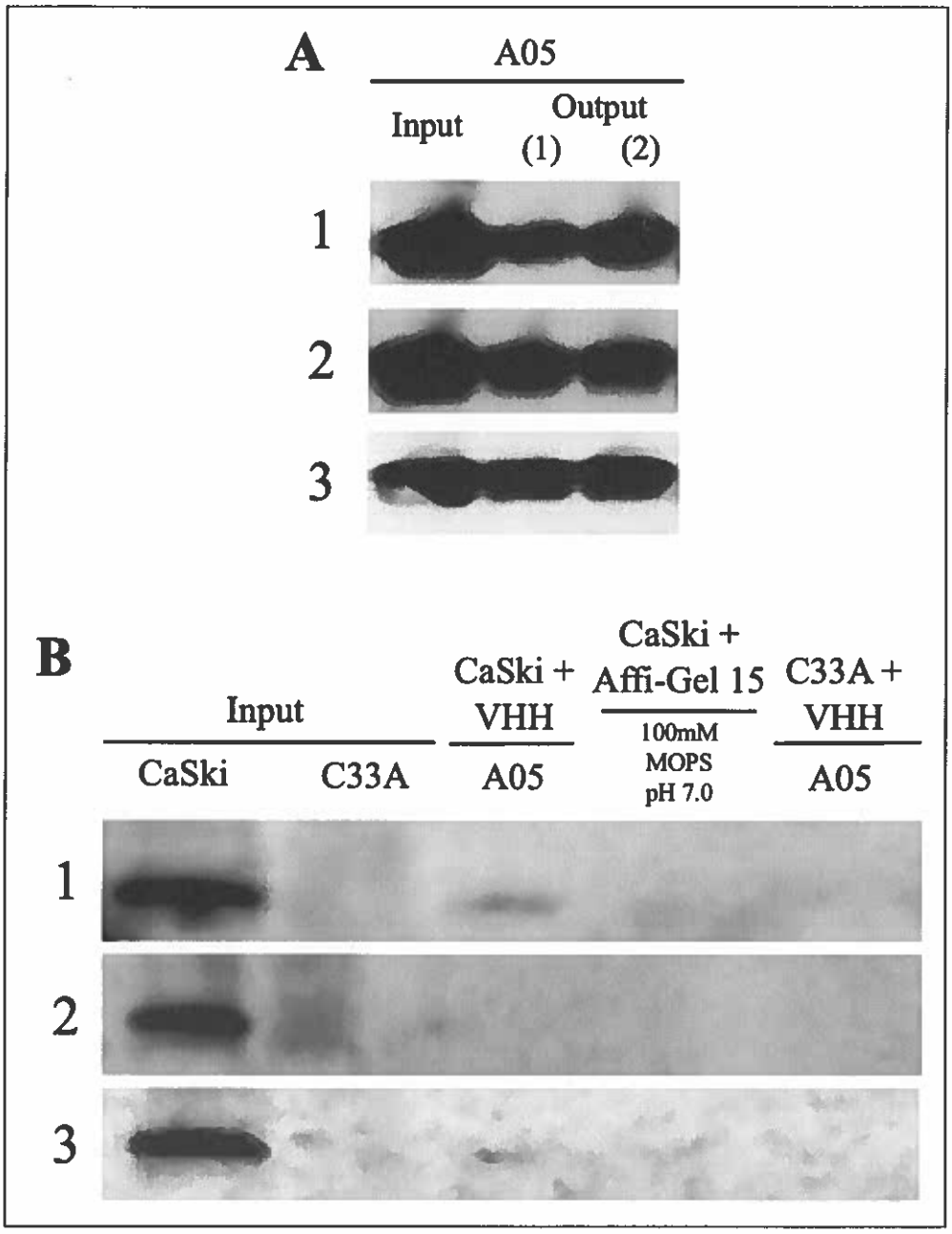

Figure 15. Co-immunoprecipitation results for A05 with Affi-Gel 15 resin. (A) VHH inputs and outputs for trial 1-3. All VHH inputs contain 40ug of A05. Method A resin division was used. Membranes visualized using 0.25uL/5mL HA-HRP antibody. (B) CaSki and C33A immunoprecipitation and resin alone control results. Membranes visualized using 12.33uL 6F4 anti-E6 antibody. 500 μg of protein lysate for both CaSki and C33A were used in all trials.

3.5.2 Basic VHHs

2A03 and 2A04

Based on our dot blots (Figure 3), 2A03 and 2A04 were found to be additionally interesting candidates to try in co-immunoprecipitation. Both are basic VHHs, having isoelectric points of 8.92 and 8.03 respectively.

Observing the VHH inputs and outputs, both VHHs were found to be of average coupling ability, with consistently strong VHH input bands and some output, specifically 2A03 and 2A04 in Trial 2, and 2A04 in Trial 3 (Figure 16A.2, 3 respectively). However, the consistently stronger input bands still indicate that both VHHs had good coupling to the Affi-Gel-10 resin. Both 2A03 and 2A04 were found to immunoprecipitate E6 in Trial 1 and 3, however in Trial 2 there was very little E6 visualized (Figure 16 B). In Trial 1, non-specific bands can be seen in the C33A control, along with in the resin alone control (Figure 16B.1). Trial 2 shows minimal non-specific interactions in both controls, however with the immunoprecipitation signal so low, we deemed this a negative result overall. Trial 3 showed particularly positive results for E6 immunoprecipitation while also having decreased non-specific interactions in both the resin alone and C33A controls. Although both VHHs were able to immunoprecipitate E6 in some capacity, we are not confident to declare either as strong candidates, especially in comparison to other strong contenders such as A37 and C26 which worked much more consistently throughout the experiments at the same concentration.

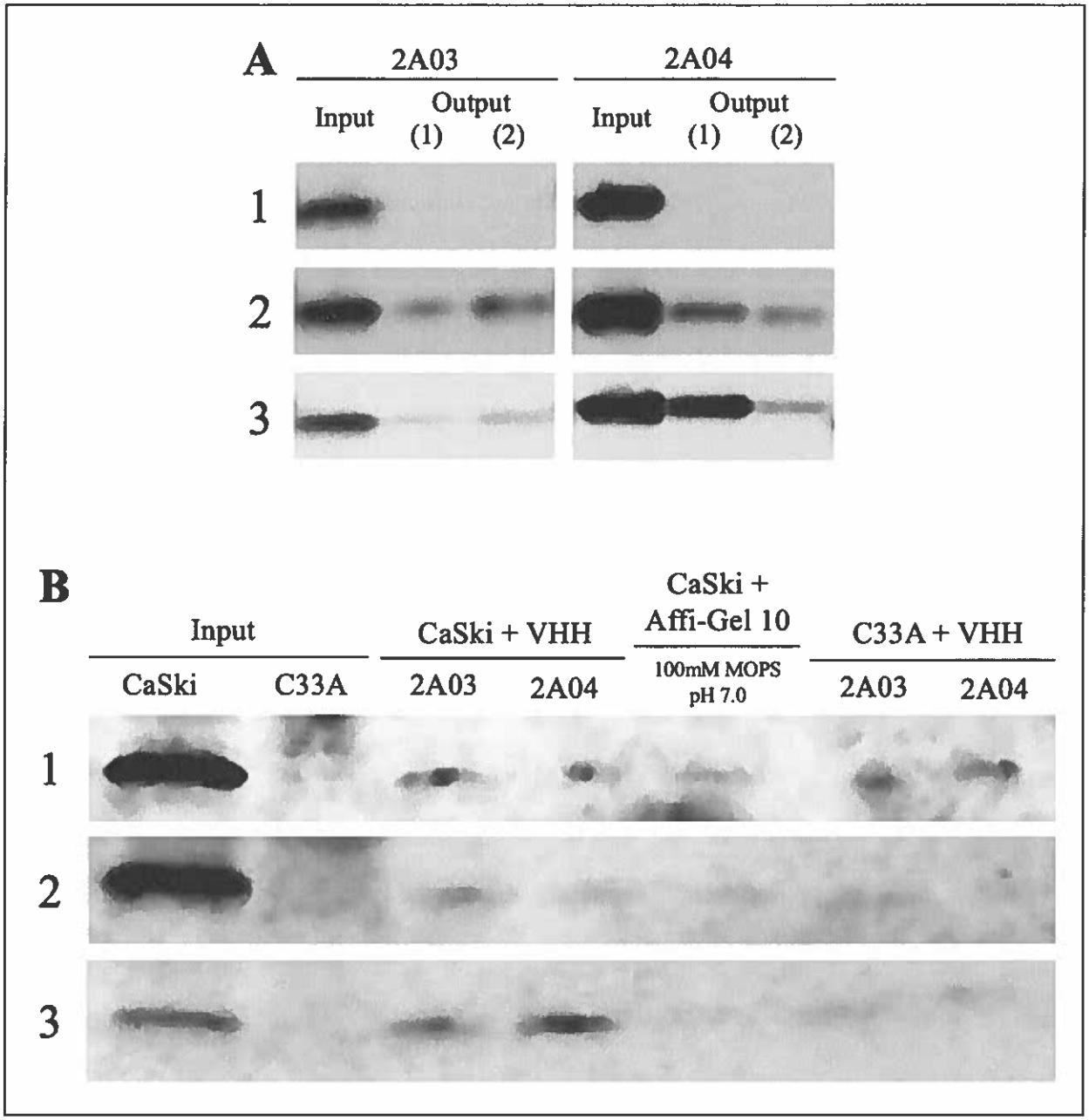

Figure 16. Co-immunoprecipitation results for 2A03 and 2A04 with Affi-Gel 10 resin. (A) VHH inputs and outputs for trial 1-3. All VHH inputs contain 40ug of 2A03 or 2A04. Method A resin division was used. Membranes visualized using 0.25uL/5mL HA-HRP antibody. (B) CaSki and C33A immunoprecipitation and resin alone control results. Membranes visualized using 12.33uL 6F4 anti-E6 antibody. 500 μg of protein lysate for both CaSki and C33A were used in all trials.

3.6 Work with Recombinant Proteins

In previous experiments, it has been shown in dot blot and Western blot that C26 binds MBP in the folded or linearized form. However, these experiments were done in the absence of an untagged E6 protein (Togtema et al. 2019). Our most recent results in the presence of E6 6C/6S indicate however that C26 may have different binding properties (Figure 3). To confirm these results, dot blots were repeated twice more to confirm that C26 binds E6 6C/6S, alongside the other five most interesting VHHs (A37, A46, 2A03, 2A04, A05). All 6 VHHs were found to preferentially bind the recombinant E6 protein with limited to no binding to the MBP protein alone (Figure 17).

As previously, discussed, we hypothesize that C26 interacts with E6 6C/6S via the CDR3 region, which is more specific and recognizes folded epitopes, while it binds the MBP protein via the less specific CDR1 or CDR2 regions. However, an alternative explanation would be that C26 recognizes an epitope on the E6 6C/6S containing one of the amino acid substitutions. These mutations are absent in the CaSki E6 protein used previously (Togtema et al. 2019). To test this hypothesis, we performed Western blots under denaturing conditions using E6 6C/6S, MBP, F47R, and 4C/4S in triplicate (Figure 18). The membranes were probed with C26, 6F4 as a positive control for E6 binding, and the secondary anti-VHH alone to exclude any unspecific binding of the secondary antibody to any protein. As expected, 6F4 recognized the recombinant E6 protein and not MBP, and the secondary alone showed no binding to any proteins (Figure 18). Interestingly, C26 reacted with the MBP-containing proteins but not with E6 6C/6S, supporting the hypothesis that C26 binds MBP or E6 by different mechanisms and CDR regions.

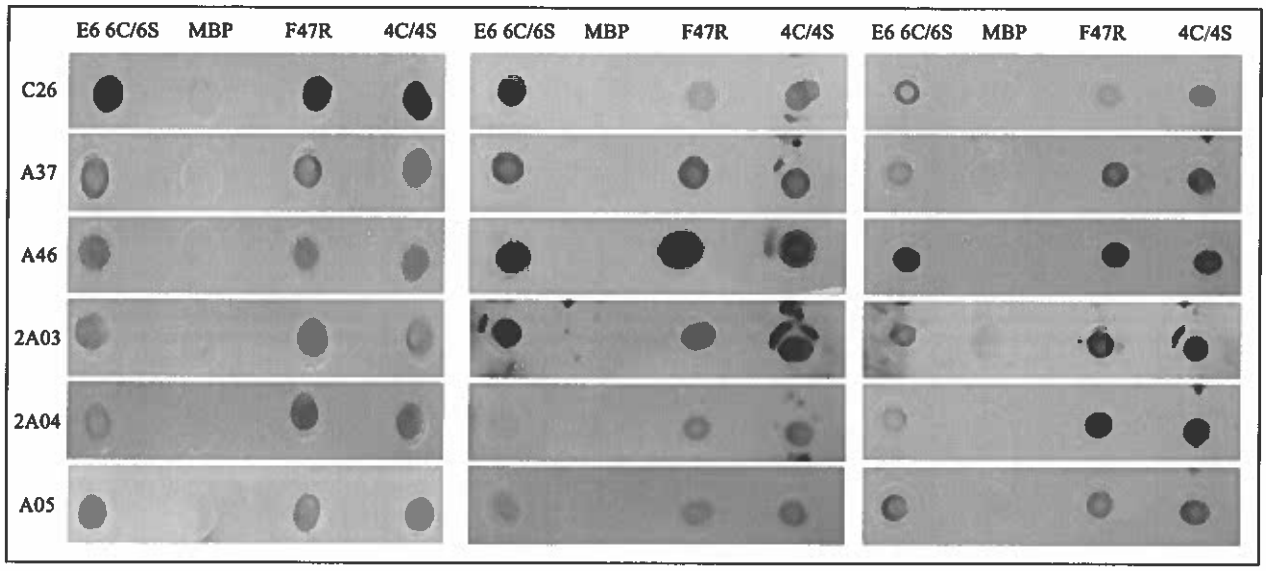

Figure 17. Triplicate dot blot results for the top 6 anti-E6 VHHs selected based on successful co-IP. (Left) Dot blot results from original dot blot experiment (Figure 3). (Middle and Right) Dot blot experiments performed during my MSc. Each spot contains 4 μL of the respective recombinant E6, E6-MBP, or MBP protein at a concentration of 0.5 μg/μl. Membranes were incubated overnight in a 5 mL blocking solution containing 5.4 μg/μL of the respective VHH, followed by a secondary antibody incubation with MonoRabTM: Rabbit Anti-Camelid VHH Antibody [HRP] in blocking solution overnight. Membranes were visualized through chemiluminescence, UVP™ Gel Imaging System, and VisionWorks software.

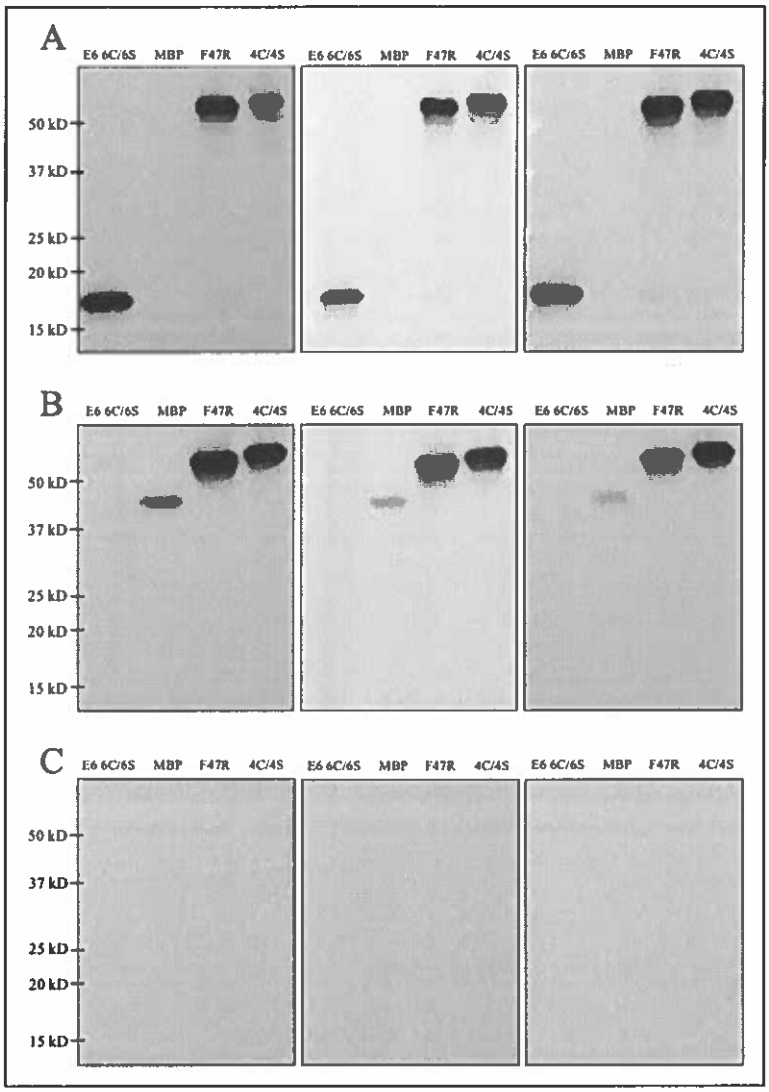

Figure 18. C26 Western blots under denaturing conditions. (A) Membrane incubated with anti-E6 6F4 antibody. (B) Membrane incubated with C26. (C) Membrane incubated with secondary antibody only (Negative Control). 10 ng of recombinant E6, E6-MBP, or MBP protein was prepared and denatured for each lane respectively. Gels were run at 120V for 75 minutes, followed by transfer 100V, 0.35A for 60 minutes. Membranes were incubated with 2.69 μg/μL (A) Anti-E6 6F4, (B) C26, (C) non-supplemented blocking solution overnight, followed by 1:5000 of HRP-Anti Mouse antibody for 1 hour. Membranes were visualized through chemiluminescence, UVP™ Gel Imaging System, and VisionWorks software.

3.7 VHH Transfection

3.7.1 Transfection with HiPerFect Transfection Reagent

After identifying C26B, C26, and A37 as competent E6 binders, we sought to evaluate if their E6 binding ability had any therapeutic potential. To achieve this, we first had to identify a method of transfection that allows our VHHs to enter our target cells. The HiPerFect transfection reagent is one of many cationic lipid-based transfection reagents originally designed for RNA/DNA delivery, although it has been further adapted for the delivery of mouse monoclonal antibodies against the E6 protein (Courtête et al. 2007, Togtema et al. 2012). However, for efficient protein delivery using HiPerFect, the protein must contain a sequence of anionic residues to interact with the cationic lipids, allowing the transfection to occur. Previous research in the Zehbe lab has used HiPerFect to deliver two mouse monoclonal antibodies to CaSki and SiHa cells (Togtema et al. 2012); we therefore evaluated our VHHs based on this existing protocol, however without success.

To achieve transfection, various trouble-shooting experiments were performed where notably, we varied the amount of VHH used (0.4 μg/mL to 80 μg/mL) and varied the amounts of HiPerFect (3 μL and 10 μL). Due to its similar co-immunoprecipitation of E6 and our ample stock, C26B was used for many of the troubleshooting experiments, before trying the final protocol with C26 and A37 (Appendix B). Unfortunately, despite our efforts, little to no VHH was visualized using the HiPerFect transfection reagent, with the final result of our HiPerFect methodology after troubleshooting presented in Figure 19.

In this experiment, C26 and A37 were evaluated using two different concentrations of VHH (8 μg/mL and 40 μg/mL). Tubulin was used as a positive control to verify our methodology due to previous successful uses in our lab (Togtema et al. 2012). No signal was

observed for C26 with either concentration while little to none of the VHH was observed with A37 at 40 µg/mL (only 3 spots were observed in the entire field) (Figure 19). However, in cells treated with A37 without the addition of the transfection reagent, similar spots were also observed, even in fields with no cells. In drastic contrast, the tubulin antibody was easily detected throughout the entire field of cells (Figure 19).

This lack of transfection efficiency is most likely due to the isoelectric point of the VHHs tested. Personal communication with technical support at Thermo Scientific revealed that when using cationic transfection reagents, the isoelectric point of the protein of interest should be below 5 to ensure their negative charge at physiological pH (the pH of the reaction). This allows, in our case the HiPerFect, to complex with our proteins, resulting in a successful protein transfection. Unfortunately, our VHHs having isoelectric points of 7.21 (C26), 8.91 (A37), and 7.02 (C26B) were therefore unlikely to be complexed with the HiPerFect, explaining the low transfection efficiency observed. The previous antibodies tested, 4C6 and F127-6G6 (Togtema et al. 2012), have never been sequenced (personal communication with Johannes Schweizer, Arbor Vita Corporation) and the tubulin antibody's sequence is proprietary. Therefore, their isoelectric points and the potential presence of anionic stretches is unknown and limited our ability to adapt the conditions of our VHH transfection accordingly.

The main issue we encountered with HiPerFect delivery of VHHs is that the amount of protein delivered would not allow any final analysis of the therapeutic effect of our molecules. The Coronavirus pandemic and the development of mRNA vaccines have popularized the use of mRNA molecules to treat disease as well as progressing the development of clinically approved mRNA delivery. Considering our ultimate goal is to deliver our VHHs as therapeutics, we

decided to focus our attention on this area of research in search of a more clinically suited transfection methodology.

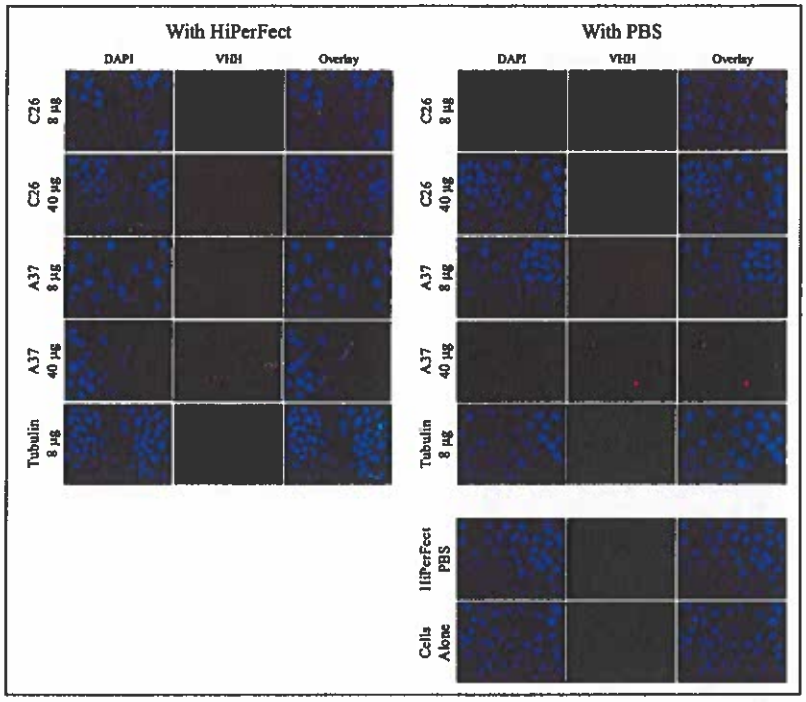

Figure 19. Immunodetection of C26 and A37 (8 µg/mL and 40 µg/mL) transfected in CaSki cells with 10 µL HiPerFect. With HiPerFect represents wells transfected with VHH + HiP. With PBS represents wells transfected with VHH + PBS to serve as a negative control for transfection. Tubulin wells were transfected with either Tubulin + HiP as a positive control, or Tubulin + PBS as a negative control. HiPerFect PBS and Cells Alone controls represent wells treated with HiP + PBS or only Complete DMEM media respectively, serving as controls for cell growth when exposed to HiPerFect or not respectively. VHHs were detected using 1:400 Alexa Fluor 594 + while tubulin was detected with 1:400 Alexa Fluor 488 Donkey anti-mouse IgG diluted in BSA. Nuclei were visualized using DAPI followed by imaging with the Zeiss Axiovert 200 fluorescence microscope equipped with an LD A-Plan 40x/0.50 Ph2 objective and a CCD camera with 12-bit capability and edited using ImageJ software version1.53a. Note that DAPI staining for A37 40 µg was similar to A37 µg, however representative images were taken in areas without cells to show similar red spots in the PBS control compared to the HiPerFect wells at the same concentration of VHH.

3.7.2 mRNA Transfection

Due to the coronavirus pandemic and the resulting vaccine development, we had a new technique to explore for the delivery of our VHHs to our target cells hoping to maximize transfection of out VHHs. mRNA transfection is a technique designed to allow RNA to enter a range of cell types, with minimal cellular toxicity. Delivering RNA opposed to DNA or protein avoids transcriptional regulation effects by delivering the RNA directly to the cytoplasm, where it can then be processed and expressed. Instead of using HiPerFect, these experiments will use the Mirus *Trans*IT-mRNA Transfection Kit, which has been used to deliver a variety of RNA molecules including mRNAs and viral RNAs. We ordered the C26 and A37 mRNA without any tags to avoid any tag-interference as they will be more similar to molecules used in a clinical context. The mRNA was produced by TriLink Biotechnologies with CleanCap® and a poly-A tail. Additionally, the mRNA was modified with 5-methooxyuridine, allowing for fast expression of the protein, and reduced innate immune response. We also selected these modifications as they were identical to the modifications present on their control mCherry mRNA, providing us with an ideal control for our experiments.

To prepare for our functional assays to follow, we evaluated C26 and A37 using the supplier protocol for a 48-well plate and the recommended RNA amount (1X) or two-times (2X) the recommend amount (250 ng or 500 ng) in chamber slides. We organized various controls along with the experimental samples; the conditions tested for both amounts of mRNA are referred to as the following: C26, A37, Both, mCherry, Reagent Alone (mRNA dilution storage buffer), and No Transfection. C26 and A37 refer to wells transfected with either C26 or A37 mRNA, while Both refers to wells transfected with C26 and A37 together. The mCherry wells have been transfected with mCherry mRNA, which when expressed displays a bright red

fluorescence under the microscope. Respectively, Transfection Reagent Alone and No Transfection represent negative controls to ensure the transfection reagent is not damaging or causing effects in the cells, and that the non-transfected cells were healthy.

Using 1X mRNA, strong signal was observed in experiment wells C26, A37, and Both indicating that the VHHs were transfected and expressed in all three cell types (Figure 20). Of the three cell types, the signals in CaSki appeared the least strong, followed by C33A and SiHa overall. As the positive control, mCherry showed very bright signals across all cell types, while the negative controls (Transfection Reagent Alone and No Transfection) showed little to no signal as expected (Figure 20). In the overlay, much of the observed signal was present in the nucleus of the cells, with residual signal observed inside and surrounding CaSki, SiHa and C33A cells. Overall, the transfection observed with 1X mRNA is quite strong compared to previous experiments with HiPerFect.

Using 2X mRNA for the transfection proved to successfully increase the signal observed in all cell lines for C26, A37, and Both (Figure 21) compared to when using 1X mRNA (Figure 20). As before, most of the signal in all cases was found to be nuclear, which is evident in observing the overlay for all cell types and experimental conditions. Some signal was also detected in the cytoplasm, which could be due to the abundant expression of the VHHs. As in the previous experiment, the mCherry control also displayed strong nuclear signals in all cell types, indicating a successful transfection. In comparison, the negative controls both Transfection Reagent Alone and No Transfection showed no signal present in any of the cell types. Overall, 60-80% of the cells were positive for the VHH after transfection depending on the cell type. Although the results for the 2X mRNA were brighter, the signal with 1X was more than

sufficient to allow us to perform functional assays. Therefore, we decided to use this condition for further experimentation.

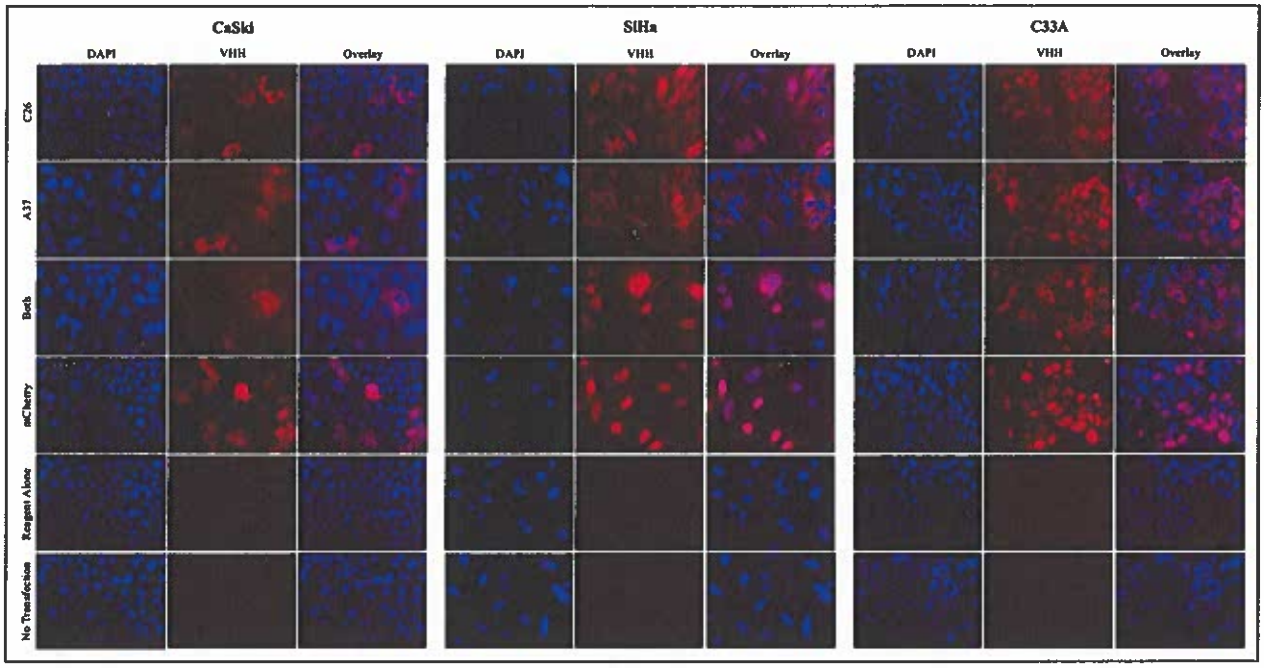

Figure 20. Immunodetection of C26, A37, and mCherry 48-hours after 1X (250 ng) mRNA transfection. 12 000 – 24 000 cells (CaSki, SiHa and C33A) were seeded 48-hours prior to transfection, with fresh media added 4-hours post transfection. Transfection was performed using the Mirus *Trans*IT-mRNA Transfection Kit following manufacturer protocols. 48-hours post transfection, slides were prepared for analysis. VHHs were detected using 1:400 Alexa Fluor 594 +. Nuclei were visualized using DAPI followed by imaging with the Zeiss Axiovert 200 fluorescence microscope equipped with an LD A-Plan 40x/0.50 Ph2 objective and a CCD camera with 12-bit capability and edited using ImageJ software version1.53a.

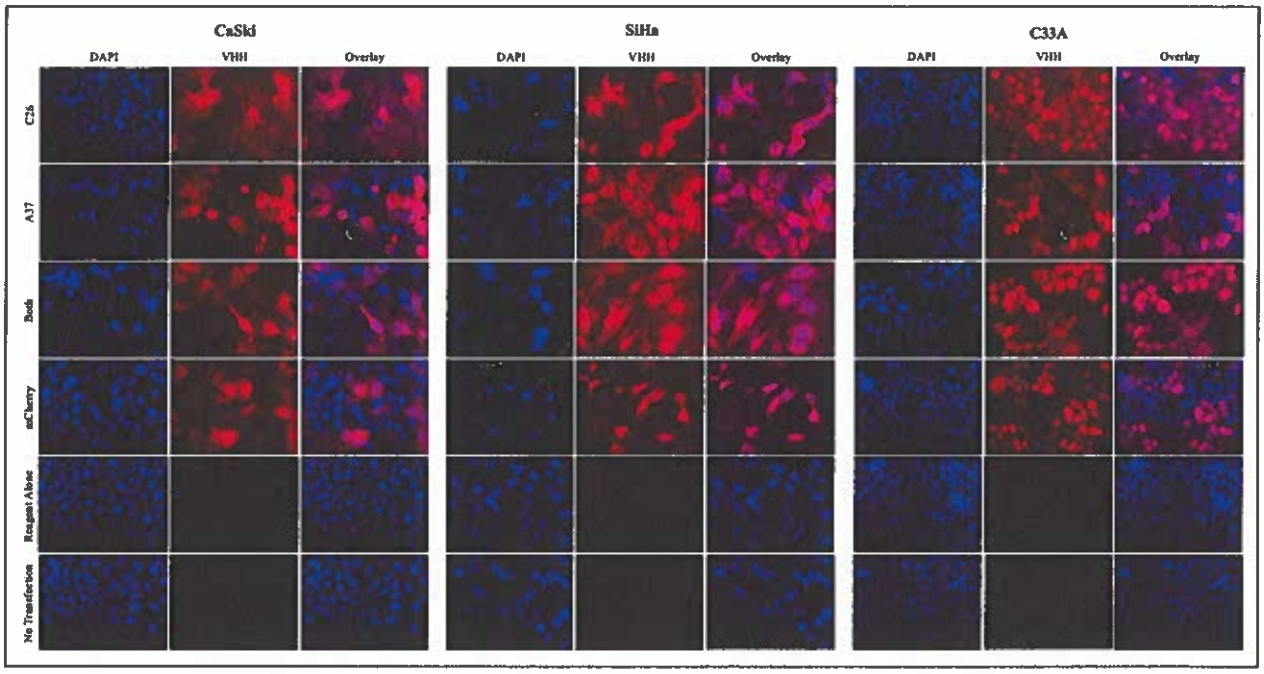

Figure 21. Immunodetection of C26, A37, and mCherry 48-hours after 2X (500 ng) mRNA transfection. 12 000 – 24 000 cells were seeded 48-hours prior to transfection, with fresh media added 4-hours post transfection. Transfection was performed using the Mirus *Trans*IT-mRNA Transfection Kit following manufacturer protocols. 48-hours post transfection, slides were prepared for analysis. VHHs were detected using 1:400 Alexa Fluor 594 +. Nuclei were visualized using DAPI followed by imaging with the Zeiss Axiovert 200 fluorescence microscope equipped with an LD A-Plan 40x/0.50 Ph2 objective and a CCD camera with 12-bit capability and edited using ImageJ software version1.53a.

3.8 Functional Assays

It is expected that antibodies blocking the E6 protein will influence p53 and restore its activity. Activation of p53 could lead to apoptosis induction which can be monitored by PARP-1 cleavage, an early marker of apoptosis. However, it has been observed in some instances that antibodies against the E6 protein reduce cell proliferation or induce apoptosis in a p53-independent manner (Lagrange et al. 2007). To account for all these possibilities, we performed proliferation assays using CaSki, SiHa, and C33A cells. Additionally, should our VHHs have a significant effect on p53 restoration, these differences may be observed at a single-cell level. To observe these cellular changes, after mRNA transfection of our VHHs to CaSki, SiHa, and C33A cells, we co-stained each slide with antibodies to detect p53 or PARP-1 cleavage alongside our regular VHH secondary antibodies. As a positive control for p53 activation and PARP-1 cleavage, we treated all cell types with Actinomycin D to elicit apoptosis. With this method, we can evaluate the number of cells successfully transfected with VHH, while observing if these cells show a difference in p53 expression or evidence of PARP-1 cleavage.

3.8.1 Proliferation Assays

Triplicate proliferation assays were performed to evaluate the cell viability 48-hours post mRNA transfection. Each mRNA transfection was performed on two HPV16 E6+ cells lines (CaSki and SiHa) as well as one HPV16 E6 – cell line (C33A) to account for any E6 independent side-effects caused by the VHHs. Each cell line was transfected with C26 mRNA, A37 mRNA, and both C26 and A37 mRNA. We anticipate that cells transfected with both C26 and A37 could allow multiple binding sites on the E6 protein to be targeted at once, facilitating the complete inactivation of the E6 protein. The mCherry mRNA, and sodium citrate (mRNA dilution storage

buffer) (Reagent Alone) transfection were used as controls as described above. Cells without transfection (No Transfection) were also analyzed as a baseline for comparison and normalization.

CaSki cells transfected with C26 mRNA showed a significant decrease in cell proliferation compared to cells transfected with A37 mRNA, C26 + A37 (Both) mRNA, and the mCherry mRNA control ($P<0.05$ for all; A37 $P=0.003$, C26+A37 $P=0.0002$, mCherry $P=0.03$), however no significant difference was observed compared to the Reagent Alone control ($P>0.05$) (Figure 22). Comparatively, SiHa cells transfected with C26 mRNA showed a significant decrease in cell proliferation compared to the Reagent Alone control, however no significant differences were observed compared to the mCherry control, A37 mRNA, or C26 + A37 (Both) mRNA ($P>0.05$) (Figure 22). C33A cells in all conditions showed no significant differences ($P>0.05$).

In our experiments, we used two controls (mCherry and Reagent Alone). These controls were used to assess the effect of the reagent on the cells as well as the effect caused by mRNA transfection. To consider that the VHHs had a therapeutic potential, the VHHs should have a significant effect compared to both controls. A37 and C26 + A37 (Both) did not significantly reduce the proliferation compared to the controls, while C26 significantly reduced proliferation in CaSki or SiHa. However, in both case it was only against one of the controls. Therefore, we can conclude that the VHH do not have a significant effect on cell proliferation overall. Nevertheless, the VHHs could have an effect at the single-cell level. Therefore, we performed single-cell analysis to see if p53 or PARP-1 cleavage was present in transfected cells.

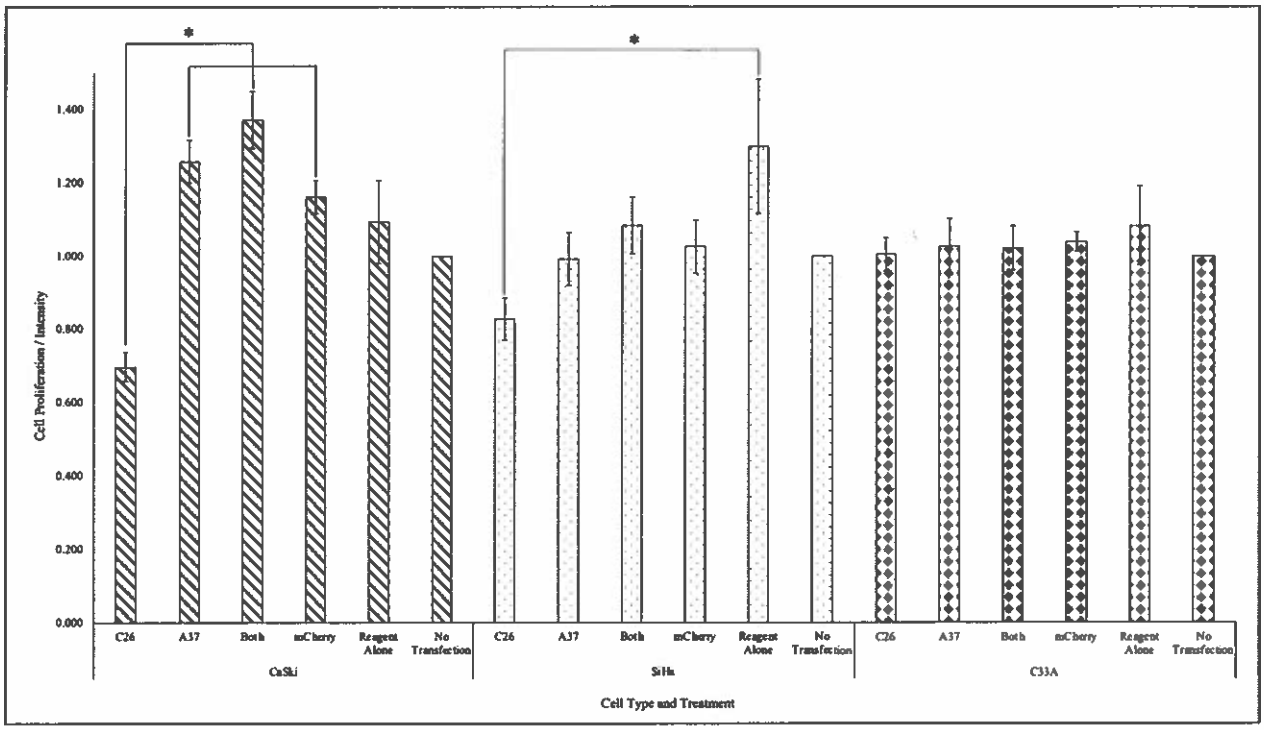

Figure 22. Cell proliferation 48-hours after mRNA transfection. Triplicate CCK8 proliferation assay data for CaSki, SiHa, and C33A were averaged and normalized against No Transfection (No Transfection = 1). mRNA transfection of C26 in CaSki cells significantly decreased cell proliferation compared to A37, C26 + A37 (Both), and mCherry ($P<0.05$ for all; A37 $P=0.003$, C26+A37 $P=0.0002$, mCherry $P=0.03$), however no significant difference was observed between C26 and the Reagent Alone control (transfection performed with mRNA dilution buffer only). mRNA transfection of C26 in SiHa cells significantly decreased cell proliferation compared to the Reagent Alone control ($P<0.05$; $P=0.02$), however no significant difference was observed between C26 and the mCherry control (transfection performed with mCherry mRNA). No significant differences in cell proliferation were observed in C33A. Statistical analysis was performed using a two-way ANOVA followed by Tukey's HSD contrasts post hoc. Data represent mean ± SEM. * denotes $P<0.05$.

3.8.2 Single-cell P53 and PARP-1 Cleavage Analysis: Actinomycin D

Before analyzing p53 and PARP-1 cleavage levels when transfected with our VHHs, we first confirmed that the p53 and PARP-1 antibodies could detect changes in p53 expression and PARP-1 cleavage. To do so, we treated cells with Actinomycin D, a known inducer of apoptosis.

As expected, untransfected cells treated with Actinomycin D showed increased expression of p53 and PARP-1 cleavage in all cell types compared to untreated cells (Figure 23). For p53, increased expression was easily observed in CaSki and SiHa cells (Figure 23A). C33A being a cervical cancer cell line overexpressing mutated p53, an abundant amount of p53 was present in both the untreated and treated samples as expected (Figure 23A). As for PARP-1 cleavage, increased expression was equally observed in all cell lines compared to the corresponding untreated cells (Figure 23B). Overall, these results confirm the functionality of our antibodies and our methodology allowing accurately analyze our experimental samples.

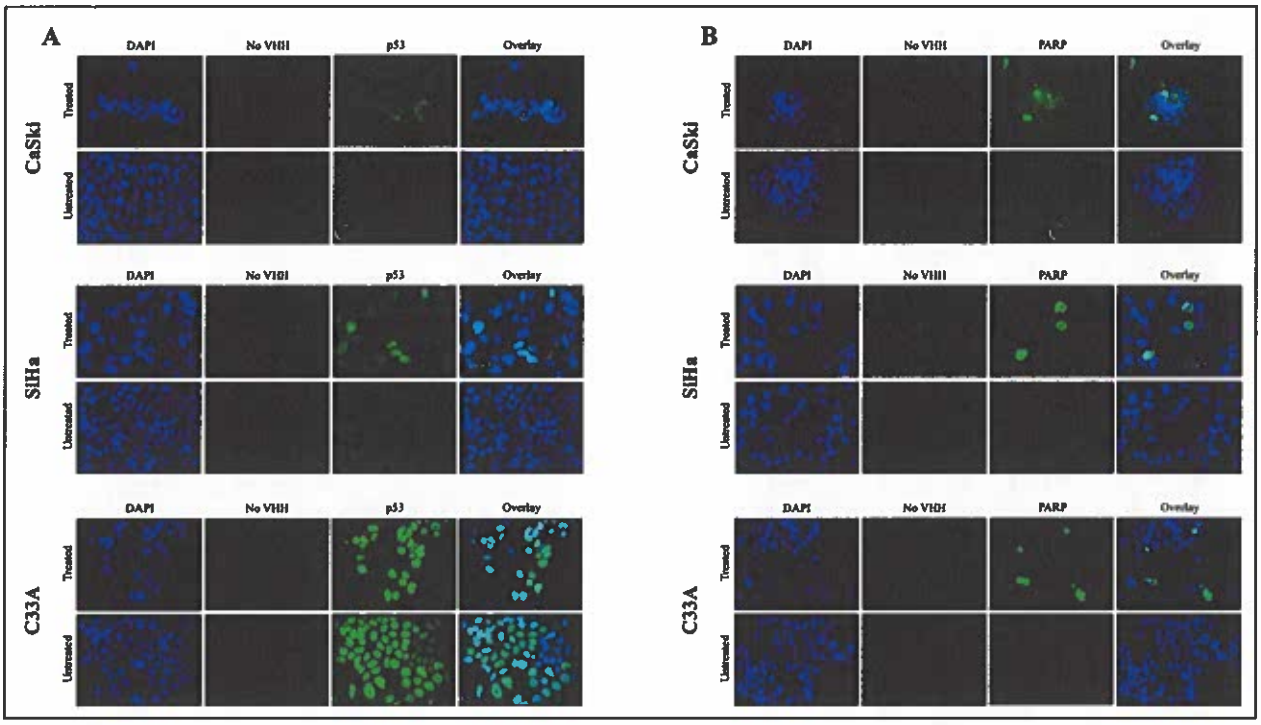

Figure 23. Immunodetection of p53 and PARP-1 cleavage in CaSki, SiHa, and C33A cells 24-hours after treatment with Actinomycin D. 12 000 – 24 000 cells were seeded 24-hours prior to treatment. After 24-hours, existing media was replaced with 300µL of Actinomycin D treatment solution (0.5µL/mL for CaSki and 0.05µL/mL for SiHa and C33A) and incubated for 24-hours. Following treatment, slides were prepared for analysis with p53 probed using 1:400 D01 p53 monoclonal antibody, PARP-1 probed using 1:760 Mouse mAb to cleaved PARP [4B5BD2], and both were detected using 1:400 Alexa Fluor 488 Donkey anti-mouse IgG. Nuclei were visualized using DAPI followed by imaging with the Zeiss Axiovert 200 fluorescence microscope equipped with an LD A-Plan 40x/0.50 Ph2 objective and a CCD camera with 12-bit capability and edited using ImageJ software version1.53a.

3.8.3 Single-cell P53 and PARP-1 Cleavage Analysis: Co-Staining Analyses

To observe changes in p53 and PARP-1 cleavage levels at a cellular level, after mRNA transfection of our VHHs to CaSki, SiHa, and C33A cells, each slide was co-stained with antibodies to detect p53 or PARP-1 cleavage alongside the VHH.

As expected, the VHH and mCherry were successfully transfected in all cell types as observed in Figure 24 and 25, lane "VHH", by the abundance of red signal detected. Additionally, no signal was observed in the Reagent Alone and No Transfection controls as no antibody was transfected in these samples (Figure 24 and 25). We observed that the signal was detected in the nucleus and/or cytoplasm of the transfected cells, indicating that the VHHs can enter the nucleus by passive diffusion. As seen in our previous 1X mRNA transfection results (Figure 20), of the three cell types, the signals in CaSki appeared the least strong, followed by C33A and SiHa overall (Figure 24 and 25).

We then observed the levels of p53 and PARP-1 cleavage in the different treated cells. No obvious differences were observed between the different cells and conditions when comparing the VHH positive cells and the VHH negative cells. Furthermore, although some cells are bright red suggesting abundant VHH expression, this is not associated with greener signal corresponding to p53 or PARP-1 cleavage (Figure 24 and 25). Finally, we also monitored the presence of pyknotic nuclei indicative of cell undergoing apoptosis. Taken together, these data indicate that the VHHs do not restore p53 activity, do not induce PARP-1 cleavage, and do not trigger apoptosis in the treated cells.

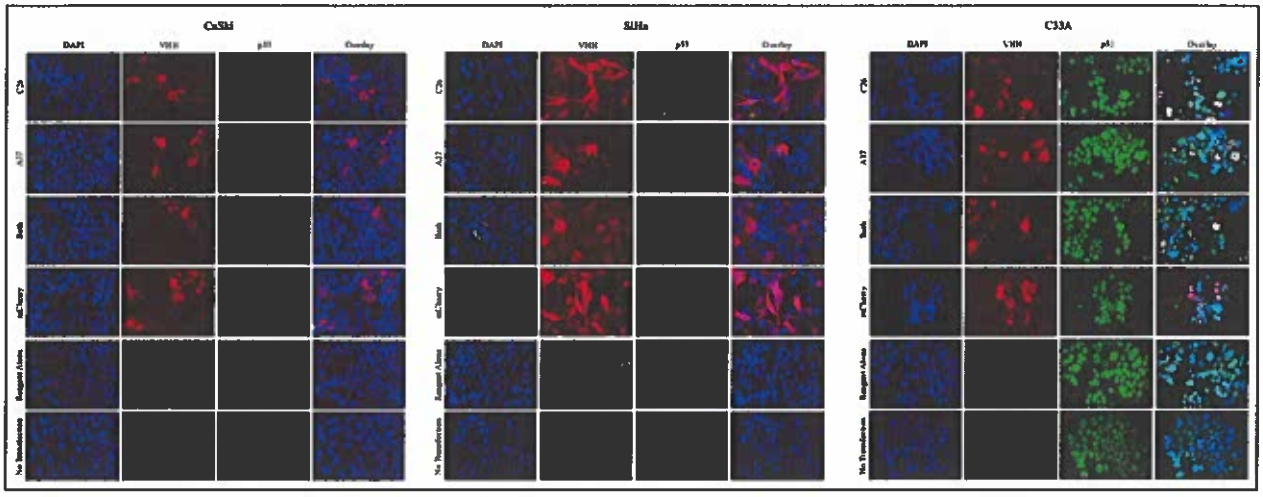

Figure 24. Immunodetection of 1X (250 ng) C26, A37, and mCherry (red) and related p53 expression (green) in CaSki, SiHa, C33A cell lines 48-hours after mRNA transfection. 12 000 – 24 000 cells were seeded 48-hours prior to transfection, with fresh media added 4-hours post transfection. Transfection was performed using the Mirus *Trans*IT-mRNA Transfection Kit following manufacturer protocols. 48-hours post transfection, slides were prepared for analysis. VHHs were detected using 1:400 Alexa Fluor 594 + while p53 was probed using 1:400 D01 p53 monoclonal antibody and detected using 1:400 Alexa Fluor 488 Donkey anti-mouse IgG. Nuclei were visualized using DAPI followed by imaging with the Zeiss Axiovert 200 fluorescence microscope equipped with an LD A-Plan 40x/0.50 Ph2 objective and a CCD camera with 12-bit capability and edited using ImageJ software version1.53a.

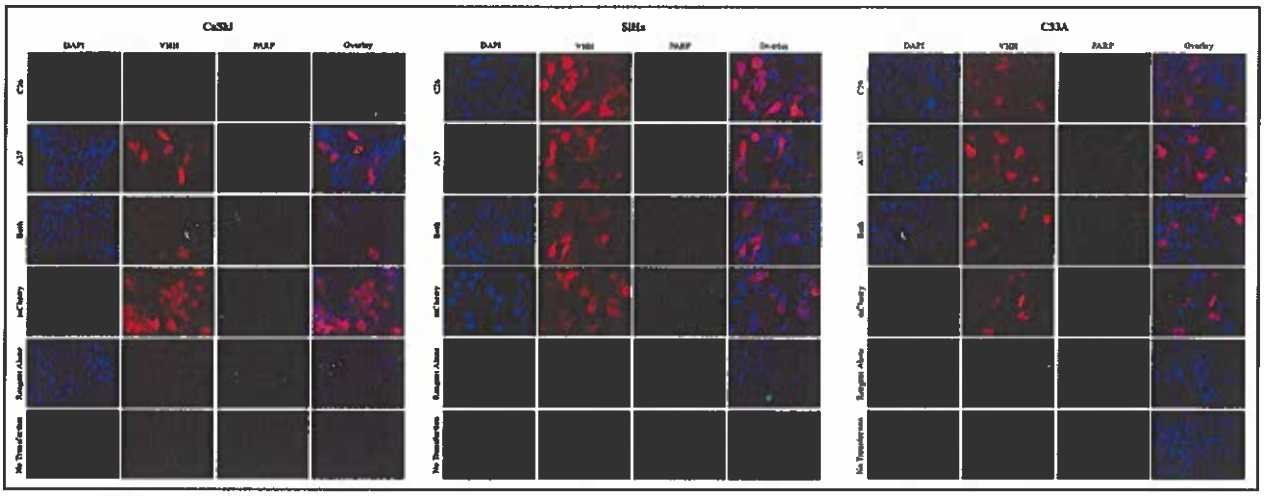

Figure 25. Immunodetection of 1X (250 ng) C26, A37, and mCherry and related PARP-1 cleavage in CaSki, SiHa, C33A cell lines 48-hours after mRNA transfection. 12 000 – 24 000 cells were seeded 48-hours prior to transfection, with fresh media added 4-hours post transfection. Transfection was performed using the Mirus *Trans*IT-mRNA Transfection Kit following manufacturer protocols. 48-hours post transfection, slides were prepared for analysis. VHHs were detected using 1:400 Alexa Fluor 594 + while PARP-1 was probed using 1:760 Ms mAb to cleaved PARP [4B5BD2] and detected using 1:400 Alexa Fluor 488 Donkey anti-mouse IgG. Nuclei were visualized using DAPI followed by imaging with the Zeiss Axiovert 200 fluorescence microscope equipped with an LD A-Plan 40x/0.50 Ph2 objective and a CCD camera with 12-bit capability and edited using ImageJ software version1.53a.

4 DISCUSSION

Persistent infection with high-risk types of HPV, such as HPV16, is the leading cause of cervical cancer worldwide, as well as an increasing number of head and anogenital malignancies affecting all genders (Senkomago et al. 2019, Van Dyne et al. 2018). Once infected, the virus begins to express crucial oncoproteins known as E6 and E7 in the host cells, the main culprits in HPV carcinogenesis. Continued expression of such oncoproteins promotes tumorigenesis through the immortilization and malignant transformation of infected cells mainly including the E6- or E7-dependent degradation of host cellular proteins leading to viral infection, persistence, and tumour promotion (Ghittoni et al. 2010, Vandepol et al. 2013, Togtema et al. 2019). Mechanistically, while E7 triggers cell proliferation by degrading pRB, the E6 protein inactivates the resulting p53-dependent apoptotic response by degrading the p53 protein in an E6AP dependent manner (Hoppe-Seyler et al. 2018). For this reason, it is anticipated that moleules inactivating E6 will restore p53 activity, leading infected cells to apoptosis. Over the years, many antibodies targeting the E6 protein have been developed, including conventional antibodies, scFvs, and VHHs, however, to the best of our knowledge, none have made the clinical transition. Our lab, as reported in Togtema et al. 2012, has previously evaluted monoclonal antibodies against the E6 protein using cationic lipids and sonoporation delivery. Using these methods, p53 expression was restored however no apoptosis was observed (Togtema et al. 2012). It has been hypothesized that the lack of apoptosis was due to the fact that only a single site on the E6 protein, and only cytoplasmic E6, were targetted (Togtema et al. 2012, 2019). E6 is known to interact with more than 50 host proteins using different binding sites (reviewed in Dayer et al. 2020, and references therein) and to exert most of its function in the nucleus of the infected cells (Togtema et al. 2019). In an attempt to overcome both issues, our lab generated several anti-E6

llama-derived VHHs whose small size of roughly ~15 kDa would allow them to enter the nucleus by passive diffusion. These VHHs showed binding affinity to recombinant E6 proteins in various assays including dot blot, western blot under non-denaturing conditions, surface plasmon resonance, and ELISA (Togtema et al. 2019). The objective of our current project was to further evaluate the binding ability of these VHHs to the endogenous E6 protein, while exploring their therapeutic potential and aptitude for diagnostics.

4.1 Work with Recombinant E6 Proteins

We have previously shown that the VHHs have varying binding affinity to different recombinant E6 proteins (E6 6C/6S, MBP, F47R, 4C/4S). In the current study, we have confirmed our results in triplicate for six of the most promising candidates (C26, A37, A46, 2A03, 2A04, and A05) (Figure 17). Interesting results were obtained with C26, the VHH previously described as an MBP binder, however using a more specific VHH secondary antibody and the addition of the untagged E6 protein has shown that C26 can bind the E6 protein and MBP most likely using two independent CDR regions. It has been shown that 30% of the VHH can interact with their target protein using only a subset of their CDR regions (Mitchell and Colwell 2018). However, it has not been suggested that VHHs could interact with two different proteins through different CDR regions simultaneously. To confirm our hypothesis, dot blots were performed with the results showing that in the presence of MBP and untagged E6, C26 favours binding to the folded E6 protein (Figure 17). On the other hand, in western blot experiments under denaturing conditions, C26 is capable of detecting the linearized MBP protein, but not the linearized E6 protein (Figure 18). Since the CDR3 regions are known to be more specific, have higher affinity for their target, and bind folded epitopes, while the CDR 1

and 2 regions are less specific and can bind only a linearized epitope (Mitchell and Colwell 2018), we conclude that C26 most likely interacts with E6 through its CDR3 region, and with MBP through either the CDR 1 or 2 regions. To the best of our knowledge, VHHs binding two different proteins using independent CDR regions have not been described. However, this peculiar C26 property is most likely due to the antibody selection process in ELISA using MBP-E6. This result indicates that the presence of the MBP-tag could have interferred with the antibody selection, which is also supported by the results obtained with 2A17 which interacts strongly with MBP-E6 but only provides extremely weak results with MBP and E6 alone (E6 6C/6S) (Figure 3).

Our VHHs were selected using MBP-E6 proteins as recombinant E6 proteins are renown to be unsoluble and have the tendency to aggregate. Therefore, antibodies produced against E6 proteins have been consistently selected using recombinant tagged E6 proteins. Giovane et al. 1999 produced three mouse monoclonal antibodies (6F4, 1F1, 4C6) using BALB/c mice immunized with glutathione S-transferase (GST)-E6 and selected in ELISA using MBP-E6 and GST-E6. Only 4C6 was capable of restoring p53 expression but without the induction of apoptosis (Courtête et al. 2007, Togtema et al. 2012). Lagrange et al. 2005 also produced three mouse monoclonal antibodies (1F5, 3B8, 3F8) against the C-terminal zinc-binding domain of the E6 protein using MBP-tagged E6 for the mouse immunization, however, none of them have shown p53 restoration capacity (Courtête et al. 2007, Lagrange et al. 2005). The scFv GTE6 was selected using MBP- or GST-E6 (Griffin et al. 2006) and the Nb9 VHH was selected using SUMO-E6 (Zhang et al. 2021), both inducing limited apoptosis. Our current data indicates that the presence of a tag during the immunization and/or antibody selection strongly interferes with the specficity of the antibody selected. It remains unclear if the generation of the above

antibodies was also negatively impacted by the use of tagged proteins as none of these antibodies fully achieved their anticipated effects. Our results strongly suggest that further generation of antibodies against the E6 protein should discontinue the use of tagged E6 and prioritize proteins such as E6 6C/6S. Alternatively, a method has been recently proposed to produce unmutated recombinant histidine-tagged E6 proteins which could be another solution (Illiano et al. 2016). Nevertheless, we believe that further antibody development should priortize such proteins, and scFvs or VHHs libraries that have been already developed could be re-screened using these proteins. It is worth mentioning that the MBP, GST, or SUMO tags are commonly used for the production of nanobodies in particular and for the production of recombinant proteins in general (Liu et al. 2018). Although such tags could help the solubility of the protein and ease their purification, our current data strongly suggests that such approaches should be considered carefully for the production of recombinant proteins used for immunization or selection of antibodies.

4.2 Binding to the Endogenous Protein

Although the VHHs have shown binding capacity to recombinant E6 proteins, these proteins have mutations or tags that are not found in mammalian cells expressing E6 such as CaSki and SiHa. Therefore, it was essential for us to determine if these VHHs could immunoprecipitate E6 from such cell lines. Initial experiments were performed using magnetic beads coated with anti-HA to take advantage of the HA-tag on the VHHs. Experiments were performed during my undergraduate degree, but no E6 immunoprecipitation was observed. We hypothesized that the binding of the anti-HA antibody to the VHHs was interferring with the binding of the VHH to E6. The size of the anti-HA antibody (150 kDa) is roughly 10X the size of the VHHs (~15 kDa) and E6 (~18 kDa). Therefore, we instead evaluated Affi-Gel resin as a

support to immobilize the VHHs. The resin binds any protein via their primary amine group found on the lysine side chain and the amino terminal. The VHHs will be bound in different orientations (one per binding site), but we anticipated that at least one of these orientations would allow the VHH to capture the E6 protein. We used this method to evaluate which of our previously produced VHHs could immunoprecipitate endogenous E6 protein in CaSki cells. Using this method, we identified C26 and A37 as our best candidates, immunoprecipitating E6 in triplicate with our optimized protocol (Figure 14). With this protocol, we had very good binding of the VHHs to the resin and clean controls overall. Although C26 and A37 interact with E6, the amount of E6 immunoprecipitated remains fairly low which could indicate that the VHHs have limited binding affinity to the E6 protein. To improve our results, a potential strategy would be to increase the amount of VHH bound to the resin, however this could lead to increased amounts of VHHs released during the elution which could ultimately lead to more unspecific bands. Alternatively, increasing the affinity of the antibodies to E6 appears to be a more interesting approach.

Based on our results, the VHHs bind the folded E6 protein which could correspond to the different zinc binding domains of E6. These domains are also known to be interacting site for various host E6 partners, such as E6AP or p53 (reviewed in Dayer et al. 2020). It can be speculated that binding the E6 protein in living cells, the VHHs may have to compete with host proteins for their binding site. Further work should therefore focus on characterizing the exact VHH sequences that interact with E6. In addition, the binding affinity of the VHHs should be evaluated in similar surface plasmon resonance experiments as previously described by Togtema et al. 2019, however using untagged recombinant E6 proteins such as E6 6C/6S. Finally, competition assays should be performed to evaluate the binding of the VHHs to E6 6C/6S in the

presence of recombinant host proteins competing for the same binding site. Such experiments were performed using 3F8, 3B8, 1F5, and 6F4 using recombinant E6, E6AP, and p53 proteins (Lagrange et al. 2005). To increase the binding affinity of the VHHs to E6, point mutations could be inserted into the VHH paratope to increase its affinity to the epitope in order to overcome the interaction of E6 with its main host targets. Such optimization will not only increase the amount of E6 immunoprecipitated, but also increase their therapeutic potential. Additionally, our results indicate that at least one C26 CDR region interacts with MBP. To further optimize C26, mutations of the CDR region should be made to disrupt C26 binding to MBP.

Nevertheless, with our current protocol, we have been able to capture the E6 protein, which is relevant for the study of E6 interactors. E6 interactome studies have been perfomred using cells expressing the E6 protein with an N-terminal or C-terminal tag. Of interest, such tags are found in the linear part of the E6 protein and the presence of the tag has been shown to interfere with E6 binding to certain host proteins, such as p53 (N-terminal). Therefore, scientists have strongly favoured tagging the C-terminal part of the protein which however interferes with PDZ-binding proteins (C-terminal) (Dayer et al. 2020, White et al. 2012). C26 and A37 are unlikely to bind the C- or N-terminal regions of the protein, indicating that their use in E6 interactome studies could potentially lead to the identification of new E6 interactors.

4.3 VHH Delivery and Functional Assays

To determine if our proteins have a therapeutic potential, our first step was to efficiently deliver our VHHs to HPV+ cells. Our initial approach was to use the HiPerFect reagent as it has been successfully used for the delivery of mouse monoclonal antibodies against the E6 protein

(Courtête et al. 2007, Togtema et al. 2012). Nevertheless, this approach did not prove successful with our VHHs, most likely due to their high isoelectric point and the characteristics of the HiPerFect transfection reagent (Figure 19, Appendix B). In our original strategy, we were interested in evaluating sonoporation as this method is more efficient for the delivery of proteins (Togtema et al. 2012). Unfortunately, key components of the methodology developed in our lab were no longer available, notably the Nunc Opticell cell culture chambers, which are not commercially available. Furthermore, due to covid restrictions, our collaborator Dr. Laura Curiel was not able to travel to Thunder Bay as much as anticipated when designing these experiements. Therefore, we investigated other approaches that are also clinically relevant. The two other strategies will be based on DNA or mRNA delivery.

As discussed in Soetens et al. 2020, the transfection of DNA plasmids containing coding sequences is one of the most straightforward and low-cost delivery methods to express a protein intracellularly. Although this may be true in research settings, transfected plasmid DNA is not easily transferrable to in vivo or clinical trials. The main concern when discussing DNA transfection surrounds insertional mutagenesis in vivo, during which the injected plasmid DNA may integrate into the genome of host somatic cells. Interestingly, delivery of mRNA has many advantages over DNA and conventional antibody delivery methods, as it allows transient and rapid expression of the encoded therapeutic antibody within the target organ, a reduction of the administered dose, and minimal risk of toxicity (Soetens et al. 2020). Additionally, one very important advantage to note is the potential increase in transfection efficiency with mRNA compared to DNA plasmid delivery. For successful plasmid DNA transfection, the plasmid must be situated in the nucleus and then be transcribed to mRNA, which depends on many factors including the cell cycle itself. However, with mRNA transfection, once the mRNA has reached

the cytoplasm it can be translated immediately to produce the desired antibody. More importantly, unlike DNA plasmids, mRNA does not need to integrate into the genome and therefore does not risk insertional mutagenesis, overcoming this common concern with plasmid DNA delivery (Zhou et al. 2020, Moradian et al. 2020). Therefore, we evaluated mRNA delivery of our VHHs to our cells of interest using the Mirus *Trans*IT-mRNA transfection reagents. Using this method, a transfection efficiency of more than 50% was obtained in each cell line investigated (Figure 20 and 21), allowing us to proceed with the functional assays. Additionally, we also observed that the VHHs were localizing within the nucleus, confirming their ability to enter the organelle by passive diffusion. This result confirms our hypothesis and is relevant for other scientists developing E6 based targeting strategies.

Although antibodies against the E6 protein are anticipated to re-establish p53, some molecules produced against E6 have been shown to induce apoptosis without restoring p53 (Lagrange et al. 2007). To account for all possibilities, we first performed proliferation assays to determine if the VHHs independently or in combination were capable of inducing an effect. Our rationale of targeting E6 with both VHHs (listed as Both in all experiements) was based on the fact that these molecules have different CDR region sequences indicating that they will bind different epitopes. Unfortunately, despite being able to interact with the endogenous E6 protein, the VHHs did not have a siginificant effect on cell proliferation compared to both controls (Figure 22). This is most likely due to low binding affinity of the VHHs to the E6 protein. As mentioned previously, further optimization of the VHHs would be needed to increase their therapeutic potential. Future work could revisit the proliferation assays to explore C26 mRNA transfection in a dose dependent manner. This could be done by transfecting various concentrations of C26 mRNA and evaluating its effects on cell proliferation, as it is possible that

higher concentrations may be required to see a significant effect. Another consideration is the cell lines evaluated in our experiments. Cells such as CaSki and SiHa have been extensively used in cell culture for several decades and it remains unclear how many mutations have occurred during that period and if these cell lines still represent cancer cells identified in the patient. Therefore, future evaluation should include newly generated cell lines by transducing the HPV genome in keratinocytes, as such cell lines may be a better representation of cervical cancer patients. Despite these results, we investigated if the VHHs had any effect at a single-cell level by evaluating p53 and PARP-1 cleavage activity in transfected cells. As anticipated based on the proliferation assay, we did not observe any p53 restoration, PARP-1 cleavage, or pyknotic nuclei in the treated cells. Nevertheless, we have developed a methodology that could be used in further experimentation to evaluate similar molecules.

5 CONCLUSIONS AND FUTURE DIRECTIONS

The objective of the current project was to evaluate the binding capacity of our VHHs and their therapeutic potential. We successfully established that a subset of our molecules is capable of binding and immunoprecipitating the endogenous E6 protein. However, none of them were capable of inducing apoptosis of the infected cells. Nevertheless, C26 appeared to have significantly reduced the proliferation of CaSki and SiHa cells but not the C33A cells. In contrast, A37 did not show any reduction of proliferation in any cell type. Taken together, these results suggest that C26 will be a better candidate for further optimization. However, C26 may need a great deal of optimization to increase its affinity and remove its unspecific binding. Therefore, a more well-suited approach would be to re-screen the original VHH library using an untagged E6 protein, such as E6 6C/6S, likely to provide more specific VHHs against the E6 protein. In the current project, we have developed a pipeline for evaluating such molecules for their binding capacity to the endogenous protein and the evaluation of their therapeutic potential, creating a path which could be followed by other researchers to continue the search for HPV-related cancer therapeutics.

Nevertheless, the C26 VHH could also be used in other applications, including diagnostics. Immunoprecipitation kits including antibodies against a specific protein are commonly used in molecular biology and research. Recently, an increasing amount of such kits are VHH-based instead of monoclonal antibody-based. The development of such kits using the C26 antibody could support the research on E6 as well as being adaptable for diagnostic purposes. Cervical cancer especially affects women in isolated areas or with low-income who do not have access to regular PAP tests. Companies such as Arbor Vita Corporation have developed easy to use kits for HPV-screening based on monoclonal antibodies. Such kits could be stored at

4 °C and do not require specific equipment. These are important advantages compared to DNA screening which is commonly used in hospital settings and requires highly trained personnel and costly equipment. The development of protein-based screening kits would benefit from a protein like C26 as VHHs are both more specific and stable compared to monoclonal antibodies and can be expressed in bacteria making the cost of production far lower in comparison. This could allow the production of screening kits which would be cheaper to produce and have a longer shelf-life facilitating access and increasing screening in isolated areas.

6 REFERENCES

Amici C., Visintin M., Verachi F., Paolini F., Percario Z., Di Bonito P., Mandarino A., Affabris E., Venuti A., Accardi L. 2016. A novel intracellular antibody against the E6 oncoprotein impairs growth of human papillomavirus 16-positive tumor cells in mouse models. Oncotarget. 7, 15539-15553.

Canadian Cancer Statistics 2016 Special topic: HPV-associated cancers. Government of Canada, Canadian Cancer Society, Statistics Canada, Public Health Agency of Canada, Provincial/Territorial Cancer Registries. 2016. Accessed at: https://www.cancer.ca/~/media/cancer.ca/CW/cancer%20information/cancer%20101/Canadian%20cancer%20statistics/Canadian-Cancer-Statistics-2016-EN.pdf?la=en on April 25, 2022.

Chen Z., Terai M., Fu L., Herrero R., DeSalle R., Burk RD. 2005. Diversifying selection in human papillomavirus type 16 lineages based on complete genome analyses. J Virol. 79, 7014-7023.

Clifford GM., Rana RK., Franceschi S., Smith JS., Gough G., Pimenta JM. 2005. Human papillomavirus genotype distribution in low-grade cervical lesions: comparison by geographic region and with cervical cancer. Cancer Epidemiol Biomarkers Prev. 14, 1157-1164.

Courtête J., Sibler AP., Zeder-Lutz G., Dalkara D., Oulad-Abdelghani M., Zuber G., Weiss E. 2007. Suppression of cervical carcinoma cell growth by intracytoplasmic codelivery of anti-oncoprotein E6 antibody and small interfering RNA. Mol Cancer Ther. 6, 1728-1735.

Dayer G., Masoom ML., Togtema M., Zehbe I. 2020. Virus-Host Protein-Protein Interactions between Human Papillomavirus 16 E6 A1 and D2/D3 Sub-Lineages: Variances and Similarities. Int J Mol Sci. 21, 7980.

D'Souza G., Dempsey A. 2011. The role of HPV in head and neck cancer and review of the HPV vaccine. Prev Med. 53 Suppl 1, S5-S11.

Freund G., Sibler AP., Desplancq D., Oulad-Abdelghani M., Vigneron M., Gannon J., Van Regenmortel MH., Weiss E. 2013. Targeting endogenous nuclear antigens by electrotransfer of monoclonal antibodies in living cells. MAbs. 5, 518-522.

Ghittoni R., Accardi R., Hasan U., Gheit T., Sylla B., Tommasino M. 2010. The biological properties of E6 and E7 oncoproteins from human papillomaviruses. Virus Genes. 40, 1-13.

Giovane C., Trave G., Briones A., Lutz Y., Wasylyk B., Weiss E. 1999. Targeting of the N-terminal domain of the human papillomavirus type 16 E6 oncoprotein with monomeric ScFvs blocks the E6-mediated degradation of cellular p53. J Mol Recognit. 12, 141-152.

Griffin H., Elston R., Jackson D., Ansell K., Coleman M., Winter G., Doorbar J. 2006. Inhibition of papillomavirus protein function in cervical cancer cells by intrabody targeting. J Mol Biol. 355, 360-378.

Han H., Lee H., Kim K., Kim H. 2017. Effect of high intensity focused ultrasound (HIFU) in conjunction with a nanomedicines-microbubble complex for enhanced drug delivery. J Control Release. 266, 75-86.

Harmsen MM., Ruuls RC., Nijman IJ., Niewold TA., Frenken LG., de Geus B. 2000. Llama heavy-chain V regions consist of at least four distinct subfamilies revealing novel sequence features. Mol Immunol. 37, 579-590.

Hoppe-Seyler K., Bossler F., Braun JA., Herrmann AL., Hoppe-Seyler F. 2018. The HPV E6/E7 Oncogenes: Key Factors for Viral Carcinogenesis and Therapeutic Targets. Trends Microbiol. 26, 158-168.

Illiano E., Demurtas OC., Massa S., Di Bonito P., Consalvi V., Chiaraluce R., Zanotto C., De Giuli Morghen C., Radaelli A., Venuti A., Franconi R. 2016. Production of functional, stable, unmutated recombinant human papillomavirus E6 oncoprotein: implications for HPV-tumor diagnosis and therapy. J Transl Med. 14, 224

Kang TH., Seong BL. 2020. Solubility, Stability, and Avidity of Recombinant Antibody Fragments Expressed in Microorganisms. Front Microbiol. 11, 1927.

Kanodia S., Fahey LM., Kast WM. 2007. Mechanisms used by human papillomaviruses to escape the host immune response. Curr Cancer Drug Targets. 7, 79-89.

Lagrange M., Boulade-Ladame C., Mailly L., Weiss E., Orfanoudakis G., Deryckere F. 2007. Intracellular scFvs against the viral E6 oncoprotein provoke apoptosis in human papillomavirus-positive cancer cells. Biochem Biophys Res Commun. 361, 487-492.

Lagrange M., Charbonnier S., Orfanoudakis G., Robinson P., Zanier K., Masson M., Lutz Y., Trave G., Weiss E., Deryckere F. 2005. Binding of human papillomavirus 16 E6 to p53 and E6AP is impaired by monoclonal antibodies directed against the second zinc-binding domain of E6. J. Gen. Virol. 86, 1001–1007

Li S, Hong X, Wei Z, Xie M, Li W, Liu G, Guo H, Yang J, Wei W, Zhang S. Ubiquitination of the HPV Oncoprotein E6 Is Critical for E6/E6AP-Mediated p53 Degradation. Front Microbiol. 2019 Oct 31;10:2483. doi: 10.3389/fmicb.2019.02483. PMID: 31749782; PMCID: PMC6842930.

Liu Z., Huang D., Fu X., Cheng P., Du E. 2018. Comparison of three commonly used fusion tags for the expression of nanobodies in the cytoplasm of *Escherichia coli*. Biotechnol. Biotechnol. Equip. 32, 462-469.

Lu RM., Hwang YC., Liu IJ., Lee CC., Tsai HZ., Li HJ., Wu HC. 2020. Development of therapeutic antibodies for the treatment of diseases. J Biomed Sci. 27, 1.

Masson M., Hindelang C., Sibler AP., Schwalbach G., Travé G., Weiss E. 2003. Preferential nuclear localization of the human papillomavirus type 16 E6 oncoprotein in cervical carcinoma cells. J Gen Virol. 84, 2099-2104.

Meissner JD. 1999. Nucleotide sequences and further characterization of human papillomavirus DNA present in the CaSki, SiHa and HeLa cervical carcinoma cell lines. J. Gen. Virol. 80, 1725–1733.

Mitchell LS., Colwell LJ. 2018. Analysis of nanobody paratopes reveals greater diversity than classical antibodies. Protein Eng Des Sel. 31, 267-275.

Moradian H., Roch T., Lendlein A., Gossen M. 2020. mRNA Transfection-Induced Activation of Primary Human Monocytes and Macrophages: Dependence on Carrier System and Nucleotide Modification. Sci Rep. 10, 4181.

Pattillo RA., Hussa RO., Story MT., Ruckert AC., Shalaby MR., Mattingly RF. 1977. Tumor antigen and human chorionic gonadotropin in CaSki cells: A new epidermoid cervical cancer cell line. Science 196, 1456–1458.

Postupalenko V., Sibler AP., Desplancq D., Nominé Y., Spehner D., Schultz P., Weiss E., Zuber G. 2014. Intracellular delivery of functionally active proteins using self-assembling pyridylthiourea-polyethylenimine. J Control Release. 178, 86-94.

Rui M., Chen Y., Zhang Y., Ma D. 2002. Transfer of anti-TFAR19 monoclonal antibody into HeLa cells by in situ electroporation can inhibit the apoptosis. Life Sci. 71, 1771-1778.

Sanofi Press Release, FDA Approves Cablivi® (Caplacizumab-Yhdp), the First Nanobody®-Based Medicine, for Adults with Acquired Thrombotic Thrombocytopenic Purpura (aTTP). Available online: http://hugin.info/152918/R/2233733/878824.pdf (accessed on April 25 2022).

Sarker A., Rathore AS., Gupta RD. 2019. Evaluation of scFv protein recovery from E. coli by in vitro refolding and mild solubilization process. Microb Cell Fact. 18, 5.

Senkomago V., Henley SJ., Thomas CC., Mix JM., Markowitz LE., Saraiya M. 2019. Human Papillomavirus-Attributable Cancers - United States, 2012-2016. MMWR Morb Mortal Wkly Rep. 68, 724-728.

Sibler AP., Nordhammer A., Masson M., Martineau P., Travé G., Weiss E. 2003. Nucleocytoplasmic shuttling of antigen in mammalian cells conferred by a soluble versus insoluble single-chain antibody fragment equipped with import/export signals. Exp Cell Res. 286, 276-287.

Slastnikova TA., Ulasov AV., Rosenkranz AA., Sobolev AS. 2018. Targeted Intracellular Delivery of Antibodies: The State of the Art. Front Pharmacol. 9, 1208.

Soetens E., Ballegeer M., Saelens X. 2020. An Inside Job: Applications of Intracellular Single Domain Antibodies. Biomolecules. 10, 1663.

Togtema M., Pichardo S., Jackson R., Lambert PF., Curiel L., 2012. Zehbe I. Sonoporation delivery of monoclonal antibodies against human papillomavirus 16 E6 restores p53 expression in transformed cervical keratinocytes. PLoS One. 7, e50730.

Togtema M., Hussack G., Dayer G., Teghtmeyer MR., Raphael S., Tanha J., Zehbe I. 2019. Single-Domain Antibodies Represent Novel Alternatives to Monoclonal Antibodies as Targeting Agents against the Human Papillomavirus 16 E6 Protein. Int J Mol Sci. 20, 2088.

Trenevska I., Li D., Banham AH. 2017. Therapeutic Antibodies against Intracellular Tumor Antigens. Front Immunol. 8, 1001.

United States Cancer Statistics - Incidence: 1999 - 2016, WONDER Online Database. United States Department of Health and Human Services, Centers for Disease Control and Prevention and National Cancer Institute; 2019. Accessed at http://wonder.cdc.gov/cancer-v2016.html on April 25, 2022.

Van Dyne EA., Henley SJ., Saraiya M., Thomas CC., Markowitz LE., Benard VB. 2018. Trends in Human Papillomavirus-Associated Cancers - United States, 1999-2015. MMWR Morb Mortal Wkly Rep.67, 918-924.

Vande Pol SB., Klingelhutz AJ. 2013. Papillomavirus E6 oncoproteins. Virology. 445, 115-37.

Vats A, Trejo-Cerro O, Thomas M, Banks L. Human papillomavirus E6 and E7: What remains? Tumour Virus Res. 2021 Jun;11:200213. doi: 10.1016/j.tvr.2021.200213. Epub 2021 Feb 8. PMID: 33716206; PMCID: PMC7972986.

Wang R., Brattain MG. 2007. The maximal size of protein to diffuse through the nuclear pore is larger than 60kDa. FEBS Lett. 581, 3164-70.

White EA., Kramer RE., Tan MJ., Hayes SD., Harper JW., Howley PM. 2012. Comprehensive analysis of host cellular interactions with human papillomavirus E6 proteins identifies new E6 binding partners and reflects viral diversity. J Virol. 86, 13174-13186.

Zehbe I., Richard C., DeCarlo CA., Shai A., Lambert PF., Lichtig H., Tommasino M., Sherman L. 2009. Human papillomavirus 16 E6 variants differ in their dysregulation of human keratinocyte differentiation and apoptosis. Virology 383, 69–77.

Zhang W., Shan H., Jiang K., Huang W., Li S. 2021. A novel intracellular nanobody against HPV16 E6 oncoprotein. Clin Immunol. 225, 108684.

Zhao Y., Brown TL., Kohler H., Müller S. 2003. MTS-conjugated-antiactive caspase 3 antibodies inhibit actinomycin D-induced apoptosis. Apoptosis. 8, 631-637.

Zhou X., Hao R., Chen C., Su Z., Zhao L., Luo Z., Xie W. 2020. Rapid Delivery of Nanobodies/V_HHs into Living Cells via Expressing *In Vitro*-Transcribed mRNA. Mol Ther Methods Clin Dev. 17, 401-408.

zur Hausen H. 2002. Papillomaviruses and cancer: from basic studies to clinical application. Nat Rev Cancer. 2, 342-350.

7 APPENDICES

7.1 Appendix A: Preliminary Co-IP Results for 2A04, 2A10, and 2A15

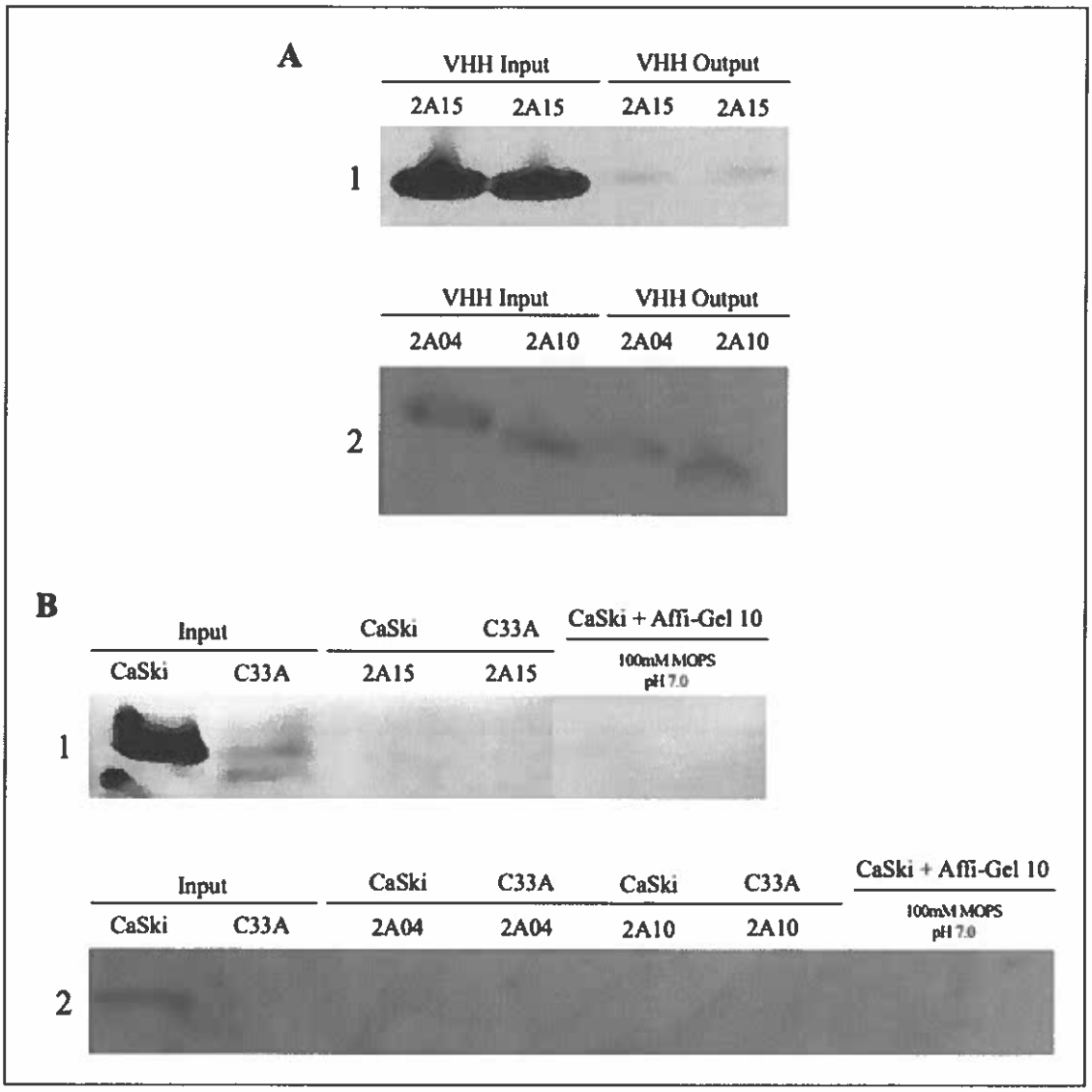

Figure A1: Preliminary co-immunoprecipitation results for 2A04, 2A10, and 2A15 using Affi-Gel 10 resin and 100 mM MOPS pH 7.0. (A) VHH inputs and outputs for experiment 1 and 2. Each input contains 10ug of the respective VHH. Method B resin division was used in both trials. Membranes were visualized using 0.25uL/5mL HA-HRP antibody. (B) CaSki and C33A immunoprecipitation results, and resin alone control results for experiment 1 and 2. Membranes visualized using 12.33uL 6F4 anti-E6 antibody. 500 μg of protein lysate for both CaSki and C33A were used in both trials.

7.2 Appendix B: HiPerFect Transfection Results

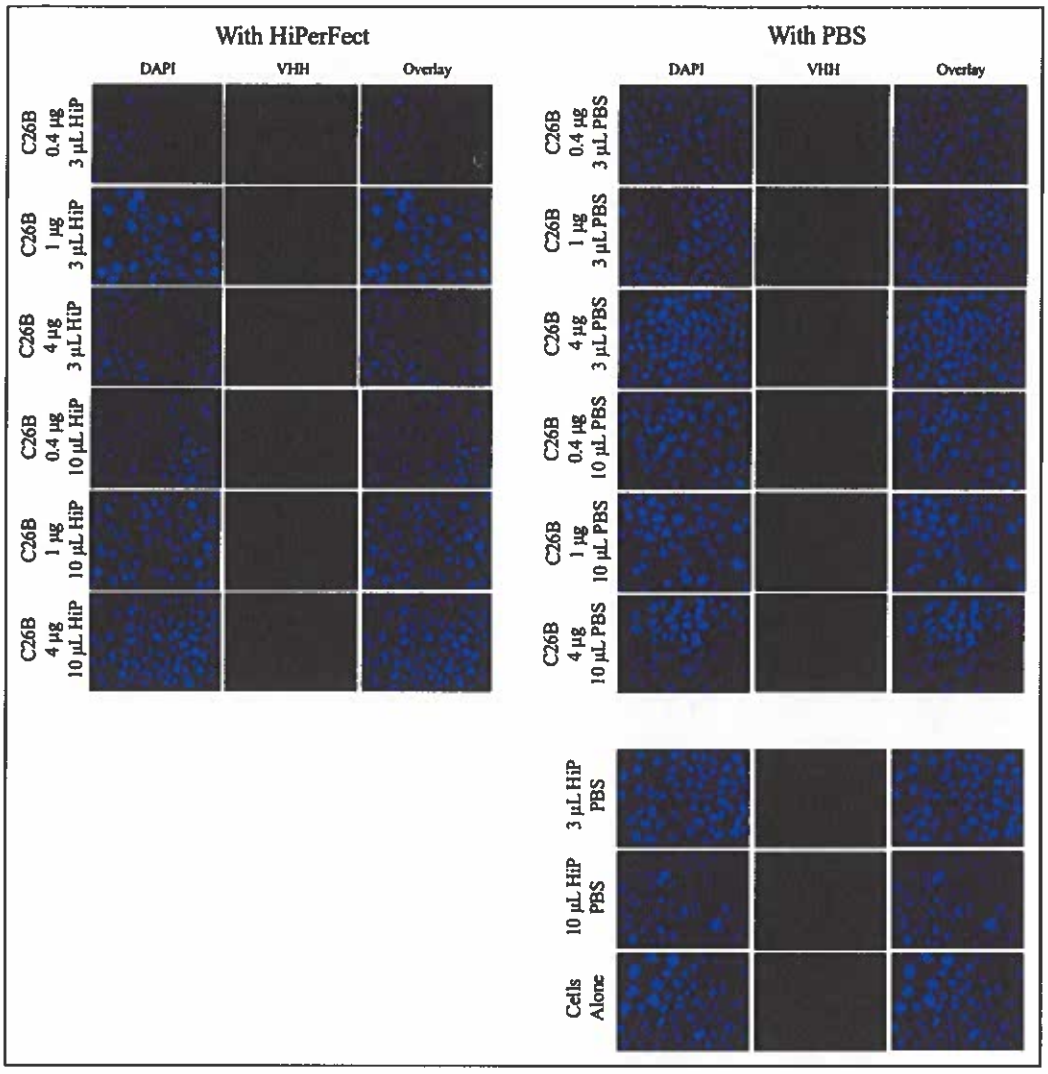

Figure B1: Immunodetection of C26B (0.4 µg/mL, 1 µg/mL, 4 µg/mL) transfected in CaSki cells with 3 µL or 10 µL of HiPerFect. With HiPerFect represents wells transfected with VHH + HiP. With PBS represents wells transfected with VHH + PBS to serve as a negative control for transfection. HiPerFect PBS and Cells Alone controls represent wells treated with HiP + PBS or only Complete DMEM media respectively, serving as controls for cell growth when exposed to HiPerFect or not respectively. VHHs were detected using 1:400 Alexa Fluor 594 +. Nuclei were visualized using DAPI followed by imaging with the Zeiss Axiovert 200 fluorescence microscope equipped with an LD A-Plan 40x/0.50 Ph2 objective and a CCD camera with 12-bit capability.

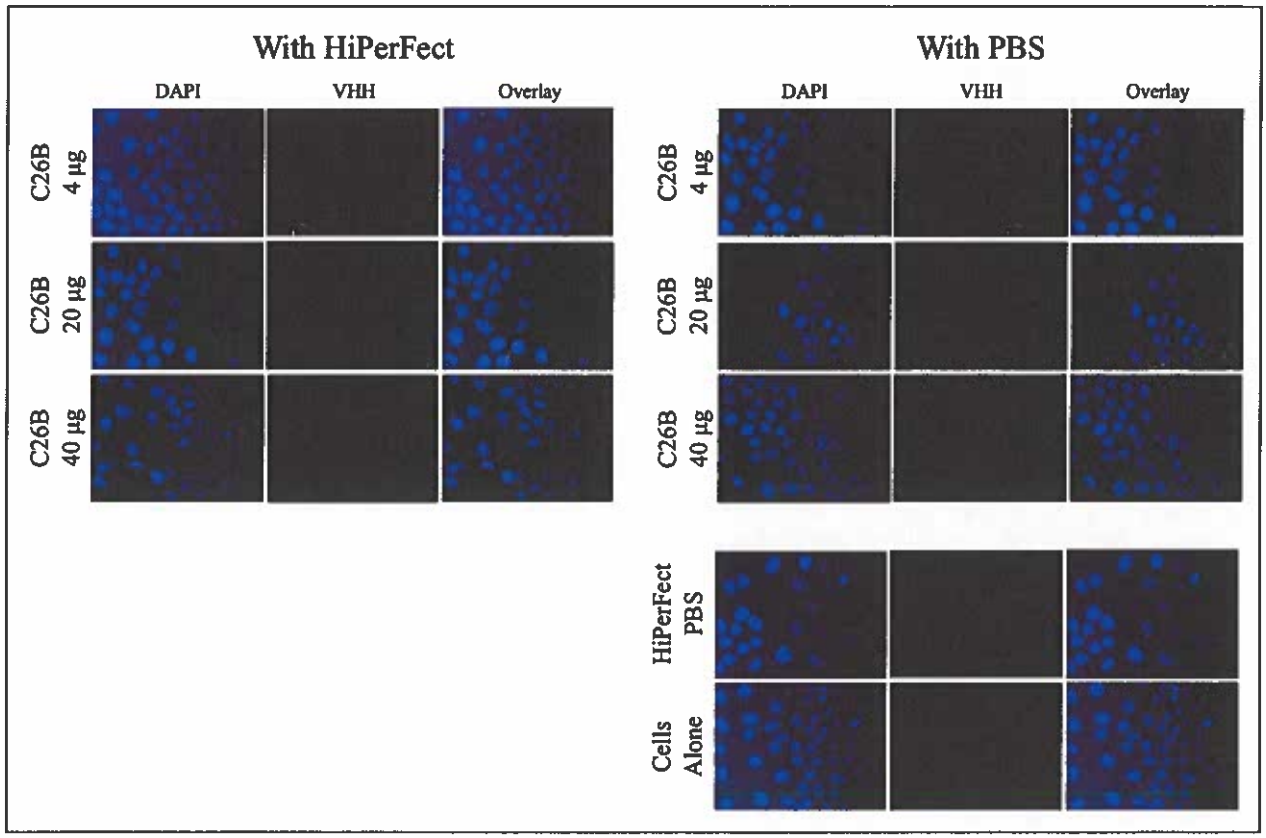

Figure B2: Immunodetection of C26B (4 µg/mL, 20 µg/mL, 40 µg/mL) transfected in CaSki cells with 3 µL of HiPerFect. With HiPerFect represents wells transfected with VHH + HiP. With PBS represents wells transfected with VHH + PBS to serve as a negative control for transfection. HiPerFect PBS and Cells Alone controls represent wells treated with HiP + PBS or only Complete DMEM media respectively, serving as controls for cell growth when exposed to HiPerFect or not respectively. VHHs were detected using 1:400 Alexa Fluor 594 +. Nuclei were visualized using DAPI followed by imaging with the Zeiss Axiovert 200 fluorescence microscope equipped with an LD A-Plan 40x/0.50 Ph2 objective and a CCD camera with 12-bit capability.

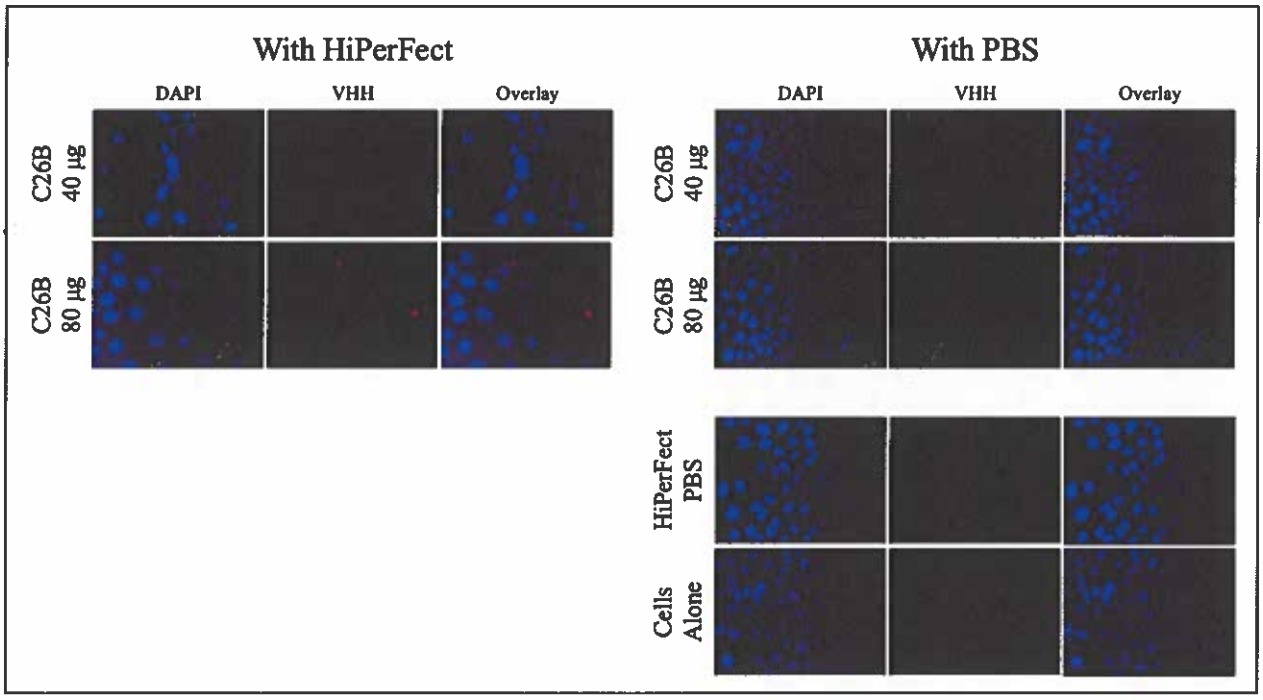

Figure B3: Immunodetection of C26B (40 µg/mL and 80 µg/mL) transfected in CaSki cells with 10 µL of HiPerFect. With HiPerFect represents wells transfected with VHH + HiP. With PBS represents wells transfected with VHH + PBS to serve as a negative control for transfection. HiPerFect PBS and Cells Alone controls represent wells treated with HiP + PBS or only Complete DMEM media respectively, serving as controls for cell growth when exposed to HiPerFect or not respectively. VHHs were detected using 1:400 Alexa Fluor 594 +. Nuclei were visualized using DAPI followed by imaging with the Zeiss Axiovert 200 fluorescence microscope equipped with an LD A-Plan 40x/0.50 Ph2 objective and a CCD camera with 12-bit capability.